(12) INTERNATIONAL APPLICATION PUBLISHED UNDER THE PATENT COOPERATION TREATY (PCT)

(19) World Intellectual Property Organization
International Bureau

(43) International Publication Date
20 January 2022 (20.01.2022)

WIPO | PCT

(10) International Publication Number
WO 2022/011429 A1

(51) International Patent Classification:
C07K 16/24 (2006.01) *A61K 39/395* (2006.01)
C07K 16/28 (2006.01) *A61P 35/00* (2006.01)
A61K 39/00 (2006.01)

(21) International Application Number:
PCT/AU2021/050764

(22) International Filing Date:
16 July 2021 (16.07.2021)

(25) Filing Language: English

(26) Publication Language: English

(30) Priority Data:
2020902474 17 July 2020 (17.07.2020) AU

(71) Applicants: **THE UNIVERSITY OF WESTERN AUSTRALIA** [AU/AU]; 35 Stirling Hwy, Crawley, Western Australia 6009 (AU). **TELETHON KIDS INSTITUTE** [AU/AU]; Perth Children's Hospital, 15 Hospital Avenue, Nedlands, Western Australia 6009 (AU).

(72) Inventors: **LESTERHUIS, Willem Joost**; c/- The University of Western Australia, 35 Stirling Highway, Perth, Western Australia 6009 (AU). **LASSMANN, Timo**; c/- Telethon Kids Institute, Perth Children's Hospital, 15 Hospital Avenue, Nedlands, Western Australia 6009 (AU). **ZEMEK, Rachael**; c/- The University of Western Australia, 35 Stirling Highway, Perth, Western Australia 6009 (AU). **CHIN, Wee Loong**; c/- Telethon Kids Institute, Perth Children's Hospital, 15 Hospital Avenue, Perth, Western Australia 6009 (AU).

(74) Agent: **FPA PATENT ATTORNEYS PTY LTD**; Level 46, 101 Collins Street, Melbourne, Victoria 3000 (AU).

(81) Designated States *(unless otherwise indicated, for every kind of national protection available)*: AE, AG, AL, AM, AO, AT, AU, AZ, BA, BB, BG, BH, BN, BR, BW, BY, BZ, CA, CH, CL, CN, CO, CR, CU, CZ, DE, DJ, DK, DM, DO, DZ, EC, EE, EG, ES, FI, GB, GD, GE, GH, GM, GT, HN, HR, HU, ID, IL, IN, IR, IS, IT, JO, JP, KE, KG, KH, KN, KP, KR, KW, KZ, LA, LC, LK, LR, LS, LU, LY, MA, MD, ME, MG, MK, MN, MW, MX, MY, MZ, NA, NG, NI, NO, NZ, OM, PA, PE, PG, PH, PL, PT, QA, RO, RS, RU, RW, SA, SC, SD, SE, SG, SK, SL, ST, SV, SY, TH, TJ, TM, TN, TR, TT, TZ, UA, UG, US, UZ, VC, VN, WS, ZA, ZM, ZW.

(84) Designated States *(unless otherwise indicated, for every kind of regional protection available)*: ARIPO (BW, GH, GM, KE, LR, LS, MW, MZ, NA, RW, SD, SL, ST, SZ, TZ, UG, ZM, ZW), Eurasian (AM, AZ, BY, KG, KZ, RU, TJ, TM), European (AL, AT, BE, BG, CH, CY, CZ, DE, DK, EE, ES, FI, FR, GB, GR, HR, HU, IE, IS, IT, LT, LU, LV, MC, MK, MT, NL, NO, PL, PT, RO, RS, SE, SI, SK, SM, TR), OAPI (BF, BJ, CF, CG, CI, CM, GA, GN, GQ, GW, KM, ML, MR, NE, SN, TD, TG).

Published:
— *with international search report (Art. 21(3))*

WO 2022/011429 A1

(54) Title: METHODS TO INCREASE RESPONSE TO IMMUNE CHECKPOINT MODULATION

(57) Abstract: The present invention relates to methods for treating cancer, particularly increasing the response to immune checkpoint blockade in individuals with cancer. In another aspect, the present invention provides a method of treating, preventing or minimising progression of cancer in a subject comprising administering an immune checkpoint modulator; subsequently to administering the immune checkpoint modulator, administering an interferon β (IFNβ) inhibitor, thereby treating, preventing or minimising progression of cancer in the subject.

Methods to increase response to immune checkpoint modulation

Field of the invention

The present invention relates to methods for treating cancer, particularly increasing the response to immune checkpoint modulation in individuals with cancer.

Related application

This application claims priority from Australian provisional application AU 2020902474, the contents of which are hereby incorporated by reference in their entirety.

Background of the invention

The response to immune checkpoint modulation, i.e. blockade (ICB) of suppressive immune checkpoints or activation of stimulatory immune checkpoints, in cancer is highly variable, with a majority of patients experiencing disease progression. Although the targets of ICB antibodies are known, the downstream therapeutic effector mechanisms are incompletely understood. The development of novel combination therapies is therefore mainly empiric. Specific aspects of the pre-treatment tumour microenvironment, such as PD-L1 expression, immune cell infiltration or tumour mutation burden have been shown to correlate with response, but none of these biomarkers are sufficiently robust to guide clinical decisions regarding treatment across cancers. When perturbing complex systems, some important effects may only become apparent over time. For example, in the course of an immune response, some inflammatory mediators need to be switched off, not only to resolve inflammation, but also to mediate a transition from innate to adaptive immunity. Similar mechanisms may underpin an effective anti-tumour immune response. However, it is difficult to obtain repeated tumour samples from patients during treatment and analyses of patient tumours are challenging due to inter-individual differences in germline and cancer genetics, tumour microenvironment composition and environmental influences.

There therefore remains a need for new and/or improved therapies for the treatment of cancer.

Reference to any prior art in the specification is not an acknowledgment or suggestion that this prior art forms part of the common general knowledge in any jurisdiction or that this prior art could reasonably be expected to be understood, regarded as relevant, and/or combined with other pieces of prior art by a skilled person in the art.

Summary of the invention

In one aspect, the present invention provides a method of increasing the response in a subject to an immune checkpoint modulator comprising:

administering an immune checkpoint modulator;

subsequently to administering the immune checkpoint modulator, administering an interferon β (IFNβ) inhibitor,

thereby increasing the response in the subject to an immune checkpoint modulator.

In another aspect, the present invention provides a method of treating, preventing or minimising progression of cancer in a subject comprising:

administering an immune checkpoint modulator;

subsequently to administering the immune checkpoint modulator, administering an interferon β (IFNβ) inhibitor,

thereby treating, preventing or minimising progression of cancer in the subject.

In another aspect, the present invention provides a method of treating, preventing or minimising progression of cancer in a subject who has received, or who is receiving, an immune checkpoint modulator, the method comprising:

administering an interferon β (IFNβ) inhibitor,

thereby treating, preventing or minimising progression of cancer in the subject.

In any aspect of the present invention, the subject who has received, or who is receiving, an immune checkpoint modulator may have exhibited, or be exhibiting, a clinically relevant response to that immune checkpoint modulator.

In any aspect of the present invention, the subject who has received, or who is receiving, an immune checkpoint modulator may be resistant or not exhibiting a clinically relevant response to that immune checkpoint modulator.

In another aspect, the present invention provides a method of treating, preventing or minimising progression of cancer in a subject comprising the steps of:

- identifying a subject having cancer; and
- administering an immune checkpoint modulator to the subject;
- subsequently to administering the immune checkpoint modulator, administering an IFNβ inhibitor,

thereby treating, preventing or minimising progression of cancer in the subject.

In another aspect, the present invention provides a method of treating, preventing or minimising progression of cancer in a subject comprising the steps of:

- identifying a subject having cancer and being unresponsive to a treatment comprising an immune checkpoint modulator,
- administering a therapeutically effective amount of an IFNβ inhibitor to the subject,

thereby treating, preventing or minimising progression of cancer in the subject.

In another aspect, the present invention provides a method of treating, preventing or minimising progression of cancer in a subject comprising the steps of:

- identifying a subject having cancer who has received, or who is receiving an immune checkpoint modulator for the treatment of cancer,
- assessing whether the subject is responsive to the immune checkpoint modulator,

- administering a therapeutically effective amount of an IFNβ inhibitor to the subject if the subject is not responsive to the immune checkpoint modulator,

thereby treating, preventing or minimising progression of cancer in the subject.

In any aspect of the invention, the IFNβ inhibitor may be administered in a composition. In one embodiment, the composition does not include an inhibitor of IFNα, an inhibitor of a type II IFN, or an inhibitor of any other IFN. Typically, the only IFN inhibitor included in the composition is an IFNβ inhibitor. In one embodiment, the only active ingredient in the composition is the IFNβ inhibitor.

In any aspect of the invention, the immune checkpoint modulator may be an immune checkpoint inhibitor, i.e. an inhibitor of a suppressive (or negative) immune checkpoint, or an immune checkpoint stimulator or activator, i.e. a stimulator or activator of a stimulatory (or positive) immune checkpoint. Any reference to an immune checkpoint modulator herein may therefore also refer to an immune checkpoint inhibitor and/or an immune checkpoint stimulator or activator.

Further, in any aspect of the invention, the immune checkpoint modulator may be administered in a composition. Typically, the composition further comprises a pharmaceutically acceptable carrier, diluent or excipient. The composition may be formulated for intravenous administration to the subject. In other words, the composition is suitable for administration intravenously.

In any aspect, the IFNβ inhibitor is administered at least about 1 day after an immune checkpoint modulator.

In any aspect, the IFNβ inhibitor is administered not more than about 2 or about 3 months after administration of an immune checkpoint modulator.

In any aspect, the IFNβ inhibitor is administered at a time at least about 1 day after an immune checkpoint modulator but before about 2 or about 3 months after administration of an immune checkpoint modulator.

In another aspect, the present invention further provides a composition comprising, consisting essentially of or consisting of an IFNβ inhibitor and an immune checkpoint modulator, and a pharmaceutically acceptable carrier, diluent or excipient.

The composition is constructed such that in use, or when used, the IFNβ inhibitor is administered after the immune checkpoint modulator.

In another aspect, the present invention further provides a method of increasing survival of a subject having cancer comprising administering a therapeutically effective amount of an IFNβ inhibitor and an immune checkpoint modulator to a subject, thereby increasing survival of the subject having cancer, wherein the IFNβ inhibitor is administered after the immune checkpoint modulator.

In another aspect, the present invention further provides a method of minimising, reducing or preventing growth of a tumour in a subject having cancer comprising administering a therapeutically effective amount of an IFNβ inhibitor and an immune checkpoint modulator to a subject, thereby minimising, reducing or preventing growth of a tumour in the subject having cancer, wherein the IFNβ inhibitor is administered after the immune checkpoint modulator.

In another aspect, the present invention further provides a method of minimising, reducing or preventing metastasis in a subject having cancer comprising administering of a therapeutically effective amount of an IFNβ inhibitor and an immune checkpoint modulator to a subject, thereby minimising, reducing or preventing metastasis in the subject having cancer, wherein the IFNβ inhibitor is administered after the immune checkpoint modulator.

In any embodiment, the invention further provides a method of minimising, reducing or preventing cancer in a subject comprising:

- identifying a subject having a tumour at risk, or capable, of metastasising; and
- administering a therapeutically effective amount of an IFNβ inhibitor and an immune checkpoint modulator to a subject,

thereby minimising, reducing or preventing cancer in the subject, wherein the IFNβ inhibitor is administered after the immune checkpoint modulator.

In any embodiment, the invention further provides a method of minimising, reducing or preventing metastasis in a subject having cancer comprising:

- identifying a subject having a primary tumour at risk of, or capable, of metastasising;
- removing the primary tumour from the subject; and
- administering a therapeutically effective amount of an IFNβ inhibitor and a checkpoint modulator to a subject,

thereby minimising, reducing or preventing metastasis in the subject having cancer, wherein the IFNβ inhibitor is administered after the immune checkpoint modulator.

In another aspect, the present invention further provides a method of minimising, reducing or preventing growth of a tumour in at least one site distant from the site of the primary tumour in a subject comprising administering a therapeutically effective amount of an IFNβ inhibitor and an immune checkpoint modulator to a subject, thereby minimising, reducing or preventing minimising, reducing or preventing growth of a tumour in at least one site distant from the site of the primary tumour in the subject.

In any aspect of the invention, the methods described herein further comprise identifying a subject having cancer. In an embodiment, the cancer may be pre-cancerous or non-metastatic. In another embodiment, the cancer may be malignant or metastatic.

In another aspect, the present invention further provides use of a compound comprising, consisting or consisting essentially of an IFNβ inhibitor and an immune checkpoint modulator in the preparation of a medicament for treating, preventing or minimising progression of cancer in a subject. The medicament constructed such that in use, or when used, the IFNβ inhibitor is administered after the immune checkpoint modulator.

In another aspect, the present invention further provides use of a compound comprising, consisting or consisting essentially of an IFNβ inhibitor in the manufacture of a first medicament, and an immune checkpoint modulator in the preparation of a second medicament, wherein the first and second medicaments are for:

- treating, preventing or minimising progression of cancer in a subject,

- minimising, reducing or preventing growth of a tumour in a subject,
- minimising, reducing or preventing metastasis in a subject, or
- increasing survival of a subject.

Alternatively, the first and second medicaments are for any other method or use of the invention as described herein.

In another aspect, the present invention further provides use of an IFNβ inhibitor and an immune checkpoint modulator for treating, preventing, or preventing progression of cancer in a subject.

In another aspect, the present invention further provides an IFNβ inhibitor and an immune checkpoint modulator for use in treating, preventing, or preventing progression of cancer in a subject. Alternatively, the IFNβ inhibitor and the immune checkpoint modulator is for use in any other method or use of the invention as described herein.

In another aspect, the present invention further provides the use of an IFNβ inhibitor in the manufacture of a medicament for:

- treating, preventing or minimising progression of cancer in a subject who has received or who is receiving an immune checkpoint modulator,
- minimising, reducing or preventing growth of a tumour in a subject who has received or who is receiving an immune checkpoint modulator,
- minimising, reducing or preventing metastasis in a subject who has received or who is receiving an immune checkpoint modulator, or
- increasing survival of a subject who has received or who is receiving an immune checkpoint modulator.

In another aspect, the present invention further provides an IFNβ inhibitor for use in treating, preventing or minimising progression of cancer in a subject who has received or who is receiving an immune checkpoint modulator. Alternatively, the compound is for use in any other method or use of the invention as described herein.

In any aspect of the invention, the immune checkpoint inhibitor may be a PD-1, PD-L1 or a CTLA-4 checkpoint inhibitor, or any other inhibitor described herein. In an aspect, the checkpoint inhibitor is an antibody.

In any aspect of the invention, the immune checkpoint stimulator or activator is any one described herein.

In any aspect of the invention, the method or use further provides administering an IFNβ agonist prior to administering the immune checkpoint modulator.

In an embodiment of any aspect the invention, the method or use does not include administering an inhibitor of IFNα, an inhibitor of a type II IFN, or an inhibitor of any other IFN. Preferably, the only IFN inhibitor administered is an IFNβ inhibitor. Typically, the only inhibitor administered after an immune checkpoint modulator is an IFNβ inhibitor. The IFNβ inhibitor may be any as described or defined herein including inhibitors that bind to IFNβ or IFNAR, preferably IFNAR1, and inhibiting the interaction between IFNβ and IFNAR, preferably IFNAR1.

In any aspect of the invention, the IFNβ inhibitor and/or the immune checkpoint modulator may be administered by any known administration routes in the art including intraperitoneally, intratumorally, topically, orally, intravenously, subcutaneously or intramuscularly. Preferably, an IFNβ inhibitor and/ or immune checkpoint modulator are administered intravenously.

In any aspect of the invention, the cancer is selected from the group consisting of breast cancer, colorectal cancer, adenocarcinomas, mesothelioma, bladder cancer, prostate cancer, germ cell cancer, hepatoma/cholongio carcinoma, neuroendocrine cancer, pituitary neoplasm, small round cell tumour, squamous cell cancer, melanoma, atypical fibroxanthoma, seminomas, nonseminomas, stromal leydig cell tumours, Sertoli cell tumours, skin tumours, kidney tumours, testicular tumours, brain tumours, ovarian tumours, stomach tumours, oral tumours, bladder tumours, bone tumours, cervical tumours, esophageal tumours, laryngeal tumours, liver tumours, lung tumours, vaginal tumours, Wilm's tumours, pancreatic tumours, sarcomas, lymphomas or leukaemias.. The cancer or tumour may be any one described herein. Preferably, the cancer is mesothelioma or renal cell cancer.

As used herein, except where the context requires otherwise, the term "comprise" and variations of the term, such as "comprising", "comprises" and "comprised", are not intended to exclude further additives, components, integers or steps.

Further aspects of the present invention and further embodiments of the aspects described in the preceding paragraphs will become apparent from the following description, given by way of example and with reference to the accompanying drawings.

Brief description of the drawings

Figure 1: Time-dependent changes in expression of a common subset of regulators distinguish ICB responders from non-responders. a, One tumour from mice with bilateral AB1 or Renca tumours was harvested either 1 hour prior to, or 2, 4 or 6 days after ICB, whilst the remaining tumour was monitored for response (n=144). b, Expression of the top 100 regulators ranked by GENIE3 importance score plotted per mouse in time by response, genes were grouped by hierarchal clustering. c, Fraction of CD8+ T cells in responders (RS) and non-responders (NR) over time in the AB1 (top) and Renca (bottom) models. d-g, TCseq analysis was used to cluster genes with similar expression over time, identifying clusters shared by both AB1 and Renca. Gene expression over time and pathway analysis of overlapping genes between AB1 and Renca was performed for cluster 1 (d), cluster 2 (e), cluster 3 (f) and cluster 4 (g). h, AB1 responders and non-responders have a similar trend ($r>0.8$) in clusters 1-3, but not in cluster 4. i, Renca responders and non-responders have a similar trend ($r>0.8$) in clusters 1-3, but not in cluster 4.

Figure 2: Network construction approach from bulk RNA-seq data in AB1 and Renca. The inventors constructed two “direct-interaction networks”, one for AB1 and one for Renca using all responder samples for each strain across four experimental timepoints. The output from GENIE3 is a weighted, complete graph composed of all genes in the input count matrix, so we pruned this graph to isolate biologically relevant edges. To do this, the inventors integrated information from differential expression analysis and transcription factor binding site prediction results from JASPAR. The inventors identified and retained “direct connections”, defined as connections between a transcription factor (TF) to differentially expressed genes only if the transcription factor binding site (TFBS) for the TF was situated in a genomic window 400 base pairs

upstream or 300 basepairs downstream of a DE gene's transcription start site (TSS). The bottom left diagram describes the pruning schema for these networks - as illustrated, the inventors eliminate the GENIE3 edge from TF2 to differentially expressed gene 3 because gene 3 does not possess the transcription factor binding site for TF2. The right diagram demonstrates threshold selection after considering the union set of all GENIE3 weights from Renca and AB1 direct networks (red line - 0.0003125).

Figure 3: An IFN module displaying on/fast-off kinetics is associated with response to ICB. a, GENIE3 subnetwork of direct interactions between TFs and their target genes in AB1 and b, in Renca, separated into responders and non-responders, depicting gene expression over time, with fast-off IFN genes highlighted within the boxes. c, Top 10 TFs with highest GENIE3 scores between ISGs for AB1 and Renca responders (left sub-panel), with average expression for ISGs in responders across time points (right sub-panel). Hive plots of direct networks for AB1 (d) and Renca (e) with TF-to-ISG edges situated in the right upper quadrant. The top 10% of (high valued) edges by GENIE3 score are highlighted in red.

Figure 4: Single cell analysis identifies Ly6C^{hi} inflammatory monocytes as the primary source for fast-off type I IFN signalling in the responsive tumour microenvironment. a, UMAP visualization and annotation of cell subtypes from AB1 tumours prior to ICB (n = 6; 3 responders, 3 non-responders, 17935 cells) b, Differential enrichment of type I interferon production in different cell subsets between responders and non-responders, white line represents mean. c, UMAP showing a gradient of fast-off ISG enrichment located in the monocyte cluster. d, Identification of 3 distinct monocyte sub-clusters with conserved markers (e) for each cluster, separated by response. f, IFN-related TF activation across monocyte clusters. g, Flow cytometry of Irf1 gene expressing cell populations (n = 6, p-value from Mann Whitney U test, error bars represent standard deviation). h, Velocity analysis across monocyte clusters. Arrows denote transcriptional gradient from cluster 1 to cluster 2. i,j, Single cell gene set enrichment analysis of type I (i) and type II (j) interferon-related gene sets. k, Flow cytometry of poly(I:C) treated AE17 tumours from Ifnb1tm1Lky mice to identify the phenotype of IFNβ producing cells (representative sample).

Figure 5: Poly(I:C) induces IFNβ production in Ly6C+ monocytes in AB1 tumours. Tumours from AB1 bearing mice that were treated with poly(I:C) or untreated

were harvested on day 6, dissociated, stained with antibodies and FACS sorted. RNA from each population was extracted for qPCR analysis for IFNβ compared to GAPDH. a, IFNB expression in untreated compared to poly(I:C) treated tumours. b, IFNβ expression within the $CD11b^+$ $Ly6C^+$ monocyte population in untreated compared to poly(I:C) treated tumours.

Figure 6: Targeting IFNβ in a directionally opposite, time-dependent manner improves the response to ICB. a, Treatment strategy. b, Survival curves of AE17-bearing mice treated with poly(I:C), ICB followed by antibodies blocking type I and/or II IFN (n = 15 per group). c,d, Deconvolution analysis on bulk RNA seq data from AB1 (c) and Renca (d), using an IFNβ-stimulated T cell signature between responders (red) and non-responders (blue). Bars represent standard deviation. *p ≤ 0.05, **p≤ 0.01, ****p< 0.0001 from two-way ANOVA with Tukey's multiple comparisons test. e, Survival curves of AE17 bearing mice treated with poly(I:C), ICB followed by antibodies against the type I IFNs, IFNα or IFNβ compared to blocking their receptor IFNAR (n = 5 per group). f, Survival curves of Renca bearing mice treated with poly(I:C), ICB followed by antibodies against the type I and/or II IFN (n = 5 or 10 per group). g, Survival curves of AB1 bearing mice treated with ICB followed by antibodies against type I and/or II IFN (n = 5 to 15 per group).. h, Survival curves of AE17-bearing mice treated with recombinant IFNα or IFNβ and ICB followed by antibodies blocking IFNα or IFNβ (n = 6 to 10 per group). i, Survival curves of AE17-bearing mice treated with poly(I:C) and ICB, with antibodies blocking IFNβ given concurrently or 3 days after the first dose of ICB (n = 5 per group). b, e, f, g, h, i; p values from Logrank test, compared to control “Poly(I:C) + ICB + isotype” or “ICB + isotype”.

Figure 7: Therapeutically phenocopying on/off type I IFN kinetics with poly(I:C) and anti-IFNAR improves response in AB1 tumours. Mice bearing AB1 tumours were treated with poly(I:C) (day 12, 13, 14), followed by CPB (day 17), followed by an antibody against IFNAR1, IFNγ, or both (day 20, 23, 26). Pre-treatment with poly(I:C) increases the number of responders, but does not significantly increase survival (blue line, p= 0.09). Addition of anti-IFNAR significantly improves survival over ICB control (green line, p= <0.001).

Figure 8: Blocking type I IFN after ICB improves responses. To more closely recapitulate a clinical scenario, pre-treatment with poly(I:C) was omitted from the

schedule. a, AB1 tumours treated with ICB followed by anti-IFNAR or anti-IFNB showed a decrease in tumour size and delay in growth when complete response was not achieved. Growth curves were analysed longitudinally using type II ANOVA and pairwise comparisons across groups with Bonferroni correction for multiple comparisons (lower table). b, Blocking anti-IFNAR, but not IFNγ, after ICB significantly improved response in the AE17 tumour model. c, Blocking IFNβ, but not IFNα, after ICB significantly improved response in the Renca tumour model.

Figure 9: Time-dependent scheduling of type I IFN inhibition in the context of ICB. a, Schedule of pre-treatment anti-IFNAR followed by ICB. b, Dosing anti-IFNAR before ICB, rather than after, negates the effect of ICB on AE17. c, Dosing anti-IFNAR concurrently with poly(I:C) (orange line) negates the priming effect of poly(I:C); scheduling IFNAR blockade prior to ICB followed by poly (I:C) (red line) provides no improvement to ICB. d, Dosing anti-IFNβ concurrently with ICB, does not result in improved efficacy (orange versus blue line), while dosing 3 days after start of ICB does (green line).

Figure 10. Patients treated with ICB display early enrichment of the on/fast-off IFN signature. a, Gene set enrichment analysis using our dynamic interferon gene-set in glioblastoma patients within three weeks of treatment with PD-1 blockade versus controls. The dynamic interferon signal demonstrates higher normalized enrichment compared to hallmark gene sets for interferon alpha or interferon gamma gene sets. b, On/fast-off IFN-related TF activation across human peripheral blood monocytes, separated by treatment timepoint and response to ICB (C1, C3, C5; cycle of ICB, EOT; end of treatment). c-d, Comparison of human peripheral blood monocytes to Ly6chi AB1 monocytes. c, Distribution of predicted labels from mouse AB1 Ly6chi monocytes onto human peripheral blood single cell data, corresponding to human monocytes. d, Human monocytes demonstrate differential capacity for dynamic ISG activation. Applying single cell gene set enrichment using SCDE, the inventors looked at enrichment for our fast-ISG genes in responders (left) and non-responders (right) over the course of therapy. As compared to non-responder monocytes, a greater percentage of responder monocytes show dynamic IFN-related TF activation

Figure 11. Monocytes in breast cancer patients with expanded T cell following treatment with anti-PD1 display on/fast-off IFN transcriptional activity. a,

results of SCENIC network analysis showing distribution of IFN related transcription factor activation across cell subsets in the breast cancer dataset based on singleR labels. b, Results of ssGSEA showing distribution of IFN-related gene set scores across cell subsets in the breast cancer dataset based on singleR labels. c, Results of differential expression analysis comparing pre- versus on-treatment monocytes showing early downregulation of fast-off signal in patients displaying T-cell expansion in response to anti-PD1.

Detailed description of the embodiments

Reference will now be made in detail to certain embodiments of the invention. While the invention will be described in conjunction with the embodiments, it will be understood that the intention is not to limit the invention to those embodiments. On the contrary, the invention is intended to cover all alternatives, modifications, and equivalents, which may be included within the scope of the present invention as defined by the claims.

One skilled in the art will recognize many methods and materials similar or equivalent to those described herein, which could be used in the practice of the present invention. The present invention is in no way limited to the methods and materials described. It will be understood that the invention disclosed and defined in this specification extends to all alternative combinations of two or more of the individual features mentioned or evident from the text or drawings. All of these different combinations constitute various alternative aspects of the invention.

All of the patents and publications referred to herein are incorporated by reference in their entirety.

For purposes of interpreting this specification, terms used in the singular will also include the plural and vice versa.

Unless specifically indicated otherwise, all technical and scientific terms used herein have the same meaning as commonly understood by those of ordinary skill in the art to which this invention belongs. In addition, any method or material similar or equivalent to a method or material described herein can be used in the practice of the

present invention. For purposes of the present invention, the following terms are defined.

The terms "a," "an," or "the" as used herein not only include aspects with one member, but also include aspects with more than one member. For instance, the singular forms "a," "an," and "the" include plural referents unless the context clearly dictates otherwise. Thus, for example, reference to "a cell" includes a plurality of such cells and reference to "the agent" includes reference to one or more agents known to those skilled in the art, and so forth. For purposes of interpreting this specification, terms used in the singular will also include the plural and vice versa.

The terms "about" and "approximately" shall generally mean an acceptable degree of error for the quantity measured given the nature or precision of the measurements. Typical, exemplary degrees of error are within 20 percent (%), preferably within 10%, and more preferably within 5% of a given value or range of values. Alternatively, and particularly in biological systems, the terms "about" and "approximately" may mean values that are within an order of magnitude, preferably within 5-fold and more preferably within 2-fold of a given value. Numerical quantities given herein are approximate unless stated otherwise, meaning that the term "about" or "approximately" can be inferred when not expressly stated.

During the development of a tumour, tumour cells are more or less tolerated by the patient's own immune system, as they are the patient's own cells (e.g., they are self) and are not effectively recognised by the patient's immune system, allowing the tumour cells to grow and divide without proper regulatory control. Accordingly, the patient's own immune system requires stimulation to attack the cancer cells. Cancer immunotherapy involves the utilisation of the immune system of a cancer patient to reject the cancer by stimulating the patient's immune system. In turn, the activated immune system attacks the cancer cells, sparing the normal cells of the patient. A so called immunotherapy that has been shown to be useful for the treatment of cancer is the use of checkpoint modulators.

Although such immune checkpoint modulator (particularly inhibitor) cancer immunotherapies have demonstrated efficacy in some cancers, such therapies are ineffective in a significant percentage of patients, and some initial responders eventually

develop resistance to these therapies with relapsed disease. The ability of a patient to respond to an immunotherapy is dependent upon a large number of factors including individual genetic makeup, history of infection, age, nutritional status, HLA type and consumption of certain medication. Masking of tumour antigens so that the tumour cells cannot be detected by immune surveillance is also a particular problem as is the generally compromised immune status of cancer patients.

By way of example, PD-1 blockade alone has been shown to be ineffective in subsets of patients in some types of cancer such as melanoma and large B cell lymphoma. There is therefore a need for more reliable and efficacious immunotherapy regimes that have utility in the treatment of cancer.

The present inventors have unexpectedly found that when an IFNβ inhibitor is administered subsequent to (i.e. after) administration of an immune checkpoint modulator, a greater positive response to the immunotherapy is observed. This response includes a greater rate of response and depth of response. Further, this advantage is observed in tumours both intrinsically responsive and non-responsive to immune checkpoint inhibition.

The inventors have shown this remarkable effect in three different models of cancer of differing aetiology, pathogeneses and sensitivity to immune checkpoint blockade. A skilled person would therefore understand the applicability of the invention to any of the other cancers described herein. Further, the inventors have confirmed these effects are independent of immune checkpoint target as the beneficial effect was observed with inhibitors against PD-L1 and CTLA-4.

The findings described herein are significant as they establish that tumours that were previously untreatable using checkpoint modulators alone are now treatable when the combination of a checkpoint modulator and IFNβ inhibitor is used. This work therefore identifies a new immunotherapy treatment that improves response rates in patients with cancer who were previously unresponsive to immune checkpoint inhibition. Importantly, this work also identifies a new immunotherapy treatment that improves response rates in patients with cancer who are responsive to immune checkpoint inhibition.

Immune checkpoint modulator

The term "immune checkpoint modulator" includes inhibitors of suppressive (or negative) immune checkpoints and agonists or activators of stimulatory (or positive) immune checkpoints. As used herein an "immune checkpoint inhibitor" refers to any molecule that directly or indirectly inhibits, partially or completely, a suppressive or negative immune checkpoint pathway. As used herein an "immune checkpoint stimulator" or "immune checkpoint activator" refers to any molecule that directly or indirectly agonises, promotes or stimulates, partially or completely, a stimulatory or positive immune checkpoint pathway.

It is generally thought that immune checkpoint pathways function to turn on or off aspects of the immune system, particularly T cells, but also for instance myeloid cells, NK cells and B cells. Following activation of a T cell, a number of inhibitory receptors can be upregulated and present on the surface of the T cell in order to suppress the immune response at the appropriate time. Examples of immune checkpoint pathways include, without limitation, PD-1/PD-L1 , CTLA4/B7-1 , TIM-3, LAG3, By-He, H4, HAVCR2, ID01, CD276 and VTCN1, B7-H3, B7-H4, CD47, or KIR. Immune checkpoints and modulators thereof as well as methods of using such compounds are described in the literature. For instance, non-limiting examples of immune checkpoint inhibitors or modulators include fully human monoclonal antibodies, such as BMS-936558/MDX-1106, BMS- 936559/MDX-1 105, ipilimumab/Yervoy, tremelimumab, BMS-986016, Durvalumab, MEDI4736, Urelumab, CDX-1127, and Avelumab; humanized antibodies, such as CT-011 , IV1K-3475, Hu5F9-G4, CC-90002, MBG453, TSR-022, and Atezolizumab; and fusion proteins, such as AMP-224 and TTI-621 , and others. Other non-limiting examples of immune checkpoint modulators (agonists) include antibodies directed against e.g. CD40, OX40, GITR, CD137 (4-1 BB), CD27, ICOS, and TRAIL.

Non- limiting examples of agonistic immune checkpoint modulators are those that exert an agonist function in the sense that they are capable of stimulating or reinforcing stimulatory or positive immune checkpoint pathways or signals, for example those mediated by CD28, ICOS, CD137 (or 4-1BB), OX40, CD27, CD40 and GITR immune checkpoints.

Where reference is made herein to an immune checkpoint inhibitor, an immune checkpoint modulator, stimulator or activator may also be used, except in those cases where it is apparent from the context of the wording that this is not the case.

In the context of cancer, checkpoint inhibitors regulate the immune system by blocking proteins that stop the immune system from attacking cancer cells. In particular, they control how detection-evading cancer cells and T-cells interact so that T-cells can recognize tumour cells and mount an appropriate immune response against them. Non-limiting examples of checkpoint inhibitors that may be used in accordance with the methods described herein include inhibitors that target PD-1 (programmed cell death protein 1), CTLA-4 (cytotoxic T lymphocyte associated protein 4) and PD-L1 (programmed death ligand 1). A skilled person will understand that CTLA-4 and PD-1 are found on T cells and that PD-L1 is expressed on cancer cells. Other non-limiting examples include PD-L2, TIM3, LAG3, CEACAM (e.g., CEACAM-1, CEACAM-3 and/or CEACAM-5), VISTA, BTLA, TIGIT, LAIR1, CD160, 2B4, CD80, CD86, B7-H3 (CD276), B7-H4 (VTCN1), HVEM (TNFRSF14 or CD107), KIR, A2aR, SIGLEC7, NOX2, MHC class I, MHC class II, GAL9, adenosine, and TGF-beta.

Other immune checkpoints include Indoleamine 2,3-dioxygenase (IDO) and CSF-R1. Inhibitors of those proteins are also contemplated as immune checkpoint inhibitors for use in the invention.

“Programmed Death-1 (PD-1)” refers to an immunoinhibitory receptor belonging to the CD28 family. PD-1 is expressed predominantly on activated T cells in vivo, and binds to two ligands, PD-L1 and PD-L2. The term “PD-1” as used herein includes human PD-1 (hPD-1), variants, isoforms, and species homologs of hPD-1, and analogs having at least one common epitope with hPD-1. The complete hPD-1 sequence can be found under GenBank Accession No. U64863.

Upon binding of PD-1 to programmed cell death ligand 1 (PD-L1), an immune reaction is turned off so as to prevent T-cells from damaging or killing the cell. In the context of cancer, cancer cells can be covered with PD-L1 proteins to camouflage themselves as healthy cells thus avoiding an immune response. Programmed Death Ligand-1 (PD-L1) is one of two cell surface glycoprotein ligands for PD-1 (the other

being PD-L2) that downregulate T cell activation and cytokine secretion upon binding to PD-1. The term “PD-L1” as used herein includes human PD-L1 (HPD-L1), variants, isoforms, and species homologs of hPD-L1, and analogs having at least one common epitope with hPD–L1. The complete hPD-L1 sequence can be found under GenBank Accession No. Q9NZQ7.

Cytotoxic T-Lymphocyte Antigen-4 (CTLA-4) refers to an immunoinhibitory receptor belonging to the CD28 family. CTLA-4 is expressed exclusively on T cells in vivo, and binds to two ligands, CD80 and CD86 (also called B7-1 and B7-2, respectively). The term "CTLA-4 ” as used herein includes human CTLA-4 (hCTLA-4), variants, isoforms, and species homologs of hCTLA-4, and analogs having at least one common epitope with hCTLA-4. The complete hCTLA-4 sequence can be found under GenBank Accession No. AAB59385.

In accordance with this invention, the one or more immune checkpoint modulator(s) may independently be a polypeptide or a polypeptide- encoding nucleic acid molecule; said polypeptide comprising a domain capable of binding the targeted immune checkpoint and/or inhibiting the binding of a ligand to said targeted immune checkpoint so as to exert an antagonist function (i.e. being capable of antagonizing an immune checkpoint-mediated inhibitory signal) or an agonist function (i.e. being capable of boosting an immune checkpoint-mediated stimulatory signal). Such one or more immune checkpoint modulator(s) can be independently selected from the group consisting of peptides (e.g. peptide ligands), soluble domains of natural receptors, RNAi, antisense molecules, antibodies and protein scaffolds. In a preferred embodiment, the immune checkpoint modulator is an antibody. In the context of the invention, the immune check modulator antibody is used in the broadest sense and encompasses e.g. naturally occurring and engineered by man as well as full length antibodies or functional fragments or analogs thereof that are capable of binding the target immune checkpoint or epitope (thus retaining the target-binding portion). It can be of any origin, e.g. human, humanized, animal (e.g. rodent or camelid antibody) or chimeric. It may be of any isotype with a specific preference for an IgGI or IgG4 isotype. In addition, it may be glycosylated or non- glycosylated. The term "antibody" also includes bispecific or multi- specific antibodies so long as they exhibit the binding specificity described herein. Standard assays to evaluate the binding ability of the

antibodies toward immune checkpoints are known in the art, including for example, ELISAs, Western blots, RIAs and flow cytometry. The binding kinetics (e.g., binding affinity) of the antibodies also can be assessed by standard assays known in the art, such as by Biacore analysis.

Any of the checkpoint modulators described herein may be administered in the form of an antibody. An "antibody" (Ab) shall include, without limitation, a glycoprotein immunoglobulin which binds specifically to an antigen and comprises at least two heavy (H) chains and two light (L) chains interconnected by disulfide bonds, or an antigen-binding portion thereof. Each H chain comprises a heavy chain variable region (abbreviated herein as VH) and a heavy chain constant region. The heavy chain constant region comprises three constant domains, CH1, CH2 and CH3. Each light chain comprises a light chain variable region (abbreviated herein as VL) and a light chain constant region. The light chain constant region is comprises one constant domain, CL. The VH and VL regions can be further subdivided into regions of hypervariability, termed complementarity determining regions (CDRs), interspersed with regions that are more conserved, termed framework regions (FR). Each VH and VL comprises three CDRs and four FRs, arranged from amino-terminus to carboxy-terminus in the following order: FRI, CDR1, FR2, CDR2, FR3, CDR3, FR4. The variable regions of the heavy and light chains contain a binding domain that interacts with an antigen. The constant regions of the Abs can mediate the binding of the immunoglobulin to host tissues or factors, including various cells of the immune system (e.g., effector cells) and the first component (Clq) of the classical complement system.

The term “antibody” includes, by way of example monoclonal and polyclonal Abs; chimeric and humanized Abs; human or nonhuman Abs; wholly synthetic Abs; and single chain Abs. A nonhuman Ab can be humanized by recombinant methods to reduce its immunogenicity in humans. Where not expressly stated, and unless the context indicates otherwise, the term "antibody” also includes an antigen-binding fragment or an antigen-binding portion of any of the aforementioned immunoglobulins, and includes a monovalent and a divalent fragment or portion, and a single chain Ab.

An “isolated antibody” refers to an Ab that is substantially free of other Abs having different antigenic specificities (e.g., an isolated Ab that binds specifically to PD-1 is substantially free of Abs that bind specifically to antigens other than PD-1). An

isolated Ab that binds specifically to PD-1 can, however, have cross-reactivity to other antigens, such as PD-1 molecules from different species. Moreover, an isolated Ab can be substantially free of other cellular material and/or chemicals. The term “monoclonal antibody” (mAb) refers to a non-naturally occurring preparation of Ab molecules of single molecular composition, i.e., Ab molecules whose primary sequences are essentially identical, and which exhibits a single binding specificity and affinity for a particular epitope. A mAb is an example of an isolated Ab. mAbs can be produced by hybridoma, recombinant, transgenic or other techniques known to those skilled in the art.

A “human” antibody (huMAb) refers to an Ab having variable regions in which both the framework and CDR regions are derived from human germline immune globulin sequences. Furthermore, if the Ab contains a constant region, the constant region also is derived from human germline immunoglobulin sequences. The human Abs of the invention can include amino acid residues not encoded by human germline immunoglobulin sequences (e.g., mutations introduced by random or site - specific mutagenesis in vitro or by somatic mutation in vivo). However, the term “human antibody,” as used herein, is not intended to include Abs in which CDR sequences derived from the germline of another mammalian species, such as a mouse, have been grafted onto human framework sequences. The terms “human” Abs and “fully human Abs and are used synonymously.

A “humanized antibody” refers to an Ab in which some, most or all of the amino acids outside the CDR domains of a non-human Ab are replaced with corresponding amino acids derived from human immunoglobulins. In one embodiment of a humanized form of an Ab, some, most or all of the amino acids outside the CDR domains have been replaced with amino acids from human immunoglobulins, whereas some, most or all amino acids within one or more CDR regions are unchanged. Small additions, deletions, insertions, substitutions or modifications of amino acids are permissible as long as they do not abrogate the ability of the Ab to bind to a particular antigen. A “humanized" Ab retains an antigenic specificity similar to that of the original Ab.

A “chimeric antibody” refers to an Ab in which the variable regions are derived from one species and the constant regions are derived from another species, such as

an Ab in which the variable regions are derived from a mouse Ab and the constant regions are derived from a human Ab.

An "anti-antigen" Ab refers to an Ab that binds specifically to the antigen. For example, an anti-PD-1 Ab binds specifically to PD-1 and an anti-CTLA-4 Ab binds specifically to CTLA-4.

An "antigen-binding portion" of an Ab (also called an "antigen-binding fragment") refers to one or more fragments of an Ab that retain the ability to bind specifically to the antigen bound by the whole Ab.

Examples of immune checkpoints and antibody inhibitors that target those checkpoints include anti-CTLA-4 (e.g., Ipilimumab, Tremelimumab, KAHR-102), anti-TIM3 (e.g., F38-2E2. ENUM005), anti-LAG3 (e.g., BMS-986016, IMP701. IMP321, C9B7W), anti-KIR (e.g., Lirilumab, IPH2101, IPH4102), anti-PD-1 (e.g., Nivolumab, Pidilizumab, Pembrolizumab, BMS-936559, atezolizumab, Lambrolizumab, MK-3475. AMP-224, AMP-514, STI-A1110, TSR-042), anti-PD-L1 (e.g., KY-1003 (EP20120194977), MCLA-145, atezolizumab. BMS-936559, Durvalumab (MEDI-4736), MSB0010718C, AUR-012, STI-A1010. PCT/US2001/020964, Atezolizumab (MPDL3280A), AMP-224, Dapirolizumab pegol (CDP-7657), MEDI-4920), anti-CD73 (e.g., AR-42 (OSU-HDAC42, HDAC-42, AR42, AR 42, OSU-HDAC 42, OSU-HDAC-42, NSC D736012, HDAC-42, HDAC 42, HDAC42, NSCD736012, NSC-D736012), MEDI-9447), anti-B7-H3 (e.g., MGA271, DS-5573a, 8H9), anti-CD47 (e.g., CC-90002, TTI-621, VLST-007), anti-BTLA, anti-VISTA, anti-A2aR, anti-B7-1, anti-B7-H4, anti-CD52 (such as alemtuzumab), anti-IL-10, anti-IL-35, anti-TGF-β (such as Fresolumimab), anti-CSF1R (e.g., FPA008), anti-NKG2A (e.g., monalizumab), anti-MICA (e.g., IPH43), anti-CD39 and anti-TIGIT (e.g. tiragolumab).

Anti-PD-1 inhibitors and anti-PD-L1 inhibitors

Examples of suitable PD-1 inhibitors that may be used in accordance with the invention include Keytruda (pembrolizumab), Opdivo (nivolumab), AGEN 2034, BGB-A317, BI-754091, CBT-501 (genolimzumab), MEDI0680, MGA012, PDR001, PF-06801591, REGN2810 (SAR439684), and TSR-042 or those that are disclosed in US Pat. No. 8,008,449. Other anti-PD-1 mAbs have been described in, for example, US

Pat. Nos. 6,808,710, 7,488,802, 8,168,757 and 8,354,509, and PCT Publication No. WO 2012/145493.

Nivolumab (also known as "Opdivo®"; formerly designated 5C4, BMS-936558, MDX - 1106, or ONO4538) is a fully human IgG4 (S228P) PD-1 immune check point inhibitor Ab that selectively prevents interaction with PD-1 ligands (PD-L1 and PD-L2), thereby blocking the down-regulation of antitumor T-cell functions (U.S. Pat. No. 8,008,449).

Pembrolizumab (also known as "Keytruda®", lambrolizumab, and MK-3475) is a humanized monoclonal IgG4 antibody directed against human cell surface receptor PD-1 (programmed death-1 or programmed cell death-1). Pembrolizumab is described for example, in U.S. Pat. Nos. 8,354,509 and 8,900,587). Pembrolizumab has been approved by the FDA for the treatment of relapsed or refractory melanoma.

Other suitable PD-1 inhibitors include Libtayo (cemiplimab), Blincyto (blinatumomab), Dostarlimab, Spartalizumab, Cetrelimab, Pidilizumab and BI-754091.

Anti-PD-1 Abs suitable for use in the disclosed methods or compositions are Abs that bind to PD-1 with high specificity and affinity, block the binding of PD-L1 and or PD-L2 , and inhibit the immunosuppressive effect of the PD-1 signalling pathway. In any of the compositions or methods disclosed herein, an anti-PD-1 antibody includes an antigen-binding portion or fragment that binds to the PD-1 receptor and exhibits the functional properties similar to those of whole Abs in inhibiting ligand binding and upregulating the immune system.

In certain embodiments, an anti-PD-1 antibody used in the methods can be replaced with another PD-1 or anti-PD-L1 antagonist. For example, because an anti-PD-L1 antibody prevents interaction between PD-1 and PD-L1, thereby exerting similar effects to the signaling pathway of PD-1, an anti-PD-L1 antibody can replace the use of an anti-PD-1 antibody in the methods disclosed herein. In any embodiment, suitable PD-L1 inhibitors include Imfinzi (durvalumab or MEDI4736), Tecentriq (atezolizumab or MPDL3280A), Bavencio (avelumab; MSB0010718C), MS–936559 (12A4 or MDX-1105) and CX-072.

Anti - CTLA - 4 Antibodies

Anti-CTLA-4 antibodies for use in accordance with the instant invention bind to human CTLA-4 so as to disrupt the interaction of CTLA-4 with a human B7 receptor. It will be understood that because the interaction of CTLA-4 with B7 transduces a signal leading to inactivation of T cells bearing the CTLA-4 receptor, disruption of the interaction effectively induces, enhances or prolongs the activation of such T cells, thereby inducing, enhancing or prolonging an immune response.

Suitable CTLA-4 inhibitors that may be used in accordance with the invention include Yervoy (ipilimumab), Tremelimumab and AGEN 1884 or those disclosed in U.S. Pat. Nos. 6,984,720 and 7,605,238. Ipilimumab is a fully human, IgG1 monoclonal Ab that blocks the binding of CTLA-4 to its B7 ligands, thereby stimulating T cell activation. Tremelimumab is human IgG2 monoclonal anti-CTLA–4 antibody. Another is Blincyto (blinatumomab) which is a Bispecific CD19-directed CD3 T cell engager.

Interferon-β antagonist/inhibitor

As used herein, an “interferon (IFN)-β inhibitor” or “interferon (IFN)-β antagonist” includes refers to any molecule that reduces or inhibits the activity of, level of or expression of IFNβ, for example interferon (IFN)-β signalling and function and/or interferon IFNβ production. The molecule may be DNA, RNA (siRNA, antisense molecules, an sgRNA molecule for use in a CRISPR/Cas9 or related system), peptide, protein (including fusion protein), antibody or small molecules. Examples of interferon (IFN)-β inhibitors include (i) humanized or human anti-IFN-β whole antibodies or antibody fragments (Fab or scFv), antagonizing secreted IFN-β, (ii) short interfering (si) RNA or antisense oligonucleotides inhibiting IFN-β production, (iii) anti-IFNβ-receptor antibodies, mutant IFN-β/Fc fusion proteins, IFN-β receptor fusion proteins, or small molecules interfering with IFN-β signalling.

Preferably, the interferon IFNβ inhibitor does not significantly reduce or inhibit interferon (IFN)-α signalling and function and/or interferon (IFN)-α production.

Preferably, the interferon (IFN)-β inhibitor does not significantly reduce or inhibit signalling, function and/or production of one, or all type II IFNs.

In one embodiment, the only IFN the IFNβ inhibitor inhibits or reduces the signalling, function or production of, is of IFNβ.

In one embodiment, the inhibitor reduces the binding of IFNβ to its receptor, IFNAR. The inhibitor may therefore bind to IFNβ, IFNAR (particularly IFNAR1) or both IFNβ and IFNAR (particularly IFNAR1).

Exemplary IFNβ inhibitors include PF-06823859 and Anifrolumab.

In any embodiment, an IFNβ antagonist or inhibitor may inhibit the signalling of IFNβ and/or inhibit or reduce the expression or activity or level of IFNβ by at least 10%, at least 20%, at least 30%, at least 40%, at least 50%, at least 60%, at least 70%, at least 80%, at least 90% or more.

Interferon-β agonists

As used herein, an "interferon (IFN)-β agonist" includes a molecule that increases the activity of, level of, or expression of IFN-β. An IFN-β agonist also includes a “IFN-β receptor agonist” which binds to IFN-alpha/beta receptor (IFNAR), subunits IFNAR-1 or IFNAR-2, and which elicits a response typical of IFN-β. An exemplary response includes any one or more of the functions of the IFNAR, particularly those described herein. Typically the IFN-β receptor agonist comprises, consists essentially of or consists of a polypeptide.

As used herein, a fragment of interferon beta is preferably a fragment that binds to and activates an interferon beta receptor. Typically, the fragment of interferon beta binds to and activates the same receptors as full-length interferon beta.

Preferably, the fragment of the interferon beta binds to IFNAR present on the surface of a cell, preferably an immune cell, resulting in phosphorylation of one or more tyrosine residues on an IFNAR.

Non-limiting examples of IFN-β agonists include, for example, MEM-288, the IFN-β polypeptide, IFN-β1a, e.g., Avonex® (Biogen, Inc.), Rebif® (Serono, SA), SNG001 (Synairgen); IFN-β1b (Betaseron®; Betaferon ®; Bayer); Extavia (Novartis) CinnoVex ® and the like (including pegylated forms of IFN-β1a, Plegridy ® and IFN-β1b, BBT-032). Mammalian IFN-β sequences such as human (Gray and Goeddel

(1982). Nature, 298:859); rat (Yokoyama, et al., (1997). Biochem Biophys Res Commun., 232:698); canine (Iwata, et al., (1996). J Interferon Cytokine Res., 10:765); porcine (J Interferon Res., (1992).12:153) are known in the art. Another example of IFN-β receptor agonist is an IFN-β receptor agonist antibody (eg anti-IFN anti-idotypic antibody (Osheroff et al. (1985). J Immunol, 135:306).

Further non-limiting examples include Poly(I:C), or variations thereof, such as poly-ICLC (Hiltonol® from Oncovir), poly(A:U) (Innate Pharma), Rintatolimod (AIM ImmunoTech), STING agonists, including: ADU-S100 (Aduro), MK-1454 (Merck), MAVU-104 (Abbvie), BMS-986301 (BMS), GSK532 (GSK), RIG-I agonists, including: MK-4621 (Merck), KIN131A (Kineta), inarigivir (Spring bank).

Administration and dosage

In an embodiment of the invention, therapeutically effective amounts of an immune checkpoint modulator and IFNβ inhibitor are administered to the subject.

Administering refers to the physical introduction of a composition comprising a therapeutic agent to a subject, using any of the various methods and delivery systems known to those skilled in the art including those described herein. Pharmaceutical compositions may be formulated from compounds of the invention as described herein for any appropriate route of administration.

Typically, in addition to the therapeutic agent (eg an immune checkpoint modulator and/or IFNβ inhibitor, a pharmaceutical composition comprises a pharmaceutically acceptable excipient, carrier and/or diluent. Examples of suitable components for inclusion in a pharmaceutical composition are described in Martindale – The Extra Pharmacopoeia (Pharmaceutical Press, London 1993) and Martin (ed.), Remington's Pharmaceutical Sciences. Preferably, the pharmaceutically acceptable excipient, carrier and/or diluent is non-toxic.

The term "pharmaceutically acceptable carrier" refers to a substance that aids the administration of an active agent to a cell, an organism, or a subject. "Pharmaceutically acceptable carrier" refers to a carrier or excipient that can be included in the compositions of the invention and that causes no significant adverse toxicological effect on the subject. Non-limiting examples of pharmaceutically

acceptable carriers include water, NaCl, normal saline solutions, lactated Ringer's, normal sucrose, normal glucose, binders, fillers, disintegrants, lubricants, coatings, sweeteners, flavors and colors, liposomes, dispersion media, microcapsules, cationic lipid carriers, isotonic and absorption delaying agents, and the like. The carrier may also be substances for providing the formulation with stability, sterility and isotonicity (e.g. antimicrobial preservatives, antioxidants, chelating agents and buffers), for preventing the action of microorganisms (e.g. antimicrobial and antifungal agents, such as parabens, chlorobutanol, sorbic acid and the like) or for providing the formulation with an edible flavor etc. In some instances, the carrier is an agent that facilitates the delivery of a modified cancer cell to a target cell or tissue. One of skill in the art will recognize that other pharmaceutical carriers are useful in the present invention.

Suitable routes of administration for implementing the defined methods include oral, intravenous, intramuscular, topical, subcutaneous, intraperitoneal, spinal or other parenteral routes of administration, for example by injection or infusion. The phrase "parenteral administration" as used herein means modes of administration other than enteral and topical administration, usually by injection, and includes, without limitation, intravenous, intramuscular, intraarterial, intrathecal, intralymphatic, intralesional, intracapsular, intraorbital, intracardiac, intradermal, intraperitoneal, transtracheal, subcutaneous, subcuticular, intraarticular, subcapsular, subarachnoid, intraspinal, epidural and intrastemal injection and infusion, as well as in vivo electroporation. Administering can also be performed, for example, once, a plurality of times, and/or over one or more extended periods.

The phrase ‘therapeutically effective amount’ or ‘effective amount’ generally refers to an amount of an immune checkpoint modulator and/or IFN-β inhibitor, a pharmaceutically acceptable salt, polymorph or prodrug thereof of the present invention that (i) treats the particular disease, condition, or disorder, (ii) attenuates, ameliorates, or eliminates one or more symptoms of the particular disease, condition, or disorder, or (iii) delays the onset of one or more symptoms of the particular disease, condition, or disorder described herein. Undesirable effects, e.g. side effects, are sometimes manifested along with the desired therapeutic effect; hence, a practitioner balances the potential benefits against the potential risks in determining what is an appropriate "effective amount".

For instance, for the treatment of tumours, a therapeutically effective amount of the compounds or compositions described herein can inhibit tumour growth by at least about 10%, by at least about 20%, by at least about 30%, by at least about 40%, by at least about 50%, by at least about 60%, by at least about 70%, by at least about 80%, or by at least about 90% or more, relative to untreated subjects. Alternatively, the treatments described herein may cause complete regression of the tumour mass. In other embodiments of the invention, tumour regression can be observed and continue for a period of at least about 10 days, at least about 20 days, at least about 30 days, at least about 40 days, at least about 50 days or at least about 60 days, at least about 70 days, at least about 80 days, at least about 90 days, at least about 100 days or longer.

A therapeutically effective amount of a drug may also include a “preventative” or “prophylactically effective amount,” which is any amount of the an immune checkpoint modulator and/or an IFNβ inhibitor administered to a subject at risk of developing a cancer (eg a subject having a pre–malignant condition) or of suffering a recurrence of cancer, that inhibits the development or recurrence of the cancer. In certain embodiments, the prophylactically effective amount prevents the development or recurrence of the cancer entirely. “Inhibiting” or “preventing” the development or recurrence of a cancer means either lessening the likelihood of the cancer's development or recurrence, or preventing the development or recurrence of the cancer entirely.

The exact amount of the therapeutically effective amount required will vary from subject to subject, depending on the species, age and general condition of the subject, mode of administration and the like. Thus, it may not be possible to specify an exact therapeutically effective amount. However, an appropriate therapeutically effective amount in any individual case may be determined by one of ordinary skill in the art using routine experimentation. In one aspect, the dose administered to a subject is any therapeutically effective amount that reduces symptoms associated with the cancer as a result of any one of a reduction in the number of cancer cells; a reduction in the tumour size; an inhibition (i.e., slow to some extent and preferably stop) of cancer cell infiltration into peripheral organs; an inhibition (i.e., slow to some extent and preferably stop) of tumour metastasis; an inhibition, to some extent, of tumour growth; or relieving, to some extent, of one or more of the symptoms associated with the cancer. Additionally or

alternatively, the therapeutically effective amount may lead to increased survival of the subject.

In some embodiments, a therapeutically effective amount of an IFNβ inhibitor for a human subject lies in the range of about 250 nmoles/kg body weight/dose to 0.005 nmoles/kg body weight/dose. Preferably, the range is about 250 nmoles/kg body weight/dose to 0.05 nmoles/kg body weight/dose. In some embodiments, the body weight/dose range is about 250 nmoles/kg, to 0.1 nmoles/kg, about 50 nmoles/kg to 0.1 nmoles/kg, about 5 nmoles/kg to 0.1 nmol/kg, about 2.5 nmoles/kg to 0.25 nmoles/kg, or about 0.5 nmoles/kg to 0.1 nmoles/kg body weight/dose. In some embodiments, the amount is at, or about, 250 nmoles, 50 nmoles, 5 nmoles, 2.5 nmoles, 0.5 nmoles, 0.25 nmoles, 0.1 nmoles or 0.05nmoles/kg body weight/dose of the compound. Dosage regimes are adjusted to suit the exigencies of the situation and may be adjusted to produce the optimum therapeutic dose.

Typically, a therapeutically effective dosage is formulated to contain a concentration (by weight) of at least about 0.1% up to about 50% or more, and all combinations and sub-combinations of ranges therein. The compositions can be formulated to contain one or more compounds, or a pharmaceutically acceptable salt, polymorph or prodrug thereof in a concentration of from about 0.1 to less than about 50%, for example, about 49, 48, 47, 46, 45, 44, 43, 42, 41 or 40%, with concentrations of from greater than about 0.1%, for example, about 0.2, 0.3, 0.4 or 0.5%, to less than about 40%, for example, about 39, 38, 37, 36, 35, 34, 33, 32, 31 or 30%. Exemplary compositions may contain from about 0.5% to less than about 30%, for example, about 29, 28, 27, 26, 25, 25, 24, 23, 22, 21 or 20%, with concentrations of from greater than about 0.5%, for example, about 0.6, 0.7, 0.8, 0.9 or 1%, to less than about 20%, for example, about 19, 18, 17, 16, 15, 14, 13, 12, 11 or 10%. The compositions can contain from greater than about 1% for example, about 2%, to less than about 10%, for example about 9 or 8%, including concentrations of greater than about 2%, for example, about 3 or 4%, to less than about 8%, for example, about 7 or 6%. The active agent can, for example, be present in a concentration of about 5%. In all cases, amounts may be adjusted to compensate for differences in amounts of active ingredients actually delivered to the treated cells or tissue.

For administration of a checkpoint inhibitor including PD-1, PD-L1 or CTLA-4 inhibitors, the dosage can range from about 0.01 to about 20mg/kg, about 0.1 to about 10 mg/kg, about 0.1 to about 5mg/kg, about 1 to about 5mg/kg, about 2 to about 5 mg/g, about 7.5 to about 12.5 mg/kg, or about 0.1 to about 30 mg/kg of the subject's body weight. For example, dosages can be about 0.1, about 0.3, about 1, about 2, about 3, about 5 or about 10 mg/kg body weight, or, about 0.3, about 1, about 2, about 3, or about 5 mg / kg body weight. The dosing schedule is typically designed to achieve exposures that result in sustained receptor occupancy (RO) based on typical pharmacokinetic properties of an Ab. An exemplary treatment regime entails administration about once per week, about once every 2 weeks, about once every 3 weeks, about once every 4 weeks, about once a month, about once every 3 - 6 months or longer. In certain embodiments, a immune checkpoint modulator is administered to the subject about once every 2 weeks. In other embodiments, the Ab is administered about once every 3 weeks. The dosage and scheduling can change during a course of treatment. For example, a dosing schedule for anti-PD-1 therapy can comprise administering the Ab:(i) about every 2 weeks in about 6-week cycles; (ii) about every 4 weeks for about six dosages, then about every three months; (iii) about every 3 weeks; (iv) about 3-about 10 mg/kg once followed by about 1 mg/kg every about 2-3 weeks. Considering that an IgG4 Ab typically has a half-life of 2-3 weeks, a dosage regimen for an anti-PD-1 Ab of the invention comprises about 0.3–1 about 0 mg/kg body weight, 1-5 mg/kg body weight, or about 1-about 3 mg/kg body weight via intravenous administration, with the Ab being given every about 14-21 days in up to about 6-week or about 12-week cycles until complete response or confirmed progressive disease.

In some embodiments, the immune checkpoint modulator and/or IFNβ inhibitor treatment disclosed herein, is continued for at least about 1 month, at least about 2 months, at least about 3 months, at least about 4 months, at least about 5 months, at least about 6 months, at least about 7 months, at least about 8 months, at least about 9 months, at least about 10 months, at least about 11 months, at least about 1 year, at least about 18 months, at least about 24 months, at least about 3 years, at least about 5 years, or at least about 10 years.

It will be understood, that the specific dose level for any particular patient will depend upon a variety of factors including the activity of the specific compound

employed, the age, body weight, general health, sex, diet, time of administration, route of administration, and rate of excretion, drug combination i.e. other drugs being used to treat the patient), and the severity of the particular disorder undergoing therapy.

The terms "treatment" or "treating" of a subject includes the application or administration of a compound of the invention to a subject with the purpose of delaying, slowing, stabilizing, curing, healing, alleviating, relieving, altering, remedying, less worsening, ameliorating, improving, or affecting the disease or condition, the symptom of the disease or condition, or the risk of (or susceptibility to) the disease or condition. The term "treating" refers to any indication of success in the treatment or amelioration of an injury, pathology or condition, including any objective or subjective parameter such as abatement; remission; lessening of the rate of worsening; lessening severity of the disease; stabilization, diminishing of symptoms or making the injury, pathology or condition more tolerable to the subject; slowing in the rate of degeneration or decline; making the final point of degeneration less debilitating; or improving a subject's physical or mental well-being.

As used herein, minimising or preventing the progression of cancer means treating the subject so as to prevent or delay the recurrence or metastasis of a tumour, or to prevent growth of an existing tumour. Minimising or preventing the progression of cancer includes preventing or delaying the recurrence of cancer, or preventing growth of an existing tumour, following treatment of cancer. The recurrence that is being prevented includes a recurrence for example, in the tumour bed, following surgical excision. Alternatively, recurrence includes metastasis of the cancer in another part of the body. The terms “preventing recurrence” and “preventing relapse” as used herein, are interchangeable.

The present invention also includes methods of preventing the development of cancer in an individual. For example, the individual for whom prevention of cancer is required may be considered to be at risk of developing cancer, but does not yet have detectable cancer. An individual at risk of the development of cancer may be an individual with a family history of cancer, and/or an individual for whom genetic testing or other testing indicates a high risk or high likelihood of the development of cancer. The individual may have cancer stem cells but does not yet have any detectable tumours. It

will be understood that methods of preventing the development of cancer include methods of delaying the onset of cancer in a subject.

The terms “subject” and “patient” will be understood to be interchangeable. Although the invention finds application in humans, the invention is also useful for therapeutic veterinary purposes. The invention is useful for domestic or farm animals such as cattle, sheep, horses and poultry; for companion animals such as cats and dogs; and for zoo animals.

Cancer

The term “cancer” will be understood to include benign, pre-cancerous, pre-neoplastic or non-metastatic tumours or metastatic tumours.

In some embodiments, the type of cancer to be treated includes those having a benign, pre-cancerous, pre-neoplastic or non-metastatic tumour. A benign tumour will be understood to not be a malignant tumour and to not invade nearby tissue or spread to other parts of the body. Similarly non-metastatic cancer will be understood to not invade nearby tissue or spread to other parts of the body. “Pre-cancerous" or “pre–neoplasia” generally refers to a condition or a growth that typically precedes or develops into a cancer. A "pre-cancerous" growth may have cells that are characterized by abnormal cell cycle regulation, proliferation, or differentiation, which can be determined by markers of cell cycle.

In one embodiment, the cancer is a secondary cancer or metastases. The secondary cancer may be located in any organ or tissue, and particularly those organs or tissues having relatively higher hemodynamic pressures, such as lung, liver, kidney, pancreas, bowel and brain. The secondary cancer may be detected in the ascites fluid and/or lymph nodes.

Pre-neoplastic, neoplastic and metastatic cancers are particular examples to which the methods of the invention may be applied. Broad examples include breast tumours, colorectal tumours, adenocarcinomas, mesothelioma, bladder tumours, prostate tumours, germ cell tumour, hepatoma/cholongio, carcinoma, neuroendocrine tumours, pituitary neoplasm, small round cell tumour, squamous cell cancer, melanoma, atypical fibroxanthoma, seminomas, nonseminomas, stromal leydig cell tumours, Sertoli

cell tumours, skin tumours, kidney tumours, testicular tumours, brain tumours, ovarian tumours, stomach tumours, oral tumours, bladder tumours, bone tumours, cervical tumours, esophageal tumours, laryngeal tumours, liver tumours, lung tumours, vaginal tumours, Wilm's tumours, pancreatic tumours, sarcomas, lymphomas or leukaemias.

Examples of particular cancers include but are not limited to adenocarcinoma, adenoma, adenofibroma, adenolymphoma, adontoma, AIDS related cancers, acoustic neuroma, acute lymphocytic leukemia, acute myeloid leukemia, adenocystic carcinoma, adrenocortical cancer, agnogenic myeloid metaplasia, alopecia, alveolar soft-part sarcoma, ameloblastoma, angiokeratoma, angiolymphoid hyperplasia with eosinophilia, angioma sclerosing, angiomatosis, apudoma, anal cancer, angiosarcoma, aplastic anaemia, astrocytoma, ataxia-telangiectasia, basal cell carcinoma (skin), bladder cancer, bone cancers, bowel cancer, brain stem glioma, brain and CNS tumours, breast cancer, branchioma, CNS tumours, carcinoid tumours, cervical cancer, childhood brain tumours, childhood cancer, childhood leukemia, childhood soft tissue sarcoma, chondrosarcoma, choriocarcinoma, chronic lymphocytic leukemia, chronic myeloid leukemia, colorectal cancers, cutaneous T-cell lymphoma, carcinoma (e.g. Walker, basal cell, basosquamous, Brown-Pearce, ductal, Ehrlich tumour, Krebs 2, Merkel cell, mucinous, non-small cell lung, oat cell, papillary, scirrhous, bronchiolar, bronchogenic, squamous cell, and transitional cell), carcinosarcoma, cervical dysplasia, cystosarcoma phyllodies, cementoma, chordoma, choristoma, chondrosarcoma, chondroblastoma, craniopharyngioma, cholangioma, cholesteatoma, cylindroma, cystadenocarcinoma, cystadenoma, dermatofibrosarcoma- protuberans, desmoplastic-small-round-cell-tumour, ductal carcinoma, dysgerminoam, endocrine cancers, endometrial cancer, ependymoma, esophageal cancer, Ewing's sarcoma, extra-hepatic bile duct cancer, eye cancer, eye: melanoma, retinoblastoma, fallopian tube cancer, fanconi anaemia, fibroma, fibrosarcoma, gall bladder cancer, gastric cancer, gastrointestinal cancers, gastrointestinal-carcinoid-tumour, genitourinary cancers, germ cell tumours, gestationaltrophoblastic-disease, glioma, gynaecological cancers, giant cell tumours, ganglioneuroma, glioma, glomangioma, granulosa cell tumour, gynandroblastoma, haematological malignancies, hairy cell leukemia, head and neck cancer, hepatocellular cancer, hereditary breast cancer, histiocytosis, Hodgkin's disease, human papillomavirus, hydatidiform mole, hypercalcemia, hypopharynx cancer, hamartoma, hemangioendothelioma, hemangioma, hemangiopericytoma, hemangiosarcoma,

hemangiosarcoma, histiocytic disorders, histiocytosis malignant, histiocytoma, hepatoma, hidradenoma, hondrosarcoma, immunoproliferative small, opoma, ontraocular melanoma, islet cell cancer, Kaposi's sarcoma, kidney cancer, langerhan's cell-histiocytosis, laryngeal cancer, leiomyosarcoma, leukemia, li-fraumeni syndrome, lip cancer, liposarcoma, liver cancer, lung cancer, lymphedema, lymphoma, Hodgkin's lymphoma, non-Hodgkin's lymphoma, leigomyosarcoma, leukemia (e.g. B-cell, mixed cell, null-cell, T-cell, T-cell chronic, HTLV-IIassociated, lymphangiosarcoma, lymphocytic acute, lymphocytic chronic, mast-cell and myeloid), leukosarcoma, leydig cell tumour, liposarcoma, leiomyoma, leiomyosarcoma, lymphangioma, lymphangiocytoma, lymphagioma, lymphagiomyoma, lymphangiosarcoma, male breast cancer, malignant- rhabdoid-tumour-of-kidney, medulloblastoma, melanoma, Merkel cell cancer, mesothelioma, metastatic cancer, mouth cancer, multiple endocrine neoplasia, mycosis fungoides, myelodysplastic syndromes, myeloma, myeloproliferative disorders, malignant carcinoid syndrome carcinoid heart disease, medulloblastoma, meningioma, melanoma, mesenchymoma, mesonephroma, mesothelioma, myoblastoma, myoma, myosarcoma, myxoma, myxosarcoma, nasal cancer, nasopharyngeal cancer, nephroblastoma, neuroblastoma, neurofibromatosis, Nijmegen breakage syndrome, non-melanoma skin cancer, non-small-cell-lung-cancer-(nsclc), neurilemmoma, neuroblastoma, neuroepithelioma, neurofibromatosis, neurofibroma, neuroma, neoplasms (e.g. bone, breast, digestive system, colorectal, liver), ocular cancers, oesophageal cancer, oral cavity cancer, oropharynx cancer, osteosarcoma, ostomy ovarian cancer, pancreas cancer, paranasal cancer, parathyroid cancer, parotid gland cancer, penile cancer, peripheral- neuroectodermal-tumours, pituitary cancer, polycythemia vera, prostate cancer, osteoma, osteosarcoma, ovarian carcinoma, papilloma, paraganglioma, paraganglioma nonchromaffin, pinealoma, plasmacytoma, protooncogene, rare-cancers-and-associated- disorders, renal cell carcinoma, retinoblastoma, rhabdomyosarcoma, Rothmund-Thomson syndrome, reticuloendotheliosis, rhabdomyoma, salivary gland cancer, sarcoma, schwannoma, Sezary syndrome, skin cancer, small cell lung cancer (sclc), small intestine cancer, soft tissue sarcoma, spinal cord tumours, squamous-cell-carcinoma-(skin), stomach cancer, synovial sarcoma, sarcoma (e.g. Ewing's experimental, Kaposi's and mast-cell sarcomas), Sertoli cell tumour, synovioma, testicular cancer, thymus cancer, thyroid cancer, transitional-cell-cancer-(bladder), transitional-cell-cancer-(renal-pelvis-/-ureter), trophoblastic cancer, teratoma, theca cell tumour, thymoma, trophoblastic tumour,

urethral cancer, urinary system cancer, uroplakins, uterine sarcoma, uterus cancer, vaginal cancer, vulva cancer, Waldenstrom' s-macroglobulinemia and Wilms' tumour.

The existence of, improvement in, treatment of, or minimisation of progression of cancer may be determined by any clinically or biochemically relevant method as described herein or known in the art. A positive response to treatment or a minimisation of progression of a cancer may be determined by any method known in the art and may include the determination of:

- a reduction in the number of cancer cells;
- a reduction in the tumour size;
- an inhibition (i.e., slow to some extent and preferably stop) of cancer cell infiltration into peripheral organs;
- an inhibition (i.e., slow to some extent and preferably stop) of tumour metastasis;
- a reduction or complete prevention of tumour metastasis following removal of the primary tumour;
- an inhibition, to some extent, of tumour growth;
- relieving, to some extent, of one or more of the symptoms associated with the cancer; and/or
- increased survival of the subject.

The determination of any of the above may be considered to be a positive response to an immune checkpoint modulator and/or a IFNβ inhibitor described herein.

In an embodiment of the invention, the subject may have previously received treatment. In an embodiment the previous treatment is an immune checkpoint modulator which may be in the form of an inhibitor of PD-1, PD-L1 or CTLA-4. In a preferred embodiment, the checkpoint modulator is in the form of an antibody.

The subject who has received the treatment for cancer may be in partial or complete remission. In other words, the subject, having received a treatment for cancer,

as described above, may have a 10%, 20%, 30%, 40%, 50%, 60%, 70%, 80%, 90% or greater reduction in the measurable parameters of tumour growth as may be found on physical examination, radiologic study, or by biomarker levels from a blood or urine test. Alternatively, where the subject is in complete remission, there is a complete disappearance of all detectable manifestations of disease, such that the subject does not have any detectable signs of cancer. The subject may have substantially undetectable signs of cancer. A cancer that is "substantially undetectable" generally refers to a circumstance where therapy has depleted the size, volume or other physical measure of a cancer so that using relevant standard detection techniques such as *in vivo* imaging, the cancer, as a consequence of the therapy, is not clearly detectable.

The objective or outcome of treatment with an immune checkpoint modulator and/or IFNβ inhibitor may be to reduce the number of cancer cells; reduce the primary tumour size; inhibit (i.e., slow to some extent and preferably stop) cancer cell infiltration into peripheral organs; inhibit (i.e., slow to some extent and preferably stop) tumour metastasis; inhibit, to some extent, tumour growth; and/or relieve to some extent one or more of the symptoms associated with the disorder.

Efficacy of treatment can be measured by assessing the duration of survival, time to disease progression, the response rates (RR), duration of response, and/or quality of life.

In one embodiment, the method is particularly useful for delaying cancer progression. In one embodiment, the method is particularly useful for extending survival of the subject, including overall survival as well as progression free survival. It will be understood that overall survival is the length of time from either the date of diagnosis or the start of treatment of a cancer, that patients diagnosed with the cancer are still alive. It will be understood that progression free survival is the length of time during and after the treatment of a cancer that a patient lives with the disease but it does not get worse.

Survival analysis can be performed using well known techniques in the art including the Kaplan-Meier method. The Kaplan-Meier method estimates the survival function from life-time data. In medical research, it can be used to measure the fraction of patients living for a certain amount of time after treatment. A plot of the Kaplan-Meier method of the survival function is a series of horizontal steps of declining magnitude

which, when a large enough sample is taken, approaches the true survival function for that population. The value of the survival function between successive distinct sampled observations ("clicks") is assumed to be constant.

An important advantage of the Kaplan-Meier curve is that the method can take into account "censored" data- losses from the sample before the final outcome is observed (for instance, if a patient withdraws from a study). On the plot, small vertical tick-marks indicate losses, where patient data has been censored. When no truncation or censoring occurs, the Kaplan-Meier curve is equivalent to the empirical distribution.

In one embodiment, the method is particularly useful for providing a complete response to therapy whereby all signs of cancer in response to treatment have disappeared. This does not always mean the cancer has been cured. In one embodiment, the method is particularly useful for providing a partial response to therapy whereby there has been a decrease in the size of one or more tumours or lesions, or in the extent of cancer in the body, in response to treatment.

Kits

In another embodiment there is provided a kit or article of manufacture comprising an immune checkpoint modulator and/or an IFNβ inhibitor as described herein, a pharmaceutically acceptable salt, diluent or excipient and/or pharmaceutical composition as described above. Further, the kit may comprise instructions for use in any method or use of the invention as described herein.

In other embodiments there is provided a kit for use in a therapeutic and/or prophylactic application mentioned above, the kit comprising:

- a container holding a therapeutic composition in the form of an immune checkpoint modulator and/or an IFNβ inhibitor as described herein, and/or a pharmaceutically acceptable salt, diluent or excipient or pharmaceutical composition;

- a label or package insert with instructions for use in any method or use of the invention as described herein..

In certain embodiments the kit may contain one or more further active principles or ingredients for treatment of cancer.

The kit or "article of manufacture" may comprise a container and a label or package insert on or associated with the container. Suitable containers include, for example, bottles, vials, syringes, blister pack, etc. The containers may be formed from a variety of materials such as glass or plastic. The container holds a therapeutic composition which is effective for treating the condition and may have a sterile access port (for example the container may be an intravenous solution bag or a vial having a stopper pierceable by a hypodermic injection needle). The label or package insert indicates that the therapeutic composition is used for treating the condition of choice. In one embodiment, the label or package insert includes instructions for use and indicates that the therapeutic or prophylactic composition can be used to treat a cancer described herein.

The kit may comprise (a) a therapeutic or prophylactic composition; and (b) a second container with a second active principle or ingredient contained therein. The kit in this embodiment of the invention may further comprise a package insert indicating the composition and other active principle can be used to treat a cancer or prevent progression of a cancer described herein.

Examples

Despite the extensive use of antibodies that block immune checkpoints in cancer, many patients do not respond. The biological determinants of response remain incompletely understood, which limits the development of novel effective treatment combinations. In particular, little is known about dynamic biological events that underpin the therapeutic response. Here, the transcriptional events in responding and non-responding tumours were mapped in two independent mouse models at four time points during treatment with antibodies against multiple immune checkpoints (i.e. CTLA4 and PD-L1). Responding tumours displayed fast-off kinetics of type I interferon (IFN) signalling, while in non-responding tumours activation of type I IFN signalling was delayed with diminished intensity. The cells producing this type I IFN were tumour-infiltrating Ly6c^{hi} inflammatory monocytes that were more abundant in responders at the start of treatment, but swiftly differentiated towards a Ly6c^{lo} phenotype. Phenocopying of this fast-off kinetics using time-dependent sequential dosing of IFN agonists and neutralizing antibodies markedly improved efficacy, but only when IFNβ or its receptor IFNAR1 were blocked, not IFNα. Together, the results suggest that fast-off dynamics of

IFNβ signalling underlie the therapeutic response to immune checkpoint therapy in cancer.

Example 1 – Materials and methods

Mice

BALB/cArc, Balb/cAusB, C57BL6/J or Ifnb1^{tm1Lky}/J mice 8-12 weeks of age were used for all experiments. BALB/cArc or C57BL6/J mice were obtained from the Animal Resource Centre (Murdoch, WA), Balb/cAusB mice were obtained from the Harry Perkins Institute for Medical Research Bioresources Centre South (Murdoch, WA). Ifnb1tm1Lky/J mice, generated by knock-in of a yellow fluorescent protein (YFP) reporter cas-sette into the endogenous Ifnb locus (Scheu, Dresing and Locksley, *Proc Natl Acad Sci USA,* 105(51), 20416-20421 (2008)), were imported from The Jackson Laboratory (Bar Harbour, Maine) and maintained at the Harry Perkins Institute for Medical Research Bioresources Centre South (Murdoch, WA). All mice were housed at the Harry Perkins Institute of Medical Research Bioresources Facility North under specific pathogen free conditions. Mice were fed Rat and Mouse cubes (Specialty Feeds, Glen Forrest, Australia) and had access to water ad libitum. Cages (Techniplast, Italy) were individually ventilated with filtered air, contained aspen chips bedding (Tapvei, Estonia) and were supplemented with tissues, cardboard rolls and wood blocks as environmental enrichment, and were changed every 14 days. Mice were housed at 21-22°C with 12-hour light/dark cycle (06:00 – 18:00). Sentinel mice (n = 3) in the animal facility were screened monthly for a standard panel of bacteria and fungi, ectoparasites, endoparasites, non-pathogenic protozoa and viruses (Cerberus Sciences, Australia). All experiments were conducted in compliance with the institutional guidelines provided by the Harry Perkins Institute for Medical Research animal ethics committee (approval numbers AE047, AE091, AE157, AE201).

Cell culture

Cell lines AB1 and AE17 were obtained from CellBank Australia. Cell line Renca was kindly donated by Dr E. Sotomayor and Dr F. Cheng (University of South Florida, Tampa, FL). Cell lines were maintained in RPMI 1640 (Invitrogen, Mulgrave, Australia) supplemented with 20 mM HEPES, 0.05 mM 2-mercaptoethanol, 100 units/ml penicillin/streptomycin (Thermo Fisher), and 10% FCS (Invitrogen). Cells were grown to

70-80% before passage and passaged 3-5 times before inoculation. Cells were frequently tested for mycoplasma by PCR and remained negative. Cell lines were validated yearly by flow cytometry for MHC class I molecules H2-K^b (consistent with C57BL/6) and H2-K^d (consistent with BALB/c), and for fibroblast markers E-cad, EpCam and PDGFRα (negative) and by PCR for mesothelin (positive for AB1, negative for Renca).

In vivo treatments

When cell lines were 70-80% confluent, they were harvested and washed 3 times in PBS. 5 x 10^5 cells in 100 µl were inoculated subcutaneously (s.c.) onto the lower right-hand side (RHS) flank (for single inoculations) or both flanks (for dual tumour inoculations) using a single 26G needle per injection. Mice were randomized when tumours became palpable, approximately 3-5 days after tumour inoculation.

Surgery experiments

A detailed protocol for the surgery experiments has been previously described in Zemek, R. M. *et al. Nat Protoc*, doi:10.1038/s41596-020-0299-3 (2020). For the pre-treatment samples, tumours were resected eight (AB1) or 10 (Renca) days post tumour inoculation, when tumours were ~ 9 mm^2, and mice were administered ICB 1 hour after surgery. For the post-treatment samples, tumours were resected 2, 4 or 6 days after administration of ICB. Mice were dosed with 0.1 mg/kg buprenorphine in 100 µl s.c. (30 min prior) and anesthetized using isoflurane (4% in 100% oxygen at a flow rate of 2 L/min). Whole tumours and the corresponding draining inguinal lymph node on the RHS were removed by surgical excision and immediately immersed in RNAlater (Life Technologies, Australia). The wound was closed with staples (Able Scientific, Australia). Mice were placed in a heat box for recovery. The remaining tumour was monitored for response as an indicator of response for the removed tumour. Mice were designated as responders when their tumour completely regressed and they remained tumour free for up to 4 weeks after treatment. Mice were designated as non-responders if their tumours grew to 100 mm^2 within 4 weeks after start of treatment, similar to saline-treated controls. Mice that had a delay in tumour growth or partial regression were designated as intermediate responders and excluded from the analysis. For internal consistency, the inventors only used experiments in which mice displayed a dichotomous response,

i.e. in any cage there had to be at least one non-responder amongst responders or vice versa.

In vivo ICB treatment

The anti-PD-L1 hybridoma (clone MIH5) and the anti-CLTA4 hybridoma (clone 9H10) were cultured in IMDM containing 1% of FCS and gentamycin at Bioceros (Utrecht, The Netherlands). Clarified supernatants were used to purify the antibody using affinity chromatography. The antibodies were sterile formulated in PBS. Alternatively, antibodies from the same clones were obtained from BioXcell (New Hampshire, US). Mice received an intraperitoneal (i.p.) dose of 100 µg of anti-CTLA4 and 100 µg anti-PDL1 combined in 100 µl phosphate-buffered solution (PBS). Mice received additional doses of 100 µg anti-PDL1 two and four days later. The inventors had not found any difference in effect of control IgG versus PBS, and therefore vehicle controls received PBS alone.

Tumour preparation for RNA sequencing

Whole tumours and lymph nodes were surgically resected, the surrounding tissue was removed and immediately submerged in RNAlater (Life Technologies, Australia). Samples were stored at 4°C for 24 hours, after which supernatant was removed and samples transferred to -80°C. Frozen tumours were dissociated in Trizol (Life Technologies, Australia) using a TissueRuptor (QIAgen, Australia). RNA was extracted using chloroform and purified on RNeasy MinElute columns (QIAgen, Australia). RNA integrity was confirmed on the Bioanalyzer (Agilent Technologies, USA). Library preparation and sequencing (50 bp, single-end) was performed by Australian Genome Research Facility, using Illumina HiSeq standard protocols.

Alignment and differential expression.

The inventors processed 72 RNA-seq single-end read samples across four time points for each of our mouse models. There were an equal number of responder and non-responder samples, with 12 samples for Day 0 and 8 samples for each of the other time points (Day 2, Day 4 and Day 6). After reviewing quality control on all samples using FastQC software, the inventors used Kallisto (Bray, et al. *Nat Biotechnol* 34, 525-527, (2016); (v0.43.0)) for transcript abundance estimation. The transcript index was

created with Gencode M22 (GRCm38.p6) and each RNA-seq sample was aligned with parameters '--single', '-l 200' '-s 20', '-t 8' and '-bootstraps = 100'. Following alignment, the inventors performed differential expression analysis with Sleuth (v0.29.0) (Pimentel, H., et al. *Nat Methods* 14, 687-690, (2017)). The inventors compared responders and non-responders using a model containing time-point and response as covariates. The inventors aggregated p-values from transcript differential expression to gene-level results using Lancaster's method (Yi, et al, *Genome Biol* 19, 53, (2018)). Genes were deemed differentially expressed at a false-discovery rate of less than 5%. RNA-Seq data for this analysis are available in the Gene Expression Omnibus under accession number [GEO: GSE117358].

TCseq analysis of dynamic gene expression data

The inventors clustered time course RNAseq data using the fuzzy c-means (FCM) clustering algorithm Mfuzz (Futschik and Carlisle, *J Bioinform Comput Biol,* 3(4), 965-988 (2005)) in the TCseq package (Wu and Gu, TCseq: Time course sequencing data analysis (2020)), Z-normalised/scaled counts were used in the algorithm and expression profiles were grouped clusters (k = 6) based on their dynamic patterns. The inventors used a Pearson correlation score on trend lines to compare trends of each cluster between responders and non-responders, to identify which patterns were unique to responders. Each matching cluster between the two models had overlapping genes extracted and enrichment of per-cluster genes was performed using Enrichr (Kuleshov et al., *Nucleic Acids Res,* 8(44), W90-97 (2016)).

GENIE3 network construction.

The inventors constructed two networks, one for Renca responders and one for AB1 responders. The inventors used the GENIE3 algorithm (Huynh-Thu ,et al. *PLoS One* 5, (2010)), which achieved the best performance on the DREAM5 network inference challenge. To construct each gene regulatory network, the inventors used 36 responder samples across all time points as input to the GENIE3 algorithm. Since GENIE3 requires gene counts as input, the inventors summarised transcript abundances derived from Kallisto as gene counts using the Bioconductor tximport (Soneson, et al. *F1000Res* 4, 1521, (2015)) package. The inventors ran GENIE3 (v1.8.0) with default parameters (treeMethod ="RF", k = "sqrt", nTrees = 1000).

Next, the inventors filtered the network produced by GENIE3 to keep direct interactions between transcription factors and differentially expressed genes. For this, the inventors retained edges where the transcription factor binding site (TFBS) was located in a genomic window 400 base pairs upstream and 300 base pairs downstream of a gene's transcription start site (TSS). The inventors used the JASPAR database to obtain genome wide TFBS predictions and only retained those with a confidence score above 500 (corresponding to p-value of <0.05). The inventors also used the UCSC genome browser[35] to programmatically obtain a bedfile of TSS sites for differentially expressed genes based on our Sleuth analysis. Subsequently, the inventors used the BEDtools (Quinlan, et al. *Bioinformatics* 26, 841-842, (2010)) "window" function on these two bedfiles, with parameters "-l 400 -r 300 –sw" to obtain all direct regulatory interactions. To these direct interactions, the inventors appended their corresponding GENIE3 importance scores using the R data.table package (v1.12.2).

Network visualisation.

For visualisation, the inventors used the R igraph package (v1.2.4.2) (Csardi, et al. *InterJournal Complex Systems* 1695 (2006)). To denote confident regulatory interactions in the network, the inventors derived a numerical threshold from the KDE plots of the union set of all GENIE3 scores from AB1 and Renca responder networks using the elbow method. For each network, the inventors calculated network statistics to obtain the top 10 genes with the highest number of outgoing edges. For visualisation, the inventors used a force-directed layout and extracted a subnetwork comprising these top 10 genes with all of their first-degree outgoing neighbours. The inventors assigned colour to genes in the network by their average gene expression across time, normalised by Z-score.

Functional annotation.

In both networks, the inventors extracted dynamically changing genes between day 0 to day 2 for functional annotation. Specifically, the inventors extracted a gene list comprising the transcription factor and its surrounding first-order neighbours. The inventors used these genes as input to Enrichr's web interface (Kuleshov, et al. *Nucleic Acids Res* 44, W90-97, (2016)) to obtain GO Biological Process annotations and annotations from the LINCS1000 ligand perturbation database. The top 5 terms in both

databases, ranked by $-\log_{10}$ (p-value) were visualised using the ggplot2 R package (v3.2.1) (Wickham, H. et al. ggplot2: Elegant Graphics for Data Analysis. (Springer-Verlag, 2016)).

Analysis of IFN-stimulated genes.

The inventors obtained a list of known IFN-stimulated genes (ISGs) from the Broad Institute's MSigDB database (Liberzon, A. *et al.* The Molecular Signatures Database (MSigDB) hallmark gene set collection. *Cell Syst* 1, 417-425, (2015)). The inventors used two gene sets in the hallmark gene set collection for Type I and Type II interferon. Using BiomaRt (Smedley, D. *et al. Nucleic Acids Res* 43, (2015)), the inventors converted HGNC symbols in these gene sets to their murine (mm10) equivalents. After conversion, the inventors retained 88/97 genes from the alpha dataset and 186/200 genes from the gamma dataset. From each direct regulatory network, the inventors extracted the edge-weights of all edges containing these ISGs as the target gene. The inventors selected the top 10 TFs common to both Renca and AB1 mouse models by ranking TFs according to the sum of their edge-weights across ISGs. The inventors visualized these important TF to ISG interactions in an edge-weight matrix using the ComplexHeatmap (Gu, Z., et al. *Bioinformatics* **32**, 2847-2849 (2016)) package (v2.2.0). The edge-weight matrices were irregular (different number of elements in each row) since each ISG TSS could be surrounded by a variety of different TF binding sites, so any non-existent interactions in the matrix were set to zero prior to visualization.

Hive plot generation.

Hive plots provide an alternative approach to visualise network topology eliminating visualisation bias due to network layout. The inventors used the HiveR package (Hanson, B. A. *GitHub repository* (2017). (v0.3.42) on filtered AB1 and Renca networks to plot all direct TF to DE gene interactions, assigning genes to axes depending on (1) whether a gene was a TF, ISG or non-ISG target and (2) the importance of the TF based on sum of overall scores

Single cell sample pre-processing.

The inventors processed a total of 16 single cell samples using the cellranger3 software from 10X genomics (parameter expect-cells = 6000). For our experiments using dual checkpoint blockade, 6 of these samples were of AB1 tumours and 6 were from Renca tumours. For each model, 3 tumours were harvested from responders and 3 from non-responders, both groups from timepoint 0. The filtered matrices from cellranger output were used for downstream analysis.

Clustering, visualisation and cell annotation.

The Seurat R package (v3.0.3) was used for clustering and visualisation. Gene counts were normalised against library size and mitochondrial content. Cells were subsequently clustered using Seurat's graph-based clustering algorithm at default cluster resolution (Louvain – 0.8). To automatically label cells, the inventors used SingleR (v1.0.5) on Seurat clusters, assigning cluster identity based on top-level annotations using the mouse RNAseq reference. Subsequently, the inventors merged clusters with the same annotations for downstream analysis.

Inferring tumour cells.

Tumour clusters were inferred in a 2-stage process. First, candidate tumour clusters were identified using Seurat's label transfer functions (FindIntergrationAnchors, IntegrateData) using projection from a reference dataset. Subsequently, candidate tumour clusters were used as input to inferCNV package (Tickle, et al. *GitHub repository* (2019)), using copy number amplification as a confirmatory step. Only those clusters labelled as tumour clusters via projection which were also found to contain CNVs amplification were identified as tumour cells. For Renca cells, the inventors used transferred labels from a single cell mouse kidney dataset (Park, J. *et al. Science* 360, 758-763, (2018)) since renal cancer cells are known to recapitulate features from the normal mouse renal tubular system. For AB1, the inventors used a reference where mesothelioma tumour cells were tagged with viral hemagglutinin.

SCENIC network analysis.

Normalised count matrices from Seurat (Satija, et al. *Nat Biotechnol* 33, 495-502, (2015)). were used as input to the python SCENIC package (Aibar, S. *et al. Nat Methods* 14, 1083-1086, (2017)) to construct a single cell gene regulatory network using 38K cells across all 6 AB1 samples. Regulon (TF and downstream target genes) was computed using AUCell, with the *binarize* function to calculate on/fast-off activation status of a transcription factor within each cell. To compare TF activation on a per cluster basis between responders and non-responders, the inventors calculated the percentage of cells showing TF activation in each cluster, faceted by response. To visualise these results, the inventors created a heatmap showing the difference in percentage of TF activation per cluster for the IRF related TF (Irf1, Stat1, Stat2, Irf7 and Irf9).

Pseudotime and RNA velocity analysis.

Loom files quantifying spliced vs unspliced transcripts were first generated on a per-sample basis. These separate loomfiles were then merged using Loompy (v3.0.0). For downstream analysis, the velocyto.py package (v0.17.16) package was used on these merged loomfiles (La Manno, G. *et al. Nature* 560, 494-498 (2018)). After normalisation and feature selection and the gamma-fit and velocity calculations. The resulting velocity predictions were projected onto Seurat's UMAP embedding for visualisation.

SCDE/pagoda analysis.

Gene counts were analysed using the scde package (Butler, et al. *Nat Biotechnol* 36, 411-420, (2018)). Error models for individual cells were fitted using the knn.error.models function with cell labels supplied from singleR analysis (Aran, D. *et al. Nat Immunol* 20, 163-172, (2019)). Variance normalisation was performed with pagoda.varnorm with parameters trim = 4/ncol(cd) and max.adj.var = 5. GO analysis was performed using gene sets defined in org.Mm.eg.db using the pagoda.pathway.wPCA function. For type I interferon production the inventors used GO:0032606, and for interferon gamma production used GO:0032609. For the fast IFN stimulated genes, the same analysis with GO terms was performed with a custom R environment constructed with the gene list derived from bulk RNA seq analysis.

Cytokine stimulation estimation.

The CIBERSORT algorithm (Newman, A. M. *et al. Nat Methods* 12, 453-457, (2015)) was used to estimate the relative proportions of 7 cytokine induced T cell signatures based on the transcriptomic profiles of each sample, where the induced T cell gene signature developed by Cano-Gamez *et al. Nat Commun* 11, 1801, (2020)). was used as a reference. The inventors broadly classified the 94 samples into 7 major populations by collapsing several related sub-populations by their cytokine treatment: IFNB, Resting, Th17, Th2, Th1, Th0, iTreg to generate the reference file. Prior to analysis, gene count data for both AB1 and Renca was normalized to TPM. The data was filtered to retain genes with an TPM value > 0.3 in at least 8 samples (being the smallest experimental group size). CIBERSORT was run on AB1 and Renca separately, with quantile normalisation disabled as recommended for RNAseq data.

IFN modulation drug dosing schedules

As the inventors aimed to boost the IFN response using poly(I:C) in the tumour microenvironment prior to administration of ICB to improve response, the timing of administration of ICB antibodies was scheduled late, as to have a low background response rate to ICB. Dosing with drugs commenced on day 15 (for AE17, or day 12 for AB1 and Renca). Poly(I:C) (HMW, Invivogen) was dosed intratumourally at 50 μg daily for 3 days. ICB dosing began 2 days after the final dose of poly(I:C), on day 20. Anti-IFNAR1 (Bioxcell, clone MAR1-5A3, 0.5 mg i.p.), anti-IFNγ (Bioxcell, clone XMG1.2, 0.5 mg i.p.), anti-IFNα (Leinco, clone TIF-3C5, 1mg i.p.), anti-IFNβ (Leinco, clone HDß-4A7, 0.6 mg i.p.), or IgG2a isotype (Leinco, clone C1.18.4, 0.6 mg i.p.). Treatment began 2 days after the first day of ICB administration, on day 23, and dosed every 3rd day until the tumour reached 100 m^2 or regressed. For treatment schedules without poly(I:C), treatment with ICB commenced on day 12, followed by anti-IFN treatment 2 days after. Treatments were administered by one investigator (RMZ), while tumours were measured at least 3 times weekly using calipers by another researcher (TC) who was blinded for treatment allocation, to guarantee blinded assessment of the primary endpoint.

Flow cytometry of Irf1+ cells

For flow cytometric analysis of Irf1 gene expression in different cell subsets, AB1 tumours (n= 6) were harvested 6 days after inoculation and immediately submerged in cold PBS, cut into 1-2 mm pieces with a scalpel blade and dissociated using the GentleMACS system (Miltenyi). Fc block (anti-CD16/CD32, BD) was used for 10 minutes on ice. Cell were stained with Fixable Viability Stain 780 (BD) for 30 minutes at RT, to discriminate live cells. Cells were stained using antibodies for surface markers for 30 minutes at 4°C (Table 1). To identify Irf1+ cells, the inventors used the PrimeFlow Kit (Invitrogen). Briefly, cells were fixed in RNA fixation buffer 1, permeabilised with RNA Permeabilization buffer with RNase inhibitors, then fixed with RNA fixation buffer 2 before using Target Probes against Irf1. The signal was then amplified, followed by addition of fluorescent label probes (Alexa Fluor 647). Data were acquired on a BD Fortessa flow cytometer and analysed using FlowJo software (TreeStar). Cells were gated on Irf1+, followed by CD45+ to identify immune infiltrating cells, and CD45- non-immune cells (e.g. tumour cells). Immune cell populations were analysed by their expression of CD11b and Ly6C: Ly6C- Monocytes (CD11b+, Ly6C-); Ly6C+ Monocytes (CD11b+, Ly6C+, also F4/80-, CD3-, CD335-); Other Ly6C+ cells (CD11b+/-, Ly6C+); and remaining cells (CD11b-, Ly6C-).

Flow cytometry of YFP+ cells

For flow cytometric analysis to determine which cells express IFNB, the inventors used B6.129-Ifnb1tm1Lky/J mice, which co-express IFNβ1 and eYFP from the Ifnb1 locus (Scheu, Dresing and Locksley, *Proc Natl Acad Sci USA,* 105(51), 20416-20421 (2008)). AE17 tumours (n=3) were treated with poly(I:C) i.t. 21 days after inoculation, and harvested 24h later. Tumors were cut into 1-2 mm pieces with a scalpel blade and dissociated using the GentleMACS system (Miltenyi). Fc block (anti-CD16/CD32, BD) was used for 10 minutes on ice. Cells were stained with Fixable Viability Stain 780 (BD) for 30 minutes at RT, to discriminate live cells. Cells were stained using antibodies for surface markers for 30 minutes at 4°C (Table 1). To detect YFP+ cells, cells were fixed using a cytofix/cytoperm kit (BD), then stained using antibodies against GFP (YFP cross-reactive) in perm buffer overnight. Data were acquired on a BD Fortessa flow cytometer and analyzed using FlowJo software (TreeStar). Cells were gated for single and live cells. Cells were then gated on YFP+, which were also CD45+ indicating they

are immune infiltrating cells. Immune cell populations were analyzed by their expression of CD11b and Ly6c. YFP+ CD11b+ immune cells were MHC-II-, CD11c-, Ly6G-, CD19-, CD3- and NK1.1-.

Table 1:

Antibody	Fluorophore	Clone	Vendor
CD45	BUV395	30-F11	BD
CD3	BUV737	17A2	BD
Ly-6C	BV421	AL-21	BD
CD335 (NKp46)	BV786	29A1.4	BD
F4/80	BB700 or APC	T45-2342	BD
CD11b	PE-Cy7	M1/70	BD
Fixable Viability Stain 780			BD
Type 1 Mouse Irf1 RNA Target Probe Set	Alexa Fluor 647	VB1-3028161-PF	Invitrogen
MHC-II (I-A/I-E)	BV605	M5/114.15.2	BD
CD11c	BV711	HL3	BD
Ly-6G	AF700	1A8	BD
CD19	BV650	1D3	BD
GFP (YFP-cross reactive)	AF488	A-21311	ThermoFisher

IFNβ RT-PCR on sorted cell populations

To analyse IFNβ gene expression in different cell subsets, AB1 tumours were treated with 50 µg of Poly(I:C) (HMW, Invivogen) i.t. (n=5) or untreated (n=5), 5 days after inoculation, then harvested 24 hours later. Tumours were immediately submerged in cold PBS, cut into 1-2 mm pieces with a scalpel blade and dissociated using the GentleMACS system (Miltenyi). Fc block (anti-CD16/CD32, BD) was used for 10 minutes on ice. Cell were stained with UV Zombie live/dead (Biolegend) for 30 minutes at RT, to discriminate live cells. Cells were stained using antibodies for surface markers for 30 minutes at 4^{o}C. Cells were then sorted into RNAlater (Invitrogen) for the following populations: non-immune cells (CD45-) ; Ly6C^{hi} monocytes (CD45+ CD11b+ Ly6C^{hi} CD3- CD335-), Ly6C$^{lo/-}$ monocytes (CD45+ CD11b+ Ly6C$^{lo/-}$ CD3- CD335-), and the remaining immune cell (CD45+CD11b-). RNA was extracted using the RNAqueous-Micro Kit (Life Technologies). Resulting purified RNA was reverse transcribed using a High-Capacity cDNA Reverse Transcription Kit. Next, the inventors performed RT-PCR using TaqMan Fast Advanced Master Mix (Applied Biosystems) and TaqMan Assay

mouse IFNβ1 (Mm00439552_s1, ThermoFisher) or mouse GAPDH (Mm99999915_g1, ThermoFisher) in triplicate for each sample in a MicroAmp optical plate (Applied Biosystems) using QuantStudio 7 Flex Real-Time PCR System (Applied Biosystems). IFNβ expression was calculated as dCT of the housekeeping gene GAPDH. ΔCt = Ct (IFNβ) – Ct (GAPDH)

Statistics

The sample size calculation for *in vivo* mouse experiments was based on prior experiments in which the inventors found that the median survival time on the control treatment (ICB alone) was 35 days. Using a proportional hazards model the inventors determined that, if the true hazard ratio (relative risk) of control subjects relative to experimental subjects is 5, the inventors would need to study 10 experimental subjects and 10 control subjects to be able to reject the null hypothesis that the experimental and control survival curves are equal with probability (power) 0.8. The type I error probability associated with this test of this null hypothesis is 0.05. Differences in population frequencies in responders and non-responders using flow cytometry were determined using Mann-Whitney U testing on means. Prism software (GraphPad) was used to analyse tumour growth and to determine statistical significance of differences between groups by applying a Mann-Whitney U test. P-values were adjusted for multiple comparisons using the Benjamini-Hochberg (B-H) method; those < 0.05 were considered significant. The Kaplan-Meier method was used for survival analysis, and p-values were calculated using the log-rank test (Mantel-Cox). For comparison of deconvolution estimations, the inventors used two-way ANOVA with Tukey's multiple comparisons test.

Data availability

Raw sequencing data, both for single cell RNAseq and bulk RNAseq datasets will be deposited at GEO (accession codes will be available before publication). The computational workflow allows for programmatic downloads of processed sequencing data from a CloudStor remote repository prior to workflow execution – this processed sequencing data is available on request.

Code availability

Code for the analysis in the main manuscript and the extended data is available through GitHub (https://github.com/melvinchin/dynamic_interferon_signalling)

Network construction

Gene regulatory network inference using GENIE3

As the first step in network analysis of our bulk RNA-seq data, the inventors used the *GENIE3* R Bioconductor package for network inference. The inventors constructed two networks, one for AB1 and one for Renca using all responder samples for each strain across four experimental timepoints. The count matrices used as input to *GENIE3* were produced using the *tximport* (Soneson, et al. *F1000Research* **4**, 1521 (2015)) R package, allowing us to summarise *Kallisto's* transcript-level abundances to gene-counts. For this analysis, the inventors retained all genes with non-zero counts in at least one sample. *GENIE3* (Bioconductor version: Release (3.11)) was run on default parameters: for each target gene, the inventors used random forests, selecting the square root of the total number of candidate regulators at each tree node with a 1000-tree ensemble (treeMethod = "RF", K = "sqrt", nTrees = 1000)

Edge pruning using TFBS information and DE genes

Because the output from GENIE3 is a weighted, complete graph composed of all genes in the input count matrix, the inventors pruned this graph to isolate biologically relevant edges. To do this, the inventors integrated information from differential expression analysis and transcription factor binding site prediction results.

First, the inventors incorporated differential expression information using the R package *Sleuth*. For this, we used a likelihood ratio test with a design formula incorporating phenotype (ICB response), time and an interaction term to capture differentially expressed genes displaying time-dependent differences in expression between phenotypes. The inventors performed p-value aggregation of transcript-level results using Fisher's method (Yi et al. *Genome Biol* 19, 53 (2018)), with transcript-to-gene mapping relying on the latest Gencode reference M25 (GRCm38.p6). This

analysis yielded 4040 differentially expressed genes in AB1 and 510 differentially expressed genes in Renca at an adjusted p-value of < 0.05

Secondly, the inventors integrated JASPAR transcription factor binding site prediction (TFBS) information into our network. JASPAR provides TFBS predictions on the mm10 genome assembly using the JASPAR CORE vertebrate position frequency matrices (PFMs). The confidence of predictions is quantified by JAPAR relative scores. For their analysis, the inventors considered relative scores above 500, corresponding to a p-value of 10-5. The inventors identified and retained "direct connections", defined as connections between a transcription factor (TF) to differentially expressed genes only if the TFBS for the TF was situated in a genomic window 400 base pairs upstream or 300 base pairs downstream of a DE gene's transcription start site (TSS).

Network analysis of interferon signalling

Network visualisation

To explore these direct-interaction networks, the inventors visualised them with superimposed gene expression data. The inventors ranked regulators by connectivity (total degree), taking higher connectivity as a surrogate for greater biological influence in these networks. The inventors visualised the induced subgraph of the top ten nodes and their first order neighbours in both AB1 and Renca. To produce interpretable, reproducible diagrams of these networks with gene expression information, the inventors used the R *igraph* package to isolate these induced subgraphs and displayed them using the kamada-kawai layout. The inventors coloured nodes by scaled gene expression across time.

From inspection of these graph visualisations, the inventors confirmed in both AB1 and Renca that these subnetworks were enriched for interferon related transcription factors (Irf1, Stat1, Stat2, Irf7, Irf9) and their direct downstream targets. By visualising gene expression, the inventors also confirmed that these interferon-related genes possessed unique dynamics: only in responders, these genes showed fast-off changes by Day 2 in AB1 and Day 4 in Renca. Tthe inventors further analysed these hubs using pathway analysis using Enrichr's web-based API accessed through the R package *EnrichR*. 10 gene lists from each of the AB1 and Renca networks were used as individual inputs to Enrichr, with each gene list consisting of the one of the top 10

TFs and its first order connections. The inventors ranked term enrichment from Enrichr by their q-values and visualised the *-log10 q-value* for the top 5 terms for each gene list using Python's *seaborn* package. This analysis showed statistically significant enrichment of terms relating to both Type I and Type II interferon signalling (Figure 3), suggesting that dynamic changes in these two pathways were crucial to the checkpoint blockade response.

Transcriptional drivers of interferon signalling

Informed by our network visualisation, the inventors analysed TF-to-ISG interactions in AB1 and Renca direct networks to elucidate the key drivers of the ISG response.

Since network hubs showed enrichment of both Type I and Type II interferon, the inventors queried the regulation of ISGs involved with both signalling pathways in the AB1 and Renca networks. To identify ISGs involved in Type I and Type II interferon signalling in these direct networks, the inventors used gene sets of interferon alpha/beta signalling and interferon gamma signalling from the Molecular Signature Database (MSigDB) (Subramanian, A. *et al. Proc. Natl. Acad. Sci. U. S. A.* 102, 15545–15550 (2005); Liberzon, A. *et al. Bioinformatics* 27, 1739–1740 (2011)) converted into their murine equivalents using BioMart. The inventors visualised TF-to-ISG GENIE3 scores and expression profiles for ISGs common to both AB1 and Renca networks using the R *ComplexHeatmap* package. To aid visualization, the inventors ranked each TF's influence by the sum of GENIE3 scores on these target ISGs. By these criteria, the inventors saw regulation of fast-off ISGs confined to just 5 key interferon-related transcription factors - Irf1, Stat1, Stat2, Irf7 and Irf9, with minimal regulatory impact from other transcription factors in these networks (Figure 2).

Hive plot generation

As a final analysis, the inventors wanted to understand how the distribution of GENIE3 scores related to the interferon signalling, since stronger GENIE3 weights can be taken to represent stronger dynamic regulatory interactions in these networks. To overcome visual biases from traditional network layouts, the inventors used a hive plot visualisation. This visualisation strategy allowed the inventors to partition the edges in these networks according to the source and target genes using a consistent layout,

allowing an objective comparison between the two networks. In addition, the hive plots also allowed the inventors to visualise how the magnitude GENIE3 weights were distributed amongst the edges, and hence between genes involved in the same signalling pathways.

For each network, the inventors used a 4-axis hive plot in the *HiveR* package with the following axes, colour coded in the following way (Figure 3d, 3e):

1) Red axis – interferon related TFs (Irf1, Stat2, Stat1, Irf7 and Irf9)

2) Green axis – non-interferon related important TFs, comprising the union set of top TFs from both networks in figure 2.

3) Purple – Downstream gene targets in the "fast-off ISG set".

4) Blue – Other genes in the direct networks not in 1, 2, or 3

For axis 1 and 2, the inventors selected the union set of transcription factors in both networks based on the connectivity criterion described herein. For axis 3, the fast-ISG set was derived from k-means (k = 2) clustering on time course expression data from the AB1 responder data set. This node topology allowed the inventors to more easily visualise the "quadrant" of graph edges from IFN-related TFs to fast-off-ISGs, demonstrating that this quadrant contained edges with high value GENIE3 scores (above 0.9 quantile) denoting important dynamic regulatory links in the network.

Alignment and cell labelling of single cell data

For single cell analysis, the inventors processed FASTQ files from 6 AB1 and 6 Renca samples using cellranger v3.0 (10X genomics). For each sample, the inventors performed demultiplexing and read alignment using the Cellranger *count* function, using *cellranger*'s pre-supplied mm10 reference with an *expect-cells* parameter of 6000. The inventors used the filtered matrices from this processing step for downstream analysis. This step also produced aligned reads in binary (BAM) format and TSV files of valid cell identifiers - these files were used for velocity analysis, described in more detail herein.

Sample integration, clustering and visualisation

The inventors used a standard processing pipeline using the *Seurat* (version 3.14) R package to combine samples for downstream analysis (Stuart, T. *et al. Cell* 177, 1888-1902 (2019)). The inventors used the filtered count matrices for each sample after *cellranger* processing to construct individual Seurat objects, which were then subjected to basic filtering and QC. Specifically, the inventors excluded cells with less than 200 features and excluded genes detected in less than 3 cells. Normalisation was performed using Seurat's SCtransform function, regressing against both sequencing depth and also against the percentage of mitochondrial DNA in each cell. Subsequently, for both AB1 and Renca, all samples were merged using the FindIntergrationAnchors and IntegrateData Seurat functions. The resulting Pearson residuals from these processing steps were used for downstream PCA, cluster identification and UMAP embedding and visualisation.

Single cell labelling

To avoid subjective biases in cell identification, the inventors used an automated labelling strategy based on bulk RNAseq references. The R package *SingleR* was used in "cluster mode". For annotation, the inventors used the mouse RNAseq dataset from Benayoun et al. *Genome Res.* 29, 697–709 (2019).This dataset consisted of 358 samples, with 18 main (level 1) labels and 28 finer (level 2) labels. Labelling was performed on a per-cluster basis using clusters defined from Seurat's *FindClusters* function at default (0.8) resolution. SingleR's Level 1 annotations were used for each cluster and similarly labelled clusters were merged. The inventors confirmed that this approach was robust to cluster size by showing that labels were consistent even when cluster size was modified by changing *resolution* parameter in the *FindClusters* function. Additional annotation diagnostics are further described in herein.

Tumour cell labelling

The SingleR reference used in this labelling strategy did not contain references for tumour cells. Hence, the inventors relied on a different approach to locate tumour cells in our samples. The inventors used a strategy known as 'label transfer' in the *Seurat* package, allowing cell identities from a reference sample to be projected onto our target dataset.

Tumour labelling of AB1 mesothelioma cells

The inventors first constructed a reference set for mesothelioma cells. In tandem with the 6 AB1 and Renca samples, the inventors also sequenced 4 samples from AB1 mesothelioma tumours in which the tumour cells were tagged with influenza hemagglutinin (Marzo, et al. *Cancer Res.* 59, 1071–1079 (1999)). To detect cells containing this HA-tag, the cellranger mm10 index was rebuilt to incorporate the tag sequence. This rebuilt index was used during read alignment of these 4 reference samples. Filtered count matrices were processed similarly to our other AB1 and Renca samples as described herein. The inventors labelled any cell containing the HA-tag as a tumour cell and others as non-tumour. These labels were subsequently projected onto the combined AB1 dataset composed of 6 AB1 tumours. Clusters containing more than 10% tumour cells were deemed to be putative tumour clusters and their labels were switched from the SingleR labels to reflect these new identities

Tumour labelling of Renca renal cell carcinoma cells

To label Renca tumour cells, the inventors used a projection strategy similar to AB1 mesothelioma cells. Renal cell carcinoma is known to transcriptionally recapitulate elements of the renal tubule, so the inventors used a reference dataset of mouse kidney single cells from Park et al. *Science* 360, 758–763 (2018) in which the authors identified gene markers mapping to anatomical elements of the mouse renal tubular system. After processing count matrices in this dataset using the same approach as Renca and AB1 samples, the inventors selected clusters which expressed the highest average expression of markers specific proximal and distal tubules (Lrp2, Slc27a2). Cells in these reference clusters - which the inventors labelled as “renal tubule elements” - had their identities projected onto the Renca dataset. Cells acquiring this label in our target dataset of 6 Renca tumour samples were labelled as putative tumour clusters.

Inferring copy number changes to predict tumour cells

As a final test for tumour cell identity, the inventors inferred copy number variation in single cells. Tumour cells usually display evidence for somatic large-scale chromosomal copy number alterations, such as gains or deletions of entire chromosomes or large segments of chromosomes. For this, the inventors adopted the approach in Tirosh *et al. Science* 352, 189–196 (2016). The strategy used by these

authors is formalised by the R *inferCNV* package. In short, *inferCNV* detects CNV changes by examining changes in levels of gene expression in specific chromosomal regions against a background signal. The inventors used *inferCNV* on a per-sample basis. In both AB1 and Renca, tumour clusters labeled by *Seurat's* projection strategy were in good agreement with clusters of cells deemed to be tumour clusters based on the existence of copy number changes inferred by inferCNV. This served as an additional validation step indicating successful identification of these tumour cells in both types of tumours.

Gene set enrichment analysis on single cell data

For gene set enrichment analysis, the inventors used the SCDE/pagoda[12] package, which detects statistically significant coordinated variability at single cell level. Briefly, from the original 38K cells in our AB1 samples, the inventors constructed KNN error models for the 17K surviving default SCDE's library size filters. The inventors used raw counts and normalised variance across these cells. For speed and computational efficiency, the inventors used the multi-core implementation of the *knn.error.models* function which required the co-installation of the *WGCNA* package[13] and also supplied cell identities from SingleR (Fan, J. *et al. Nat. Methods* **13**, 241–244 (2016)). For gene sets, the inventors tested GO terms for interferon production and interferon response extracted from the *org.Mm.eg.db* Bioconductor package and also their "custom" gene set of fast-ISGs derived from bulk expression data. The inventors visualised enrichment scores using python's Seaborn scatter plot with a colour scale mapped to enrichment score intensity.

Identification of interferon sources and harmonisation of cell labels

To ascertain the source of interferon in the tumour microenvironment, the inventors used the method described above for gene set enrichment analysis on AB1 cells. Due to the quality and sequencing depth of our single cell data, the inventors found that AB1 samples showed low expression of transcripts for IFN-gamma and almost no transcripts for IFN-alpha and IFN-beta, making it difficult to interpret direct visualisations of normalised counts of these transcripts. Furthermore, the inventors wanted to study coordinated upregulation of groups of genes corresponding to a

biological pathway, so the inventors chose this analysis approach rather than inspecting and interpreting expression profiles of individual genes across our cell populations.

To accurately localise interferon sources, the inventors performed annotation diagnostics by checking cell cluster identities in our AB1 samples against the ImmGen (Heng, T. S. et al. *Nat. Immunol.* 9, 1091–1094 (2008)) reference, consisting of 252 samples of microarray data with an annotation focus on hematopoietic and immune cell types. The inventors found both references to be in agreement with the immune-orientated Immgen reference allowing us to reclassify a proportion of monocytes as dendritic cells. By inspecting conserved markers, the inventors harmonised labels (Aran, D. *et al. Nat. Immunol.* 20, 163–172 (2019)) across both reference datasets and used these labels to assign per-cell enrichment scores calculated using SCDE for interferon alpha, beta and gamma production across all cell types in our AB1 samples and in monocytes, separated by response to immune checkpoint blockade.

Single cell differential expression analysis and conserved marker analysis

Using cell labels from SingleR clustering and projection experiments, the inventors performed differential expression using *FindMarkers* function in Seurat on normalised RNA counts in the Seurat object (parameters: assay = “RNA” and slot “data”). For this analysis, cells were partitioned by response and by cell label. By default, the inventors restricted the analysis to genes which were expressed in at least 25% of all cells. The non-parametric Wilcoxon was used as the statistical test for differentially expressed genes with FDR correction. The inventors deemed genes to be differentially expressed at an absolute log-fold change of 0.5 and a q-value of below 0.05. Consistent with previous analyses in both bulk and single cell data, responder monocytes displayed high levels of interferon gamma and interferon beta signalling. DE genes in AB1 separated by cell type is provided in table 1.

The inventors also analysed 6 samples from Renca for differentially expressed genes in the same way as AB1 samples. The same strategy for label harmonisation used in AB1 was performed on Renca single cell samples showing compatible cell labels using both references. However, consistent with differential expression analysis in bulk data, the inventors observed far fewer differentially expressed genes between

responders and non-responders at Day 0 across all cell types. Consequently, the inventors observed no significant terms on pathway enrichment using *Metascape*.

The same differential expression strategy was also used to identify conserved markers in the monocyte populations (Figure 4). However, the inventors performed this using the *cellrouter* package, given that the package provided a more comprehensive set of visualisation functions for marker analysis.

Single cell analysis network

The inventors used network inference to analyse single cell data. The objective with this approach closely mirrors network analysis on bulk data - to discover co-expression modules for important transcription factors governing the checkpoint blockade response, with the potential benefit of a larger number of gene expression data points in single cell data as compared to bulk samples.

The inventors needed to analyse 38K cells from 6 AB1 samples. For this the inventors used the SCENIC pipeline (Aibar, S. *et al. Nat. Methods* 14, 1083–1086 (2017)), with the costly computational step of GRN construction performed by the *arboreto* package. This package uses a variation of the XGBoost algorithm built on python's Dask as a resource scheduler. Downstream of GRN construction, the SCENIC pipeline involves the identification of high confidence "regulons", comprising a transcription factor and its downstream effector genes. Identification was followed by regulon activity detection in individual cells using a gene set enrichment approach known as AUCell.

The inventors used counts normalised by Seurat's SCTransform negative binomial regression model for single cell network analysis. The inventors ran the analysis across cells in the AB1 dataset, with a presupplied list of mm10 transcription factors provided by the SCENIC package authors. Candidate regulons detected from this inference step were pruned, informed by a ranking database of species-specific regulatory features and a species-specific motif annotations database which were also included with this software. These "regulons" were tested for enrichment using AUCell. Automated calculation of thresholds was performed on each regulon, allowing enrichment, and hence activity of each regulon to be binarised.

The inventors summarised the result of these analyses using a difference heatmap between responders and non-responders of average binarised TF activity per Seurat cluster. Specifically, the regulon binarisation scores were averaged across clusters, separated by response and the difference between responder and non-responder averages were visualised using the R *pheatmap* package.

Velocity analysis

RNA velocity models the time derivative of the gene expression state, allowing us to quantify activity of expression for a gene of interest. By combining multiple gene velocity measurements for each of the single cells, the inventors also derive a measure of the general "transcriptional activity" of a cell in high dimensional space, which can in turn be used to predict future cell state. The inventors used RNA velocity analysis to analyse differences in the monocyte population between responders and non-responders. The inventors analysed both "general transcriptional activity", and more specifically the gene velocities of ISGs involved in the fast phase of the ICB response.

Processing pipeline and parameter specification

The inventors processed BAM files of aligned reads produced by *cellranger* as described herein. For quantification of spliced vs unspliced transcripts, we used the *veloctyo run* command from the *velocyto.py*'s command line interface on these BAM files. To mask expressed repetitive elements and prevent those counts from affecting downstream analysis, the inventors downloaded an expressed repeat annotation from UCSC genome browser in GTF format which the inventors also supplied as input to the *run* command. The resulting loomfiles produced from running individual samples were combined using the python *loompy* package. The inventors merged 6 samples from each strain into a single, combined strain-specific loomfile for downstream analysis.

Prior to the gamma-fitting step of velocity analysis, the inventors performed normalisation, filtering and feature selection on genes. The inventors normalised spliced and unspliced transcripts by total molecule count. Gene filtering and feature selection was performed using three helper functions - the first specifying gene expression cut-offs on a per-cluster basis, the second performing gene cut-offs on a per cell basis and a final feature selection step based on support vector machine regression. Genes surviving these filtering steps were used in downstream analysis. These filtered genes

were used for gamma-fitting to derive a per-gene velocity, defined as the residual between the predicted and observed unspliced transcripts. Preceding this, data smoothing using a KNN approach. The extrapolated future state of each cell was calculated using the *vlm.calculate_shift* and *vlm.extrapolate_cell_at_t* with a delta_t = 1.0.

The inventors incorporated UMAP embedding information from our Seurat analysis into the *velocytoLoom* object. Transition probabilities and embedding shifts were calculated with respect to Seurat-derived UMAP coordinates using the *vlm.estimate_transition_prob* and *vlm.calculate_embedding_shift* function. Visualisation of cell velocities was performed using matplotlib helper functions from the *velocyto.py* package.

Momentum calculations on Seurat UMAP embedding

To objectively compare responders and non responders monocytes in AB1, the inventors compared their "transcriptional momentum", which was defined as the squared L2 norm for each cell's embedding vectors with respect to their Seurat UMAP (McInes, et al. *J. Open Source Softw.* 3, 861 (2018)). These 2D embedding vectors were extracted from the "delta_embedding" slot of the *velocytoLoom* object. The inventors compared KDE distributions for momentum in various AB1 clusters, separated by response. The inventors showed from these KDE distributions that the most highly interferon-stimulated, Ly6c^{Hi} responder monocytes possessed more transcriptional momentum than their non-responder counterparts, indicating that differential transcriptional activity in this population was important to ICB response.

To compare Renca and AB1 monocytes, the inventors repeated their velocity analysis by combining 12 loom samples from AB1 and Renca with *loompy* and performed momentum calculations on an embedding derived from integrating and co-embedding all 12 samples using the method described herein. The inventors visualised the momentum from co-clustered Ly6c^{Hi} monocytes from both AB1 and Renca. On this common embedding, momentum calculations show that AB1 responders have a higher transcriptional velocity than Renca monocytes in responders, suggesting that the perceived delay in the fast-off signal originated from earlier sampling timepoints in Renca bulk RNAseq data.

Gene velocity calculations

The momentum calculation described above is derived from genes surviving feature selection and filtering. As an additional check that differences in transcriptional momentum were, in part, due to differences in interferon signalling, the inventors examined gene velocities for IFN-related TFs and ISGs in the fast-off component gene set which survived the above-mentioned filtering. The inventors extracted the normalised velocities of 42 of these genes which survived data preprocessing, which the inventors visualised in *seaborn*'s Clustermap. Hierarchical clustering showed separation of responder versus non responder monocytes based on ISG velocities.

As an additional analysis, the inventors also compared the velocity of IFN-related TF, Irf1, across their AB1 cells. Global Irf1 gene velocities displayed across the Seurat UMAP showed that the monocytes in AB1 had the largest negative velocities. These negative velocities can be interpreted as a "deceleration", where the cells actively downregulate expression of this transcription factor. The only large population of cells demonstrating negative Irf1 is the monocyte population, showing that this population is actively downregulating Irf1 expression. Taken together with high Irf1 regulon activation in this cell population, this indicates that these IFN-stimulated monocytes at Day 0 are rapidly moving to a less IFN-activated state over time by downregulating IRF-TF expression, accounting for the "shut-off" of ISG expression at Day 2 in AB1 (Figure 5).

<u>Expression analysis along pseudotime trajectories</u>

The inventors wanted to more comprehensively characterise the transcriptional behaviour of these monocytes. Having identified a monocyte pseudotemporal ordering (pseudotime) which closely tracks a gradient of interferon-related transcription, we wondered if any other important signalling pathways were also associated with this interferon signal. The inventors desired an analysis approach for gene expression along this pseudotime which allowed us to leverage information from upstream analyses. This meant retaining single cell cluster identities from Seurat's dimensionality reduction step and specifying source and target monocyte populations based on RNA velocity results. In general, such requirements are incompatible with most current pseudotime analysis software packages since they generally require a software-specific dimensionality reduction step which precedes the construction of the pseudotime manifold.

Cellrouter analysis

The chose the R *cellrouter* package to explore gene expression along our monocyte differentiation trajectory Lummertz da Rocha, E. *et al. Nat. Commun.* 9, 892 (2018). *Cellrouter* identifies trajectories using a network flow approach rather than by constructing a pseudotime manifold based on a low dimensional embedding. For this analysis, we first used *cellrouter* to calculate the cell-to-cell KNN graph using normalised counts from Seurat's SCTransform normalisation. Based on velocity analysis, the inventors specified cluster 12 as a "source" cell cluster and cluster 3 as a "target" cell cluster. All potential trajectories in the cell-to-cell KNN graph were ranked based on distance between vertices. Subsequently, the *topGenes* function was used to extract genes highly correlated with derived pseudotime, specifically those above the 0.8 quantile for positively correlated genes and those below the 0.1 quantile for negatively correlated genes. For analysis of diffusion components in the network, the inventors split the most highly correlated genes into 5 components for enrichment analysis using Metascape. Compatible with their previous results, diffusion analysis shows a component which was strongly enriched for interferon signalling, with reduced signalling intensity along pseudotime from Ly6c^{Hi} to Ly6c^{Lo} monocytes. Other components showed enrichment for terms involved in cell proliferation, cell-to-cell adhesion, and translational activity, suggesting ingress, expansion and maturation of an interferon-stimulated Ly6c^{Hi} monocyte population into the responder tumour microenvironment after ICB administration.

Phenopath analysis

The RNA velocity arrows from previous analysis indicated a trajectory from cluster 1 to cluster 2 monocytes. On this embedding, responder and non-responder monocytes share the same pseudotime axis and share similar transcriptional features, a product of analysis in a common low-dimensional embedding. Using *Cellrouter* reveals important signalling pathways correlated with this trajectory, but it does not address the potential for preferential signalling pathways along this pseudotime between responder and non-responder monocytes.

The inventors wanted a statistically robust way for determining preferential signalling pathways along monocyte responder pseudo time, so for this the inventors

used the *phenopath* R package. This Bayesian approach performs trajectory inference whilst allowing the inclusion of ICB response as an additional sample-specific covariate. In turn, it potentially reveals subtle differences between gene expression along the pseudotime trajectory which are associated with ICB response.

The preferred input to *phenopath* is a count matrix of log-normalised, variance stabilised counts of highly variable genes in the cell populations of interest. To generate this matrix, the inventors selected highly variable genes (HVGs) using the *"vst"* option using Seurat's *FindVariableFeatures* function, selecting 3000 features for analysis. From this, 253 genes were deemed to have a significant interaction with the responder phenotype, whilst 847 genes were associated with non-responder phenotype. Pathway analysis using Metascape were consistent with previous analyses. The monocyte pseudo time in responders was enriched for terms associated with interferon response and cellular migration, in turn implying ingress of an interferon-activated monocyte population into the tumour microenviroment (data not shown)

Computational workflow management using snakemake

Computational analysis was performed with snakemake (Köster, J. & Rahmann, S. *Bioinformatics* 28, 2520–2522 (2012) (version 5.14), allowing all results in these examples, including intermediate results to be regenerated.

Example 2 - Time-course transcriptomics of ICB response

The inventors optimised murine models with bilateral tumours, derived from syngeneic cancer cell lines. In these models, immune checkpoint blockade (ICB) with antibodies against CTLA4 and PD-L1 either leads to a symmetric bilateral response or a symmetric failure to respond in both tumours. This allowed characterisation of the response to ICB in entire tumours in a highly homogenous background by removing one of the tumours for analysis, and infer what the therapeutic response would have been if the inventors had left it *in situ* by observing the response of the remaining contralateral tumour.

To map the dynamic processes underlying the response to ICB, the inventors removed responsive and non-responsive tumours at 1-hour prior and at 2, 4 and 6 days following administration of anti-CTLA4/anti-PD-L1 therapy (Fig. 1a), and examined the

transcriptomes of these tumours using RNA-sequencing. To avoid bias towards one tumour type, the inventors utilised two different tumour models, AB1 mesothelioma and Renca renal cell carcinoma, and explored pathways that were consistently differentially regulated between responders and non-responders in both models.

The inventors first determined whether there were differences in cellular composition between responders and non-responders at each time point using CIBERSORT analysis (Chen et al., *Methods Mol. Biol.* 1711, 243-259 (2018)). Although some differences between responders and non-responders were observed, none of these differences were consistent between the two models, except for a significantly higher proportion of NK cells in responders prior to treatment (data not shown). Although CD8+ T cell gene signatures in baseline samples have been reported in the literature as predictors of response, the inventors observed an increase in CD8+ T cells after ICB, irrespective of response (Figure 1c).

To understand gene expression kinetics during treatment with ICB, the inventors clustered genes using *TCSeq* package (v1.14.0) (Wu and Gu, TCseq: Time course sequencing data analysis (2020)), which clusters genes based on their dynamic expression patterns, and analyzed the resulting clusters using pathway analysis. The inventors recovered four clusters that showed consistent time-dependent behavior between the two models. Clusters 1 and 2 contained genes associated with activation of myeloid cells and T cells. The expression of these genes gradually increased over time in both responders and non-responders, albeit to a greater magnitude in responders (Figure 1d and 1e), which was in agreement with earlier results obtained using CIBER-SORT (data not shown). Genes associated with cancer cell signaling (cluster 3) decreased in expression over time, but again in both responders and non-responders (Figure 1f and 1h). In contrast, cluster 4, demonstrated a kinetic profile that was strikingly different between responders and non-responders (Figure 1g and 1i). Cluster 4 contained genes associated with IFN signaling, which showed a gradual increase in expression over time in non-responders, while in responders it was initially highly expressed, followed by a rapid decrease in both AB1 and Renca (Figure 1g).

The inventors constructed gene regulatory networks for responders using the GENIE3 algorithm. For each gene, the algorithm calculates an importance score reflecting the inferred effect of the gene on all other genes. A high importance score

denotes a strong effect of a gene (putative regulator) on the dynamics of expression of a downstream gene (target) in the network. The inventors ranked putative regulators by the sum of their outgoing importance scores and plotted the expression of the top 100 regulators over time (Fig. 1b). This showed dynamic changes in regulators after treatment, with consistent differences between responders and non-responders in both mouse models, suggesting a common dynamic gene signature associated with response to ICB treatment.

Example 3 - Differential dynamics of type I IFN signalling

Having observed common regulator kinetics associated with the ICB response, the inventors focused on the top 10 known transcription factors (TF) that form central hubs in the network. For each one of these TFs, the inventors explored downstream genes that were differentially expressed between responders and non-responders and contained a binding site for the TF within their promoter (Fig. 2). Visualising the most connected TFs in the network showed multiple gene modules with increased expression early during treatment (Fig. 3a). In both AB1 and Renca, functional annotation of these modules revealed one commonly activated module in responders with similar expression kinetics, which was related to interferon (IFN) specific terms (Fig. 3a). This suggested that the IFN pathway was a common dynamic determinant of checkpoint blockade response, with a fast reduction in expression levels over the time course of the experiment, specifically day 0 to 2 in AB1 and day 2 to 4 in Renca

Next, the inventors studied the regulation of these fast-off IFN kinetics using gene sets of known IFN stimulated genes (ISGs). Because the functional annotation suggested that both type I and type II IFN contributed to the responder phenotype, the inventors obtained a list of ISGs for both type I and type II IFN from the Molecular Signatures Database hallmark gene sets and analysed direct edges from TFs to these ISGs weighted by GENIE3 importance scores. This analysis demonstrated that both AB1 and Renca showed similar on/fast-off kinetics of IFN signalling in responders, with fast-off changes by day 2 in AB1 and day 4 in Renca (Fig. 3c). In contrast, non-responders displayed a slower and less intense activation of ISGs which remained chronically active over time. The inventors confirmed that ISG expression segregated into an early and late phase, with the fast-off component containing genes stimulated by IFNg (54 of 124, 42%), IFN a/b (14 of 124, 11%) or a combination of both (58 of 125,

47%). Expression of these ISGs in both AB1 and Renca was similarly regulated (Fig. 3c). For both models, the most important TFs across ISGs were Irf1, Stat1, Stat2, Irf7 and Irf9, indicating that regulation of ISG kinetics was confined to this small subset of TFs, independent of tumour type. Likewise, the topology of the networks was highly similar in both models, reinforcing the central role of these IFN-associated TFs (Fig. 3d, e). Taken together, it is clear that fast-off dynamics in IFN signalling are associated with response to ICB, driven by common regulators across different tumour models.

Example 4 - IFN-driven changes in monocytes in responders

To further understand this fast-off IFN signal, the inventors performed single cell transcriptome sequencing one hour prior to ICB. The inventors interrogated responder and non-responder samples (Fig. 4a) and confirmed the global difference in type 1 IFN signalling in responders (Fig. 4b). Gene set enrichment analysis demonstrated that responder monocytes expressed the highest level of the fast-off ISGs (Fig. 4c). Upon closer inspection, the inventors observed a gradient of ISG enrichment across 3 distinct monocyte sub-clusters (Fig. 4d). By analysing conserved markers, the inventors found that the highest levels of fast-off ISG signalling occurred in cluster 1 monocytes (Fig. 4d), which displayed a $Ly6c^{hi}$ phenotype (Fig. 4e). Consistent with the network analysis in bulk samples, single cell network analysis in this sub-population confirmed that Irf1, Irf7, Stat1 and Irf9 and Stat2 were the major transcription factors driving the response (Fig. 4f). Flow cytometry confirmed high Irf1 expression in $CD11b^{hi}/Ly6c^{hi}$ monocytes (Fig. 4g).

The inventors exploited the fact that single cell data allows capturing of cells at various stages of response within one sample, by ordering cells by their response phenotype, and explored whether this ordering reflected the gradient in IFN signalling (Fig. 3). The inventors observed a differentiation trajectory from $Ly6c^{hi}$ to $Ly6c^{lo}$ monocytes that was more pronounced in responder samples consistent with our observation of a fast-off dynamic (Fig. 4h). Furthermore, this trajectory showed diminishing transcriptional activity of ISG genes, with a more pronounced activity in responders compared to non-responders. Along this trajectory, velocity analysis showed that monocytes downregulated transcription of ISGs such as Irf1, and this was more pronounced in responders than non-responders. Previously, the inventors saw a delayed fast-off signal in bulk RNAseq data in Renca responder samples. The inventors

demonstrated that this delayed fast-off bulk RNAseq signal in Renca was due to an earlier state of the tumour microenvironment, observed through velocity analysis of the inventors' single cell data. These dynamics are consistent with Ly6c expression over time acquired from the bulk RNAseq data. Taken together, these results suggest that the differentiation of tumour-infiltrating IFN-stimulated $Ly6c^{hi}$ monocytes towards a low interferon expressing, $Ly6c^{lo}$ phenotype is an important early event in the ICB response.

Example 5 - Dynamic targeting of type I IFN improves response rate to ICB in both ICB responsive and resistant tumour models

To explore which IFN type mediates the response, the inventors plotted the enrichment of the fast-off ISG gene set (Fig. 4c), genes involved in type I IFN (α/β) production (Fig. 4i), and IFNγ signalling (Fig. 4j). Based on this data, the inventors were unable to resolve the IFN type driving the response. As computational analysis of gene expression data did not allow robust dissection of type I and II IFN pathways, the inventors tested this experimentally. To phenocopy the active IFN signature *in vivo*, prior to ICB, the inventors pre-treated mice with intratumoural injections of poly(I:C), which is known to induce both type I and II IFNs, particularly IFNβ (Fig. 5). These studies were done in AE17 mesothelioma, which is relatively resistant to ICB. To mimic the subsequent fast-off IFN signature, ICB was followed three days later by functionally blocking either type-I or type-II IFN signalling, using antibodies against the IFNα/β receptor (IFNAR1), IFNγ, or both (Fig. 6a). Pre-treatment with poly(I:C) improved the response rate to ICB (0% vs. 26.7% complete responders), which was significantly enhanced by the subsequent blockade of type I IFN (53.3% complete response, p 0.034), but not type II IFN (Fig. 6b). The inventors confirmed these findings in the AB1 mesothelioma model (33.3% vs 53.3% complete responders, (Fig. 7). In both models, the beneficial effect of blocking type I IFN after administration was negated by blocking type II IFN simultaneously, demonstrating not only that type I IFN was responsible for the observed fast-off dynamics of IFN signalling in responders, but that these dynamics indeed played an important mediating role in the therapeutic response.

Example 6 – Switching off IFNβ increases response rate

Both IFNα and IFNβ signal through IFNAR1, but IFNβ can bind to IFNAR1 in an IFNAR2-independent manner. The inventors therefore used single cell RNAseq data

from T cells stimulated with a diverse array of cytokines, including IFNβ to construct a reference matrix using CIBERSORT. Deconvolution analysis revealed that genes associated with IFNβ signalling followed the on/fast-off IFN signature in responders in both AB1 and Renca tumour models, suggesting IFNβ was responsible for these observed dynamics (Fig. 6c, d.). To test whether indeed IFNβ was responsible for the therapeutic effect when blocking IFNAR1, the inventors treated AE17 and Renca tumour-bearing mice with antibodies against either IFNβ, IFNAR1 or IFNα (subtypes A, 1, 4, 5, 11, and 13) 3 days after administration of ICB. Mice treated with the antibody against IFNβ had a similarly increased response rate following ICB as the mice treated with the anti-IFNAR1 antibody, while mice treated with anti-IFNα displayed no increase in response versus controls (Fig. 6e). The inventors repeated these experiments in the Renca model, which exhibited the same benefit of blocking IFNAR1 or IFNβ, but not IFNγ or IFNα (Fig 6f). The inventors conclude that the beneficial effect of fast-off kinetics in type I IFN signalling after ICB is entirely dependent on switching off IFNβ.

To confirm whether monocytes were indeed the source of IFNβ in the tumor microenvironment, the inventors used B6.129-Ifnb1tm1Lky/J mice, which co-express IFNβ1 and eYFP from the Ifnb1 locus, bearing AE17 tumors (Scheu et al., *Proc Natl Acad Sci USA* 105, 20416-20421 (2008)). Tumors were analyzed by flow cytometry, one day after intra-tumoral poly(I:C), revealing YFP-positive cells were all CD45+, CD11b+, MHC-II-, F4/80-, CD11c- with the majority expressing Ly6c, consistent with the single cell RNAseq results (Figure 4k). Together, these results pinpoint CD11b+ monocytes as the key IFNβ producing cells in the tumor microenvironment.

Example 7 – Promotion of response to ICB does not require IFNβ induction

As intra-tumoural administration of poly(I:C) is not approved for use in clinical practice, the inventors tested whether similar results could be achieved in the absence of initial IFNβ induction by poly(I:C). Blockade of type I IFN again improved ICB efficacy in AB1-bearing mice, albeit to a lesser extent than after priming with poly(I:C), which was again dependent on IFNβ (Fig. 6g, Fig. 8). The inventors confirmed these findings in the AE17 and Renca models (Fig. 8).

Example 8 – Inhibiting IFNβ after ICB, not before, underlies response to ICB

To explore the biological relevance of these IFNβ dynamics, the inventors assessed the effect of blocking IFNAR1 before rather than after ICB initiation, or concomitantly with poly(I:C) prior to ICB. This treatment completely abrogated both the response to ICB and the priming effect of poly(I:C), confirming the crucial time-dependent nature of IFNβ signalling underlying the therapeutic response to ICB (Fig. 9).

Mice were inoculated with AE17, treated with poly(I:C) (blue dotted lines) followed by anti-CTLA4/anti-PD-L1 ICB (black dotted lines), with concurrent or delayed (3 days later) anti-IFNβ (Figure 9d). Dosing anti-IFNβ concurrently with ICB, does not result in improved efficacy (orange versus blue line), while dosing 3 days after start of ICB does (green line) as shown in Figure 9d.

Having established that blocking IFNAR1 abrogated the effect of poly(I:C) (Figure 9c), the inventors wanted to determine whether IFNa or IFNb activity was driving the "on" signal in responders. Using recombinant cytokines, the inventors found that priming with IFNβ, but not IFNα, increased the response to ICB (p=0.012), and mimicking the on/off IFN signature targeting IFNβ was superior to targeting IFNα (p= 0.027) (Figure 6H). Notably, the temporal aspect of scheduling the respective treatments was crucial, as treatment with anti-IFNβ concomitantly with ICB did not offer any therapeutic benefit, in contrast to administration 3 days after the first dose of ICB (Figure 6I). These results confirm that temporal restriction of IFNβ activation underlies response to ICB.

Example 9 – On/fast-off IFN kinetics correlate with response in patients treated with ICB

The inventors tested whether temporally restricted activation of IFN signaling also occurred in patients who responded to ICB therapy. To demonstrate if the on/fast-off-IFN signature occurred in responding patients early after treatment with ICB, the inventors analyzed RNAseq data from a glioblastoma study where patients were randomized to receive either neoadjuvant or adjuvant pembrolizumab (Cloughesy et al., *Nat. Med.* 25, 477-486 (2019)). In a published analysis of this dataset, neoadjuvant treatment with ICB upregulated IFN gene sets 3 weeks after anti-PD1 treatment, which correlated positively with patient survival. In the present analysis, the inventors confirmed statistical enrichment of the on/fast-off-IFN signature in the neoadjuvant cohort. When compared to the IFN gene sets previously used to analyze this dataset

(Ayers et al., *J Clin Invest* 127, 2930-2940 (2017); Moserle et al., *Cancer Res* 68, 5658-5668 (2008); Zhang et al., *Nat Med* 11, 56-62 (2005)), the on/fast-off signature showed the highest enrichment score, indicating that upregulation of this signature is an early important transcriptomic event in the response to ICB therapy (Figure 10a). Due to the limitation of having only a tumor sample at one time point after initiation of treatment in patient studies, it was not possible to adequately assess the kinetics of the on/fast-off signature over time. However, frequent serial sampling of peripheral blood has been carried out in the context of many clinical trials. The recruitment and maturation of Ly6Chi inflammatory monocytes from peripheral blood has been demonstrated to require type I IFN. Additionally, differentiation of monocyte-derived cells from a Ly6chi to Ly6clo state was previously found to be associated with response in murine models of PD1 checkpoint blockade and also in patients. From these two observations, it was postulated that IFN-driven influx of differentiating monocytes from peripheral blood into the tumor microenvironment occurs early in ICB responders. The inventors used peripheral blood data from a clinical trial investigating anti-PD1 in combination with chemotherapy in gastrointestinal cancer patients (Griffiths et al., *Proc. Natl. Acad. Sci. USA* 117, 16072-16082 (2020)). The inventors examined single cell data from four treatment time points and mapped the on/fast-off response signature to immune cell populations from peripheral blood (Figure 10b). Supporting observations in mice, the analysis of patient data showed that type I IFN signaling was activated in monocytes, but only in responders (Figure 10c-d). In these cells, upregulation of the fast-off-IFN signature occurred early after ICB administration which disappeared later, emphasizing the similarity of these IFN kinetics in patients and murine models.

In order to test whether a similar fast-off IFN signal could be identified in monocytes infiltrating into tumours in patients, the inventors used single cell RNAseq samples from breast cancer patients treated with an anti-PD1 antibody, obtained prior to treatment and 9 days after PD-1 treatment. One-third of patients displayed T cell expansion, while the rest did not.

SCENIC network analysis (Aibar et al., *Nat* Methods, 14, 1083-1086 (2017)) showed that IFN-related transcription factor activation was increased in monocytes in patients with T cell expansion (Figure 11a). Similarly, single sample GSEA identified enrichment of IFN-related gene sets in monocytes in breast cancer with T cell

expansion (Figure 11b). Importantly, comparing the pre-treatment samples with the post-treatment samples using differential expression analysis and pre-ranked GSEA, the inventors identified a faster decrease in IFN signalling activity in these monocytes in patients with T cell expansion compared to patients lacking T cell expansion similar to what they observed in the murine samples (Figure 11c).

Taken together, these results validate time dependent therapeutic IFNb modulation as a potential treatment strategy to increase treatment responses to ICB.

In summary, the inventors show that fast-off dynamics of IFNβ signalling underlie the response to ICB and that this can be therapeutically exploited using antibodies against IFNβ or its receptor IFNAR1, resulting in enhanced tumour clearing. The inventors demonstrate in intrinsically responsive tumours that type I IFN, specifically IFNβ, plays a dual role and that the response rate and depth of response can be improved by therapeutically mimicking these on/fast-off dynamics. As antibodies targeting the IFNβ/IFNAR1 pathway have been fully developed in the context of autoimmunity, these results could be readily translated into the clinic.

It will be understood that the invention disclosed and defined in this specification extends to all alternative combinations of two or more of the individual features mentioned or evident from the text or drawings. All of these different combinations constitute various alternative aspects of the invention.

CLAIMS

1. A method of increasing the response in a subject to an immune checkpoint modulator comprising:

administering an immune checkpoint modulator;

subsequently to administering the immune checkpoint modulator, administering an interferon β (IFNβ) inhibitor,

thereby increasing the response in the subject to an immune checkpoint modulator.

2. A method of treating, preventing or minimising progression of cancer in a subject comprising:

administering an immune checkpoint modulator;

subsequently to administering the immune checkpoint modulator, administering an interferon β (IFNβ) inhibitor,

thereby treating, preventing or minimising progression of cancer in the subject.

3. A method of treating, preventing or minimising progression of cancer in a subject who has received, or who is receiving, an immune checkpoint modulator, the method comprising:

administering an interferon β (IFNβ) inhibitor,

thereby treating, preventing or minimising progression of cancer in the subject.

4. A method according to claim 3, wherein the subject who has received, or who is receiving an immune checkpoint modulator may have exhibited, or be exhibiting, a clinically relevant response to that immune checkpoint modulator.

5. A method according to claim 3, wherein the subject who has received, or who is receiving, an immune checkpoint modulator may be resistant or not exhibiting a clinically relevant response to that immune checkpoint modulator.

6. A method according to claim 5, wherein the method further comprises identifying a subject having cancer and being unresponsive to a treatment comprising an immune checkpoint modulator.

7. A method according to any one of claims 1 to 6, wherein the IFNβ inhibitor is administered in a composition.

8. A method according to claim 7, wherein the composition does not include an inhibitor of IFNα.

9. A method according to claim 7, wherein the composition does not include an inhibitor of a type II IFN.

10. A method according to claim 7, wherein the composition does not include an inhibitor of any other IFN.

11. A method according to claim 7, wherein the only IFN inhibitor included in the composition is an IFNβ inhibitor.

12. A method according to any one of claims 1 to 11, wherein the immune checkpoint modulator is an inhibitor of a suppressive (or negative) immune checkpoint.

13. A method according to claim 12, wherein the suppressive immune checkpoint is PD-1, PD-L1, PD-L2, CTLA-4, TIM3, LAG3, CEACAM (e.g., CEACAM-1, CEACAM-3 and/or CEACAM-5), VISTA, BTLA, TIGIT, LAIR1, CD160, 2B4, CD80, CD86, B7-H3 (CD276), B7-H4 (VTCN1), HVEM (TNFRSF14 or CD107), KIR, A2aR, SIGLEC7, NOX2, MHC class I, MHC class II, GAL9, adenosine, and TGF-beta.

14. A method according to any one of claims 1 to 11, wherein the immune checkpoint modulator is an agonist or activator of stimulatory (or positive) immune checkpoint.

15. A method according to claim 14, wherein the stimulatory immune checkpoint is CD28, ICOS, CD137 (or 4-1BB), OX40, CD27, CD40 or GITR.

16. A method according to any one of claim 1 to 11, wherein the immune checkpoint modulator is a PD-1, PD-L1 or a CTLA-4 checkpoint inhibitor.

17. A method according to any one of claims 1 to 16, wherein the immune checkpoint modulator is an antibody.

18. Use of a compound comprising, consisting or consisting essentially of an IFNβ inhibitor and an immune checkpoint modulator in the preparation of a medicament for treating, preventing or minimising progression of cancer in a subject, wherein the medicament is constructed such that in use, or when used, the IFNβ inhibitor is administered after the immune checkpoint modulator.

19. Use of a compound comprising, consisting or consisting essentially of an immune checkpoint modulator in the manufacture of a first medicament, and an IFNβ inhibitor in the preparation of a second medicament, wherein the first and second medicaments are for:

- treating, preventing or minimising progression of cancer in a subject,
- minimising, reducing or preventing growth of a tumour in a subject,
- minimising, reducing or preventing metastasis in a subject, or
- increasing survival of a subject,

wherein the second medicament is administered after the first medicament.

20. Use of an IFNβ inhibitor in the manufacture of a medicament for:

- treating, preventing or minimising progression of cancer in a subject who has received or who is receiving an immune checkpoint modulator,
- minimising, reducing or preventing growth of a tumour in a subject who has received or who is receiving an immune checkpoint modulator,
- minimising, reducing or preventing metastasis in a subject who has received or who is receiving an immune checkpoint modulator, or
- increasing survival of a subject who has received or who is receiving an immune checkpoint modulator.

21. An IFNβ inhibitor for use in treating, preventing or minimising progression of cancer in a subject who has received or who is receiving an immune checkpoint modulator.

22. A method, use or IFNβ inhibitor for use according to any one of the preceding claims, further comprising administering an IFNβ agonist prior to administering the immune checkpoint modulator.

23. A method, use or IFNβ inhibitor for use according to any one of the preceding claims, wherein the IFNβ inhibitor and/or the immune checkpoint modulator is administered intraperitoneally, intratumorally, topically, orally, intravenously, subcutaneously or intramuscularly.

24. A method, use or IFNβ inhibitor for use according to any one of the preceding claims, wherein the IFNβ inhibitor and/ or immune checkpoint modulator are administered intravenously.

25. A method, use or IFNβ inhibitor for use according to any one of the preceding claims, wherein the cancer is selected from the group consisting of breast cancer, colorectal cancer, adenocarcinomas, mesothelioma, bladder cancer, prostate cancer, germ cell cancer, hepatoma/cholongio carcinoma, neuroendocrine cancer, pituitary neoplasm, small round cell tumour, squamous cell cancer, melanoma, atypical fibroxanthoma, seminomas, nonseminomas, stromal leydig cell tumours, Sertoli cell tumours, skin tumours, kidney tumours, testicular tumours, brain tumours, ovarian tumours, stomach tumours, oral tumours, bladder tumours, bone tumours, cervical tumours, esophageal tumours, laryngeal tumours, liver tumours, lung tumours, vaginal tumours, Wilm's tumours, pancreatic tumours, sarcomas, lymphomas or leukaemias.

26. A method, use or IFNβ inhibitor for use, according to any one of the preceding claims, wherein the cancer is mesothelioma or renal cell cancer.

Figure 1

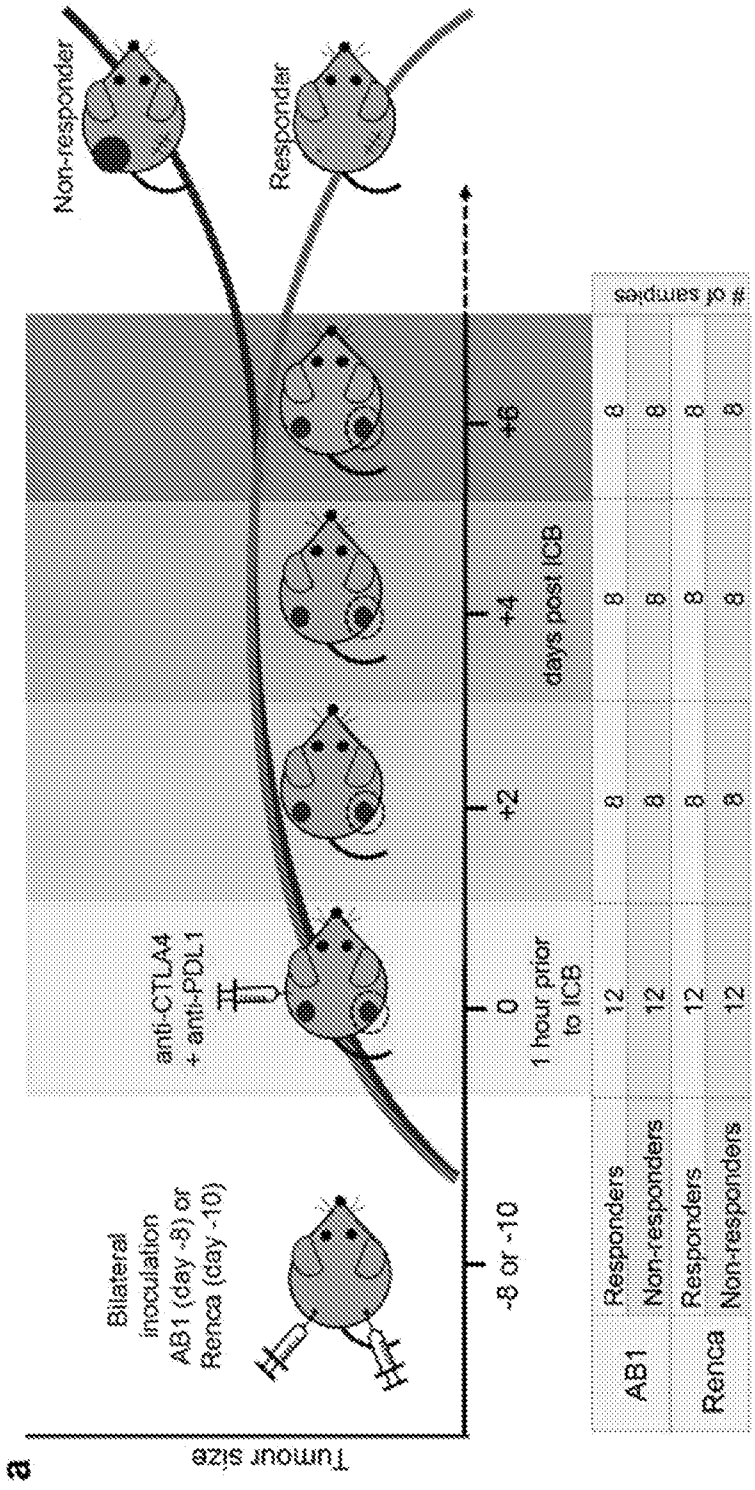
a
Tumour size
Bilateral inoculation AB1 (day -8) or Renca (day -10)
anti-CTLA4 + anti-PDL1
Non-responder
Responder
-8 or -10
0
1 hour prior to ICB
+2
+4
+6
days post ICB
# of samples
AB1
Responders
Non-responders
Renca
Responders
Non-responders
12
12
12
12
8
8
8
8
8
8
8
8
8
8
8
8

Figure 1 continued

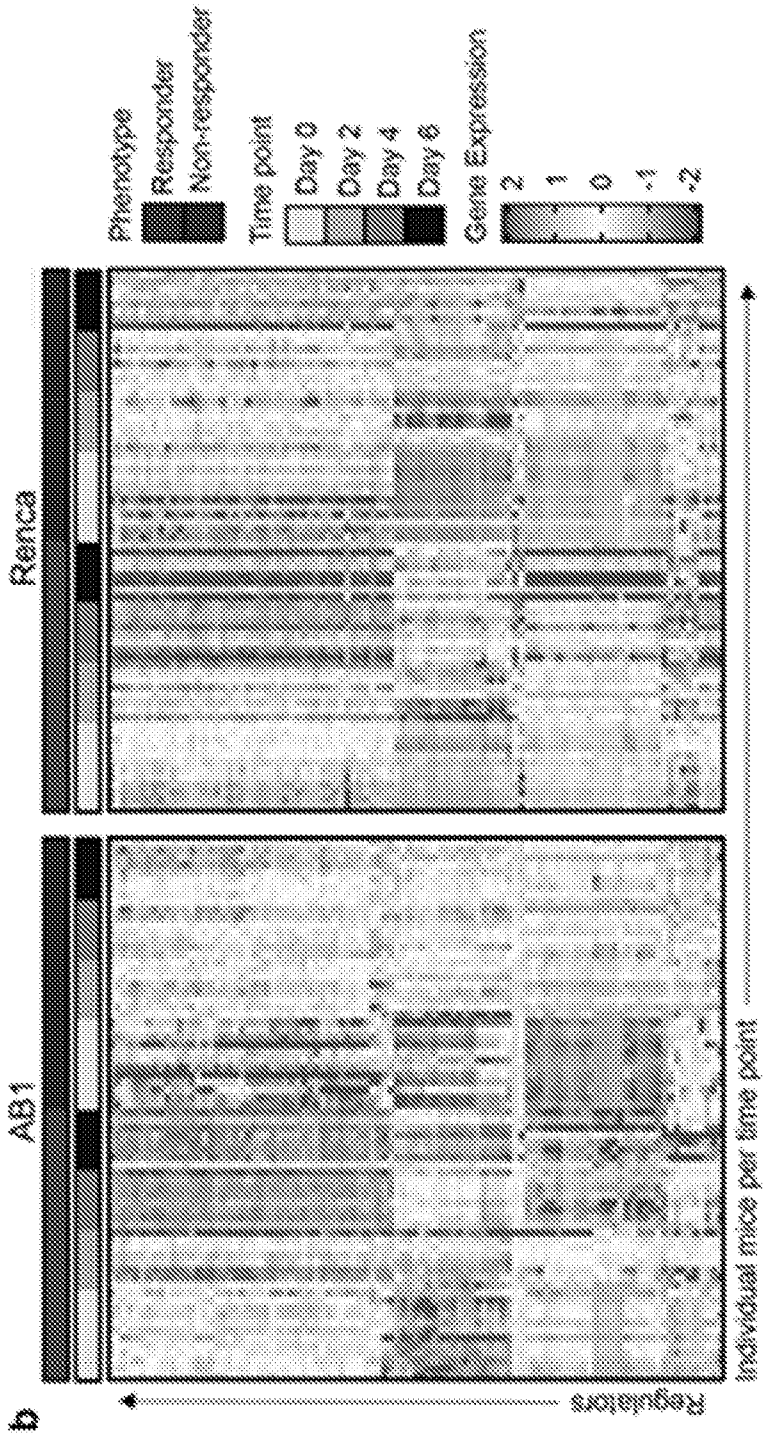

Figure 1 continued

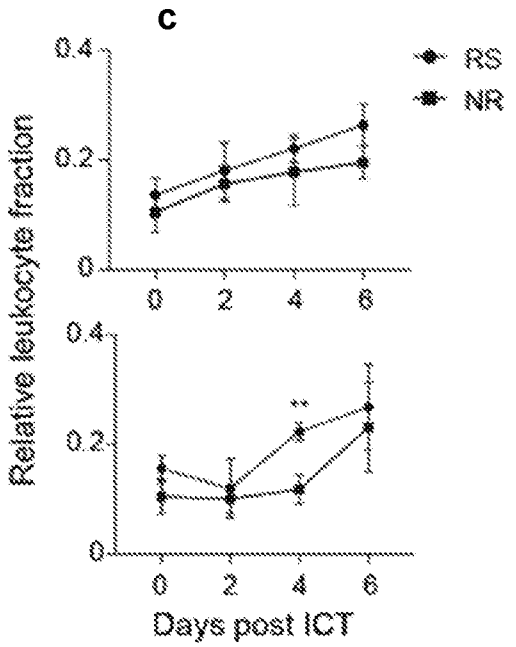

Figure 1 continued

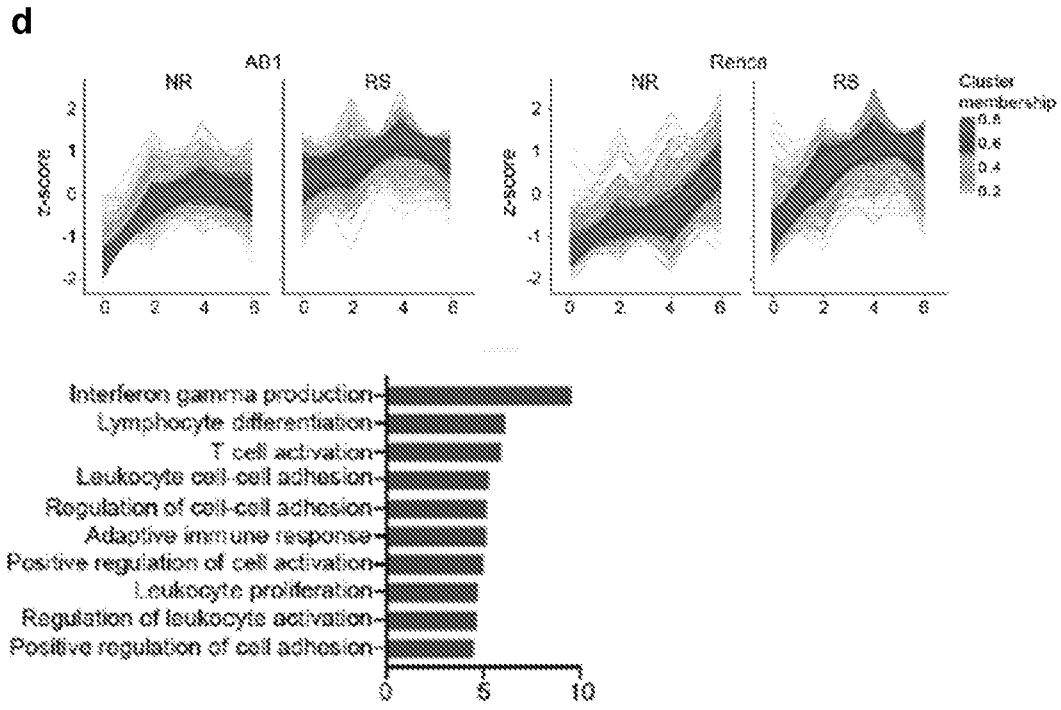

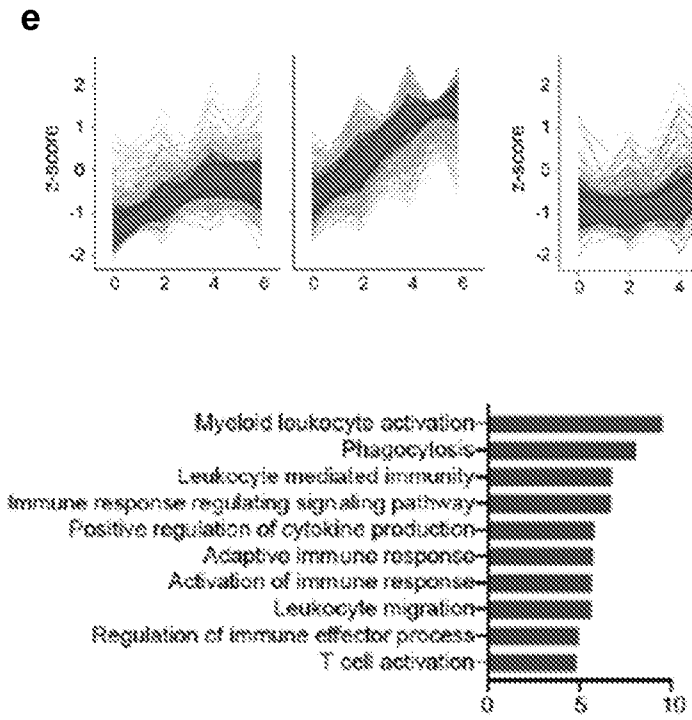

Figure 1 continued

f

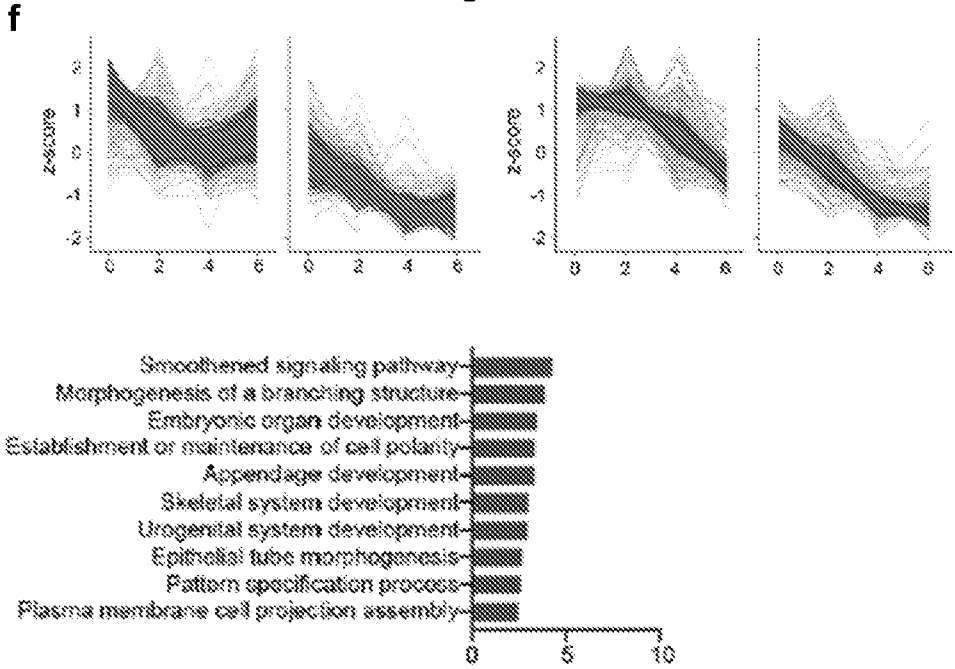

g

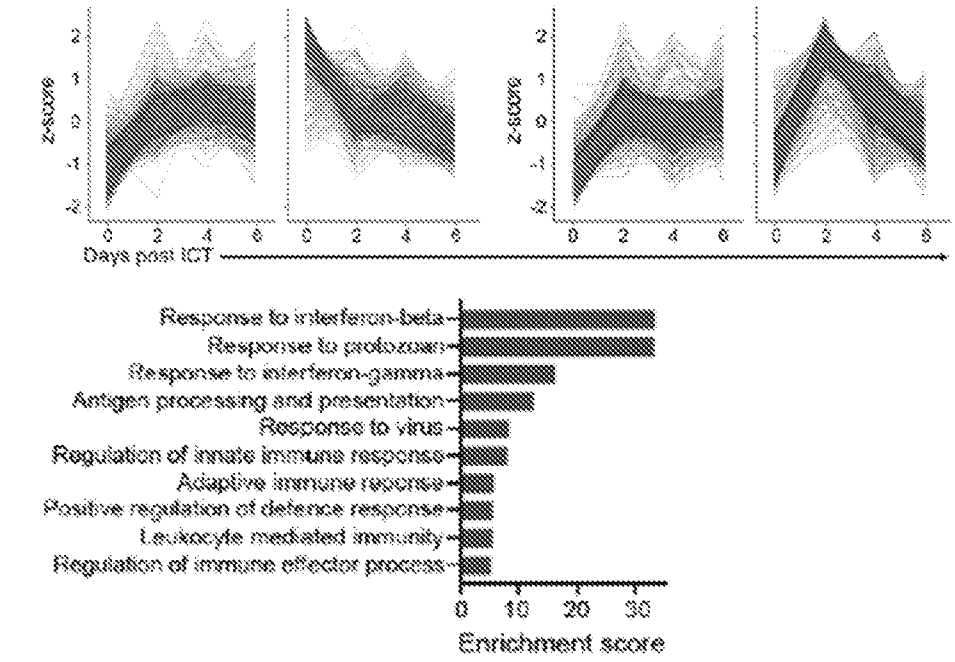

Figure 1 continued

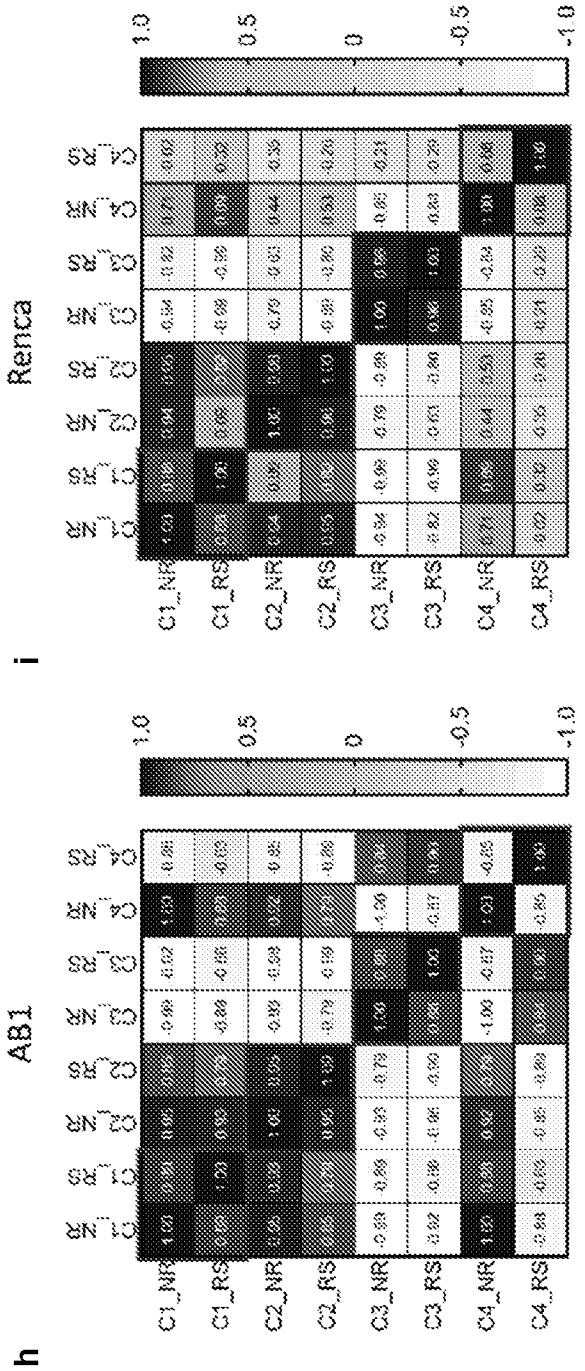

Figure 2

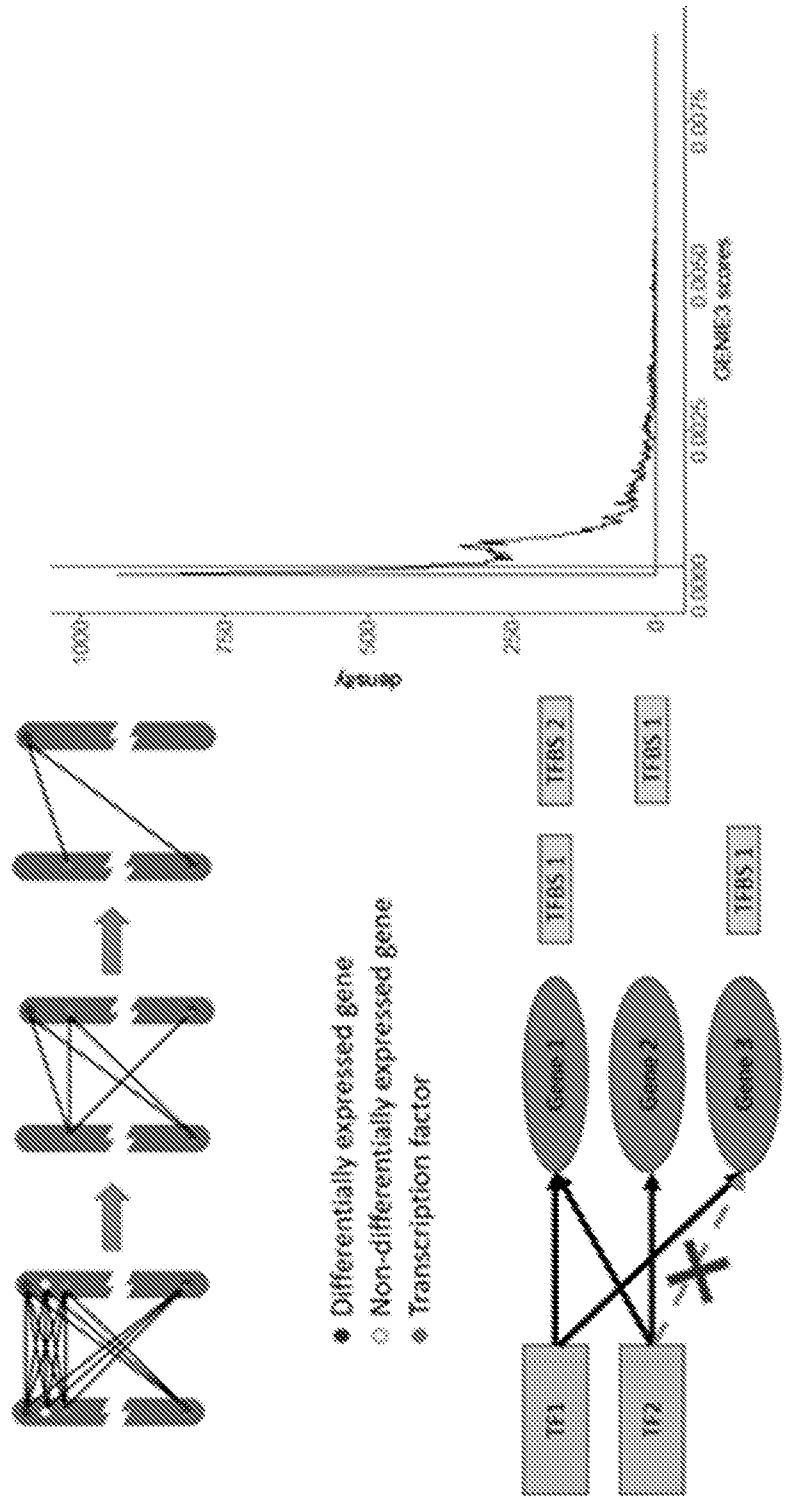
Differentially expressed gene
Non-differentially expressed gene
Transcription factor
TF1
TF2
Gene 1
Gene 2
Gene 3
TBS 1
TBS 2
TBS 1
TBS 1
-log10
CRMD3 scores

Figure 3

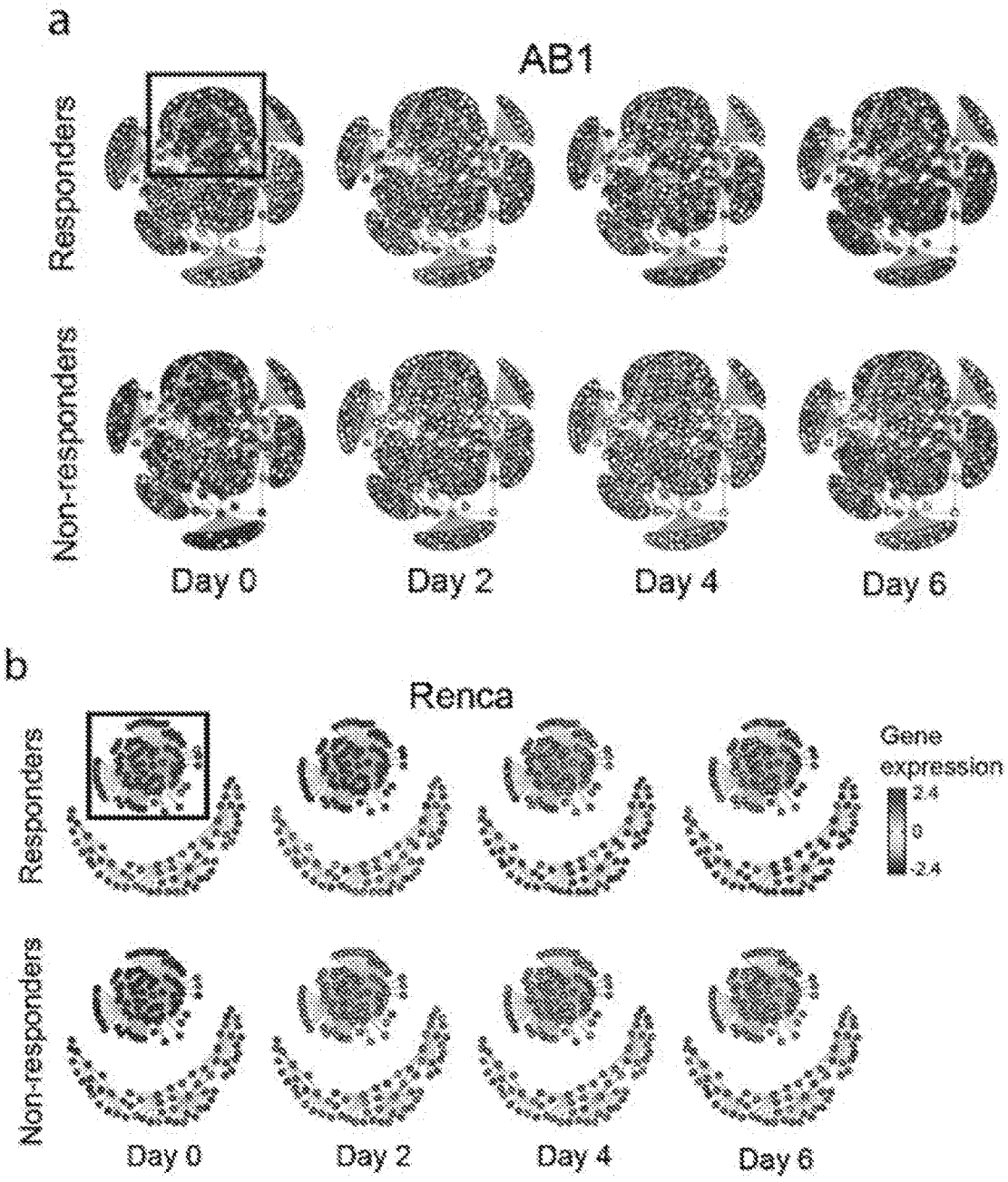
a
AB1
Responders
Non-responders
Day 0
Day 2
Day 4
Day 6
b
Renca
Responders
Non-responders
Gene expression
2.4
0
-2.4
Day 0
Day 2
Day 4
Day 6

Figure 3 continued

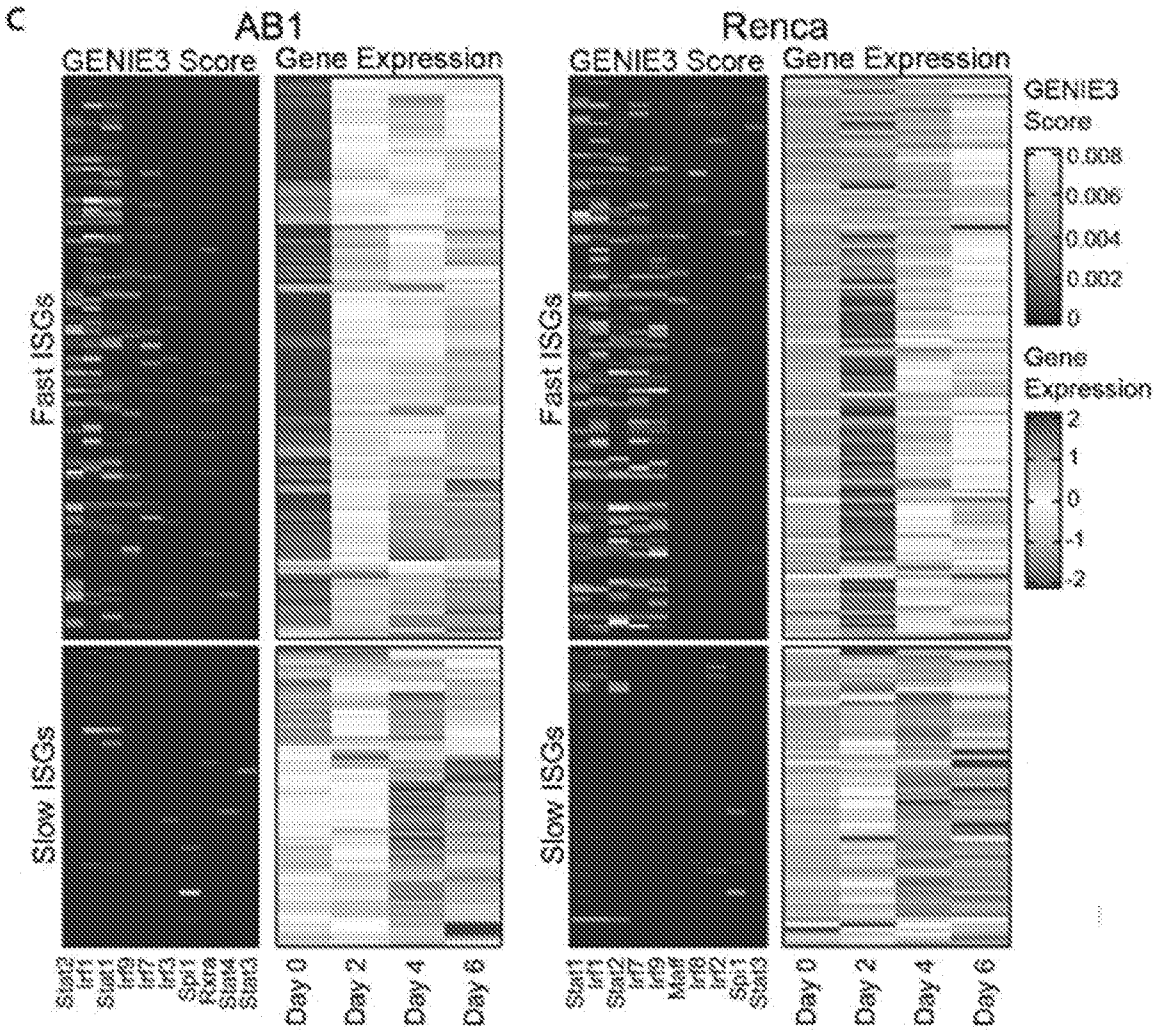

Figure 3 continued

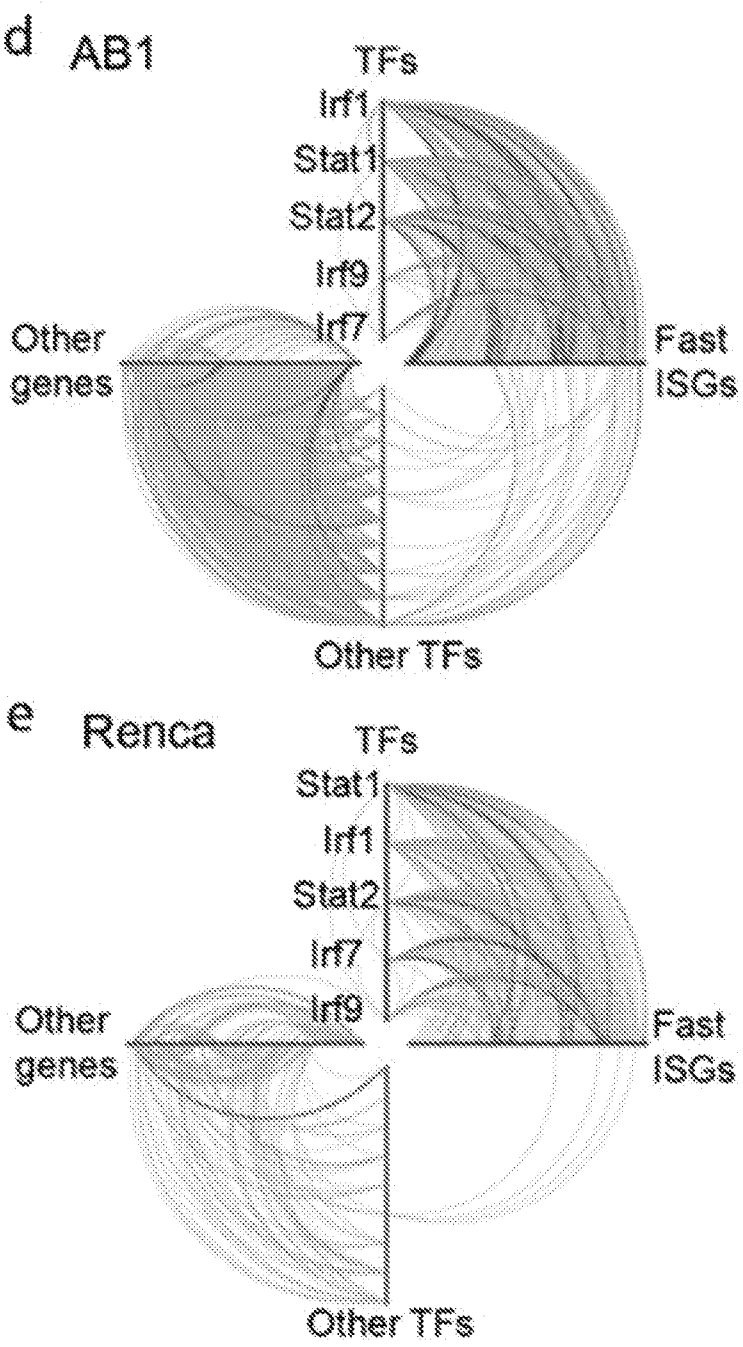

Figure 4

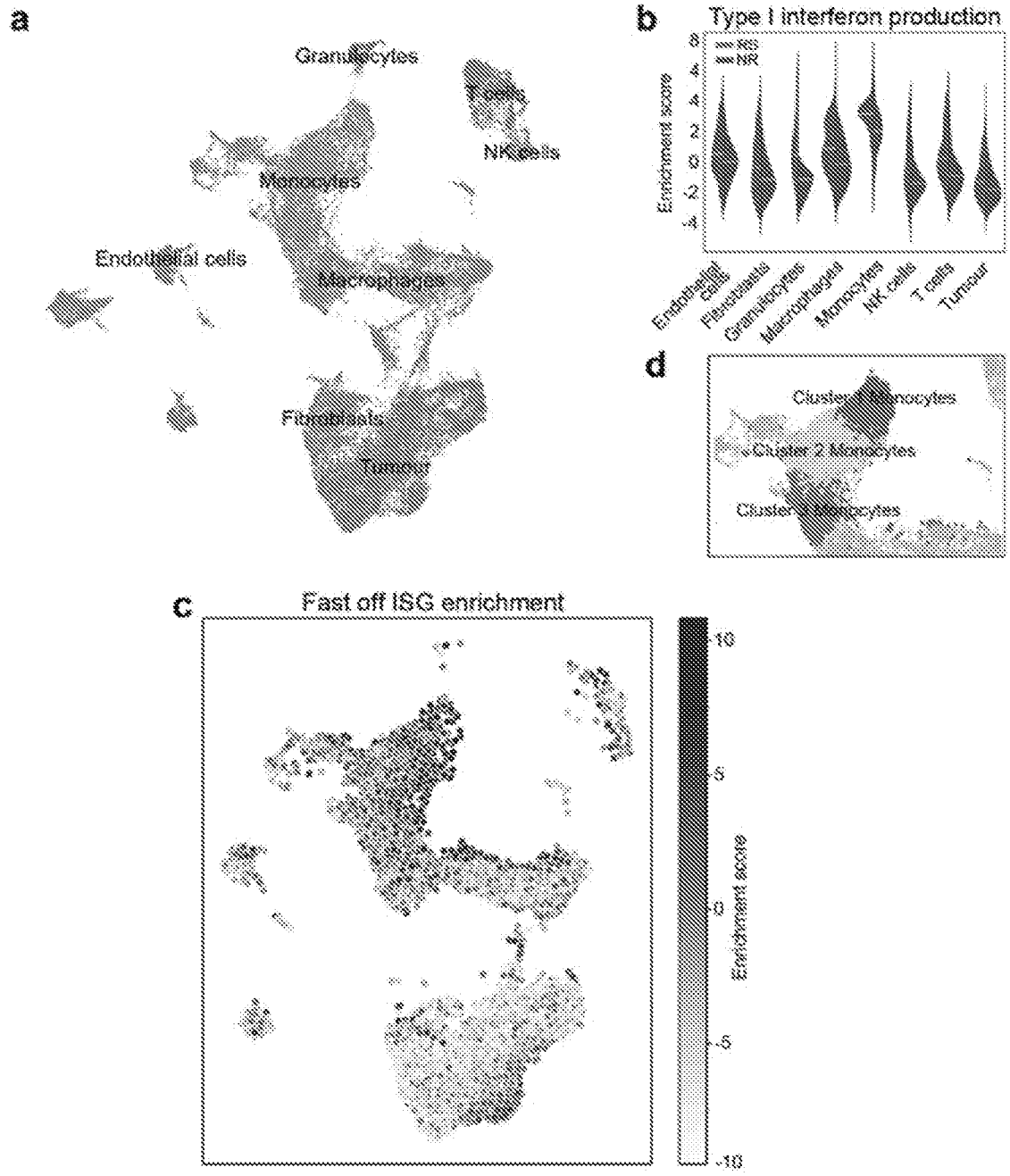
a
Granulocytes
T cells
NK cells
Monocytes
Endothelial cells
Macrophages
Fibroblasts
Tumour
b
Type I interferon production
KO
NR
Enrichment score
8
6
4
2
0
-2
-4
Endothelial cells
Fibroblasts
Granulocytes
Macrophages
Monocytes
NK cells
T cells
Tumour
d
Cluster 1 Monocytes
Cluster 2 Monocytes
Cluster 3 Monocytes
c
Fast off ISG enrichment
10
5
0
-5
-10
Enrichment score

Figure 4 continued

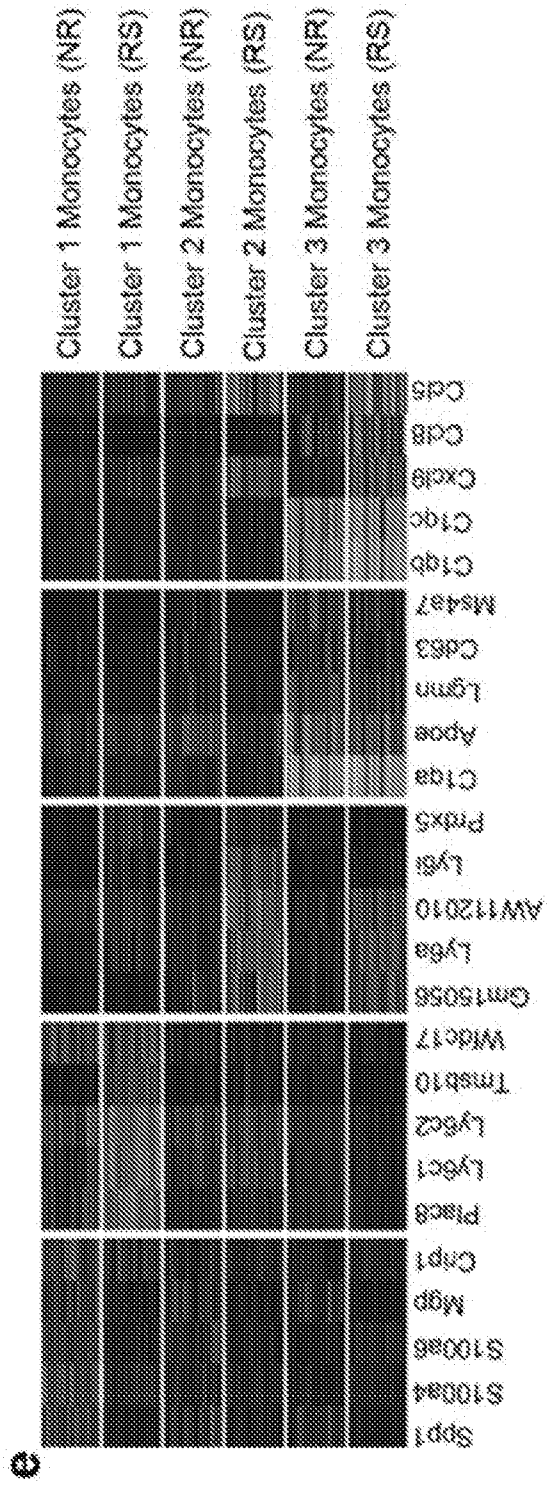

Figure 4 continued

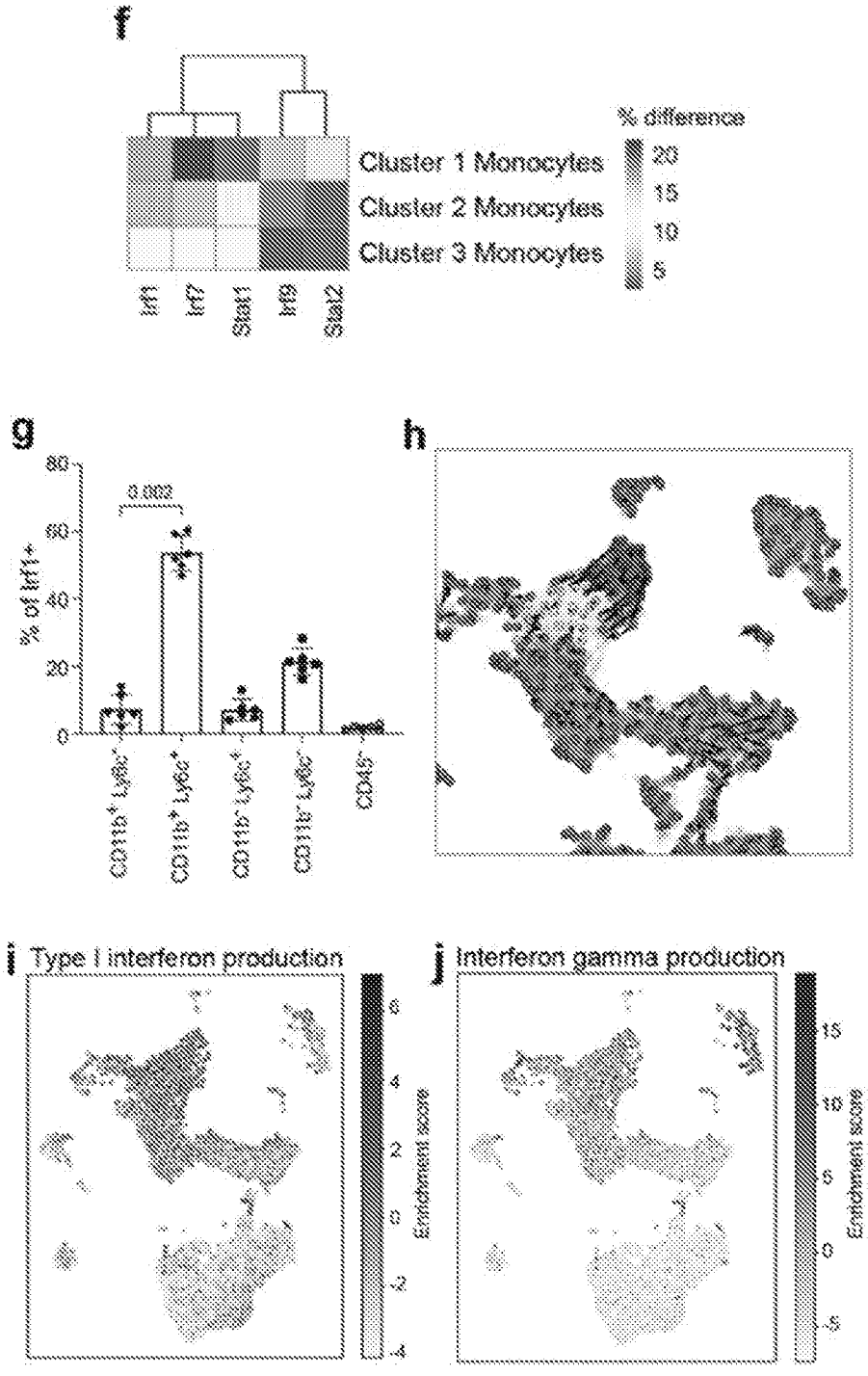

Figure 4 continued

k

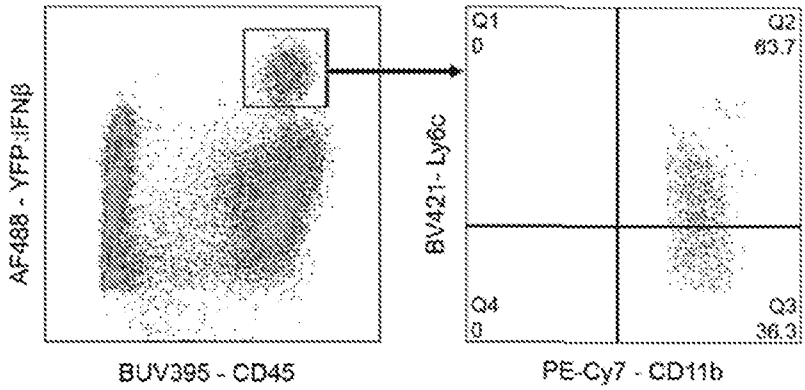

Figure 5

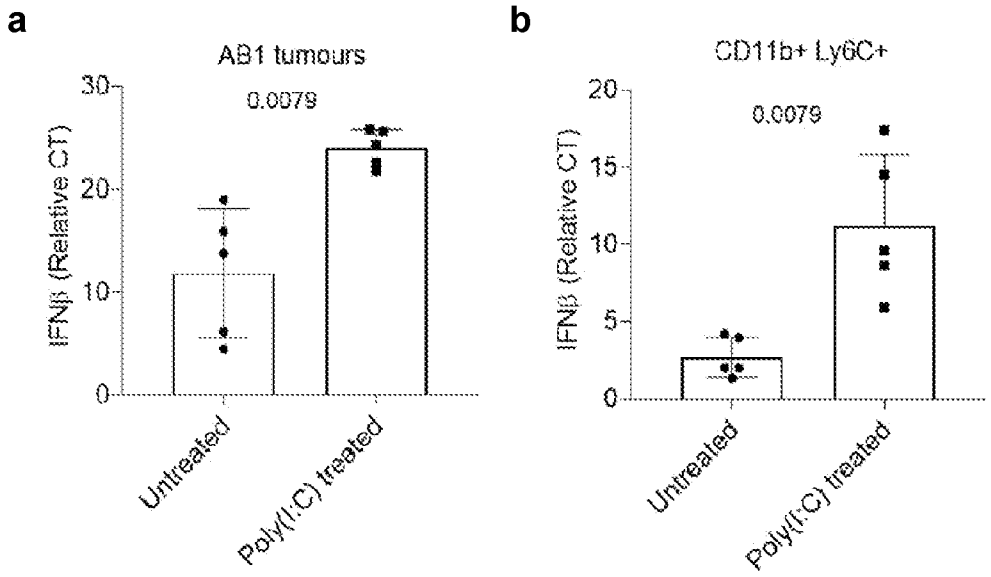
a
AB1 tumours
0.0079
IFNβ (Relative CT)
30
20
10
0
Untreated
Poly(I:C) treated
b
CD11b+ Ly6C+
0.0079
IFNβ (Relative CT)
20
15
10
5
0
Untreated
Poly(I:C) treated

Figure 6

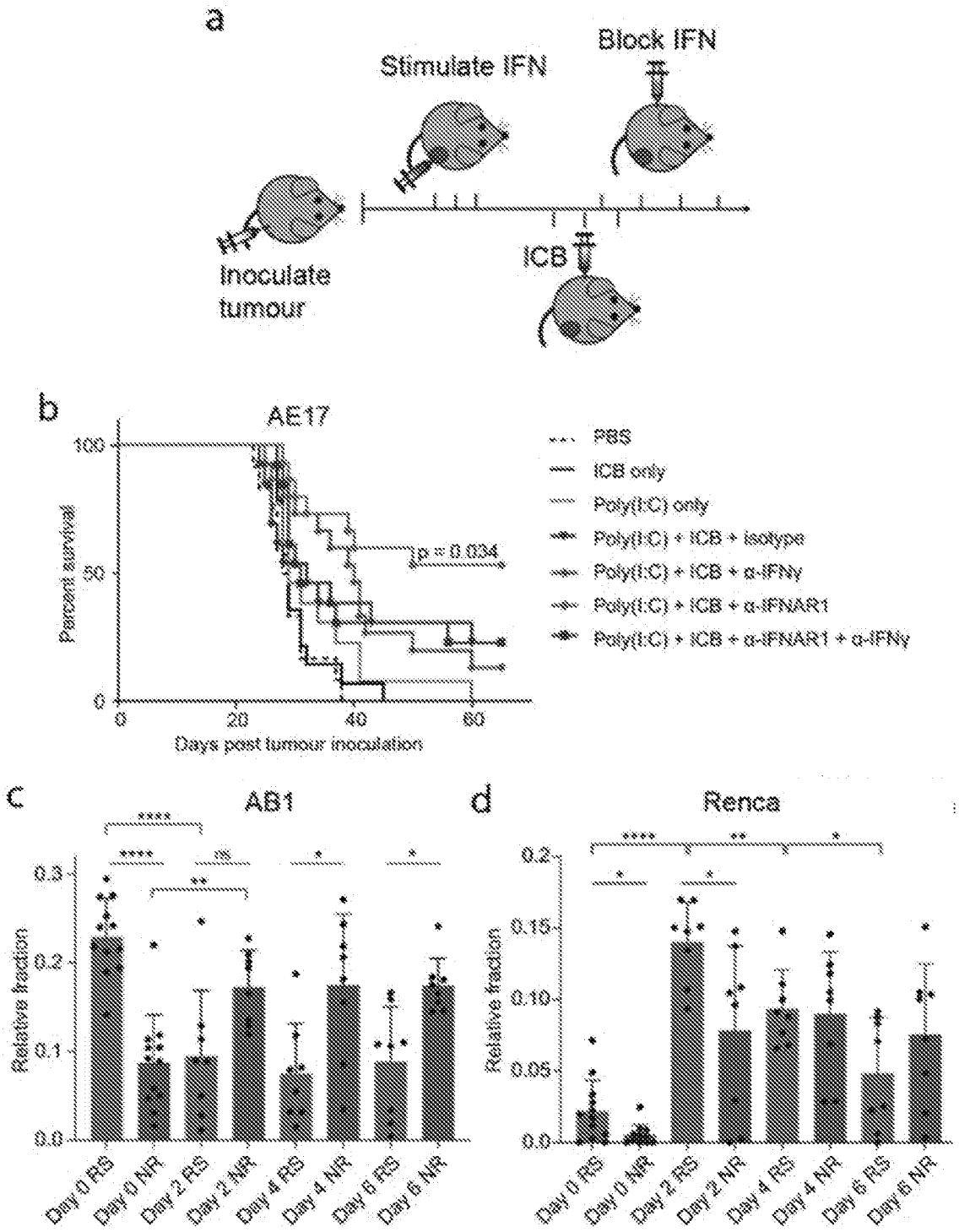
a
Stimulate IFN
Block IFN
Inoculate tumour
ICB
b
AE17
Percent survival
Days post tumour inoculation
p = 0.034
PBS
ICB only
Poly(I:C) only
Poly(I:C) + ICB + isotype
Poly(I:C) + ICB + α-IFNγ
Poly(I:C) + ICB + α-IFNAR1
Poly(I:C) + ICB + α-IFNAR1 + α-IFNγ
c
AB1
Relative fraction
Day 0 RS
Day 0 NR
Day 2 RS
Day 2 NR
Day 4 RS
Day 4 NR
Day 6 RS
Day 6 NR
d
Renca
Relative fraction

Figure 6 continued

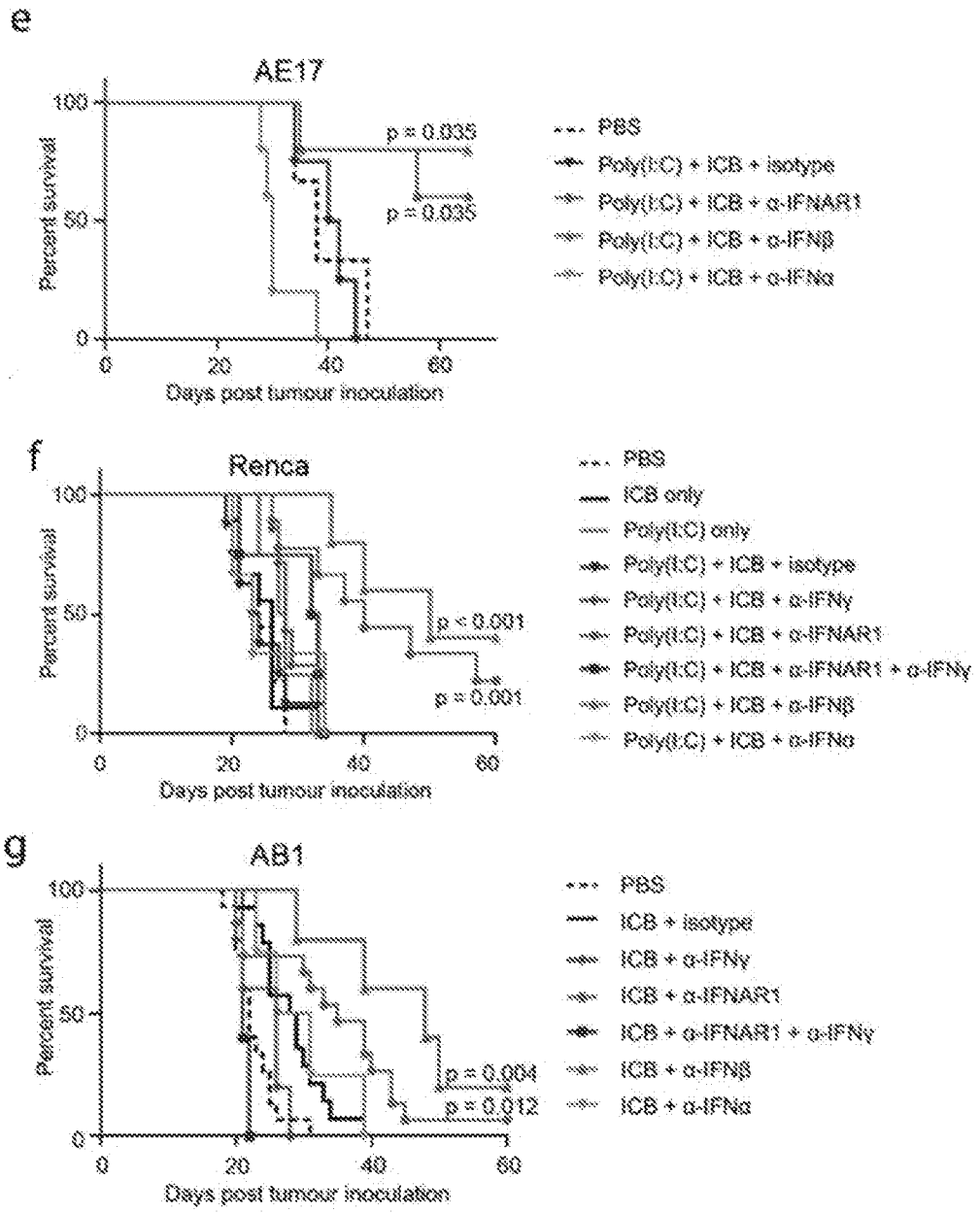

Figure 6 continued

h

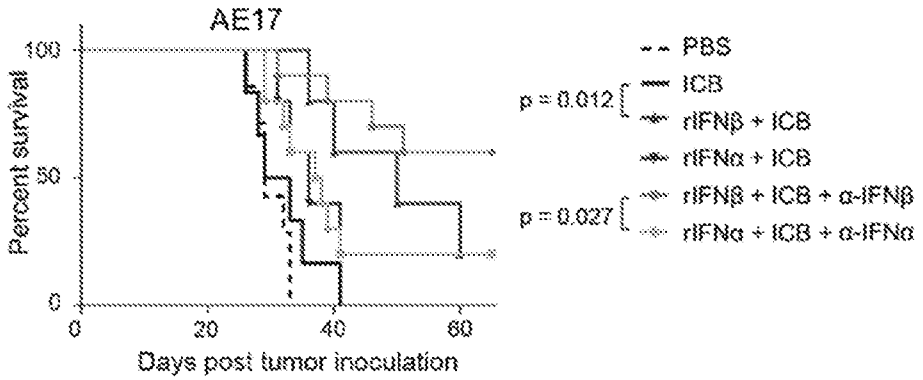

i

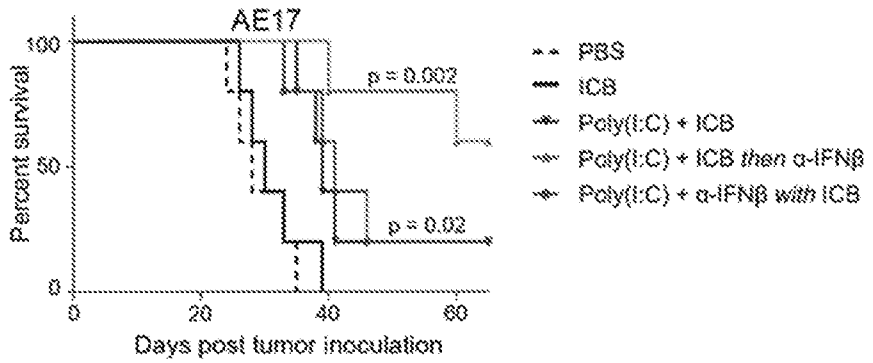

Figure 7

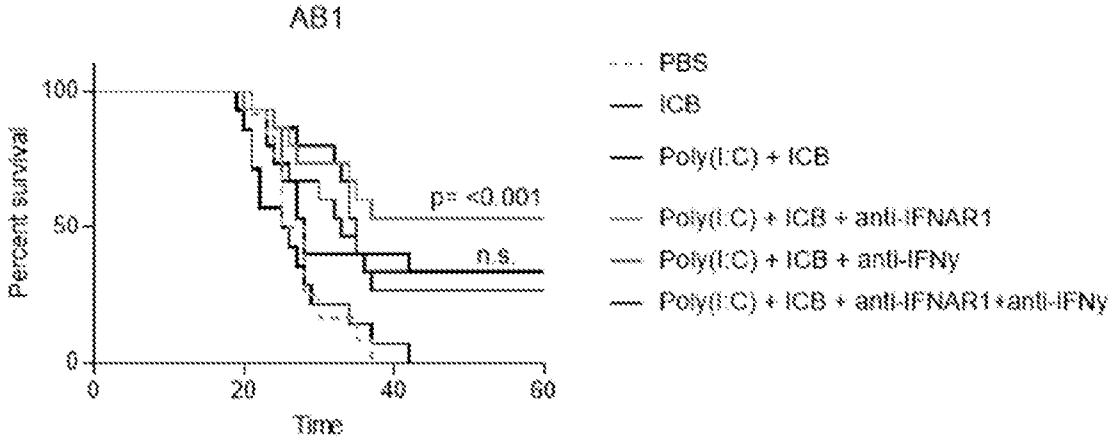
AB1
Percent survival
100
50
0
0
20
40
60
Time
p= <0.001
n.s.
PBS
ICB
Poly(I:C) + ICB
Poly(I:C) + ICB + anti-IFNAR1
Poly(I:C) + ICB + anti-IFNγ
Poly(I:C) + ICB + anti-IFNAR1+anti-IFNγ

Figure 8

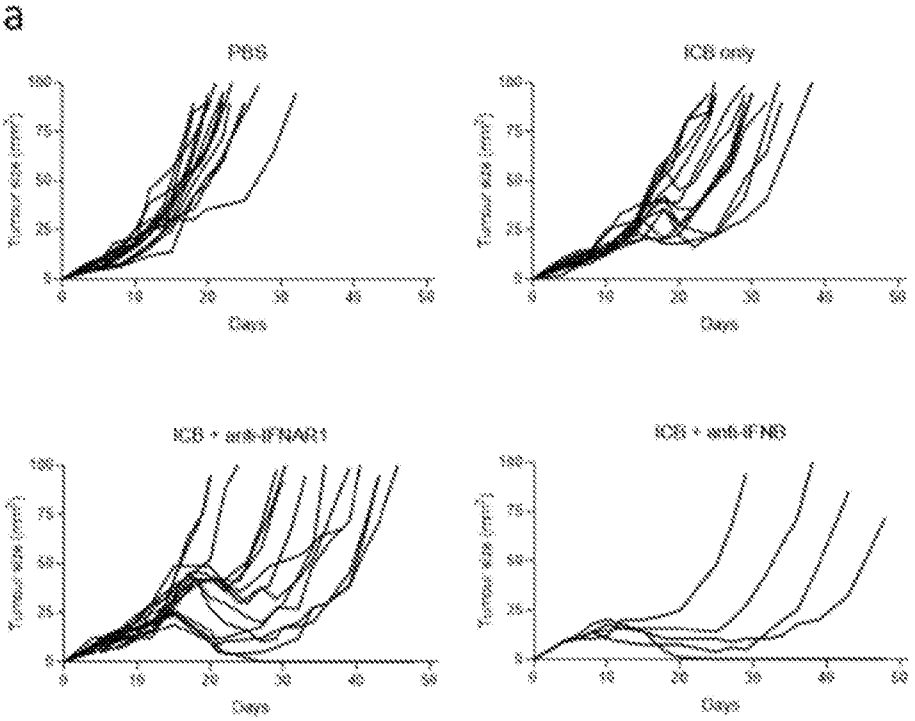

Group	Comparison	Contrast	Df	Pvalue	PvalueAdj
PBS	ICB only	0.055 [0.011;0.099]	49.88	0.0146	0.0890
PBS	ICB + anti-IFNAR	0.095 [0.052;0.138]	47.83	<0.0001	0.0003
PBS	ICB + anti-IFNB	0.143 [0.085;0.200]	39.43	<0.0001	<0.0001
ICB only	ICB + anti-IFNAR	0.040 [-0.002;0.081]	40.92	0.0591	0.3546
ICB only	ICB + anti-IFNB	0.087 [0.031;0.144]	36.13	0.0032	0.0192
ICB + anti-IFNAR	ICB + anti-IFNB	0.048 [-0.008;0.103]	35.11	0.0887	0.5324

P-value adjustment: bonferroni

Figure 8 continued

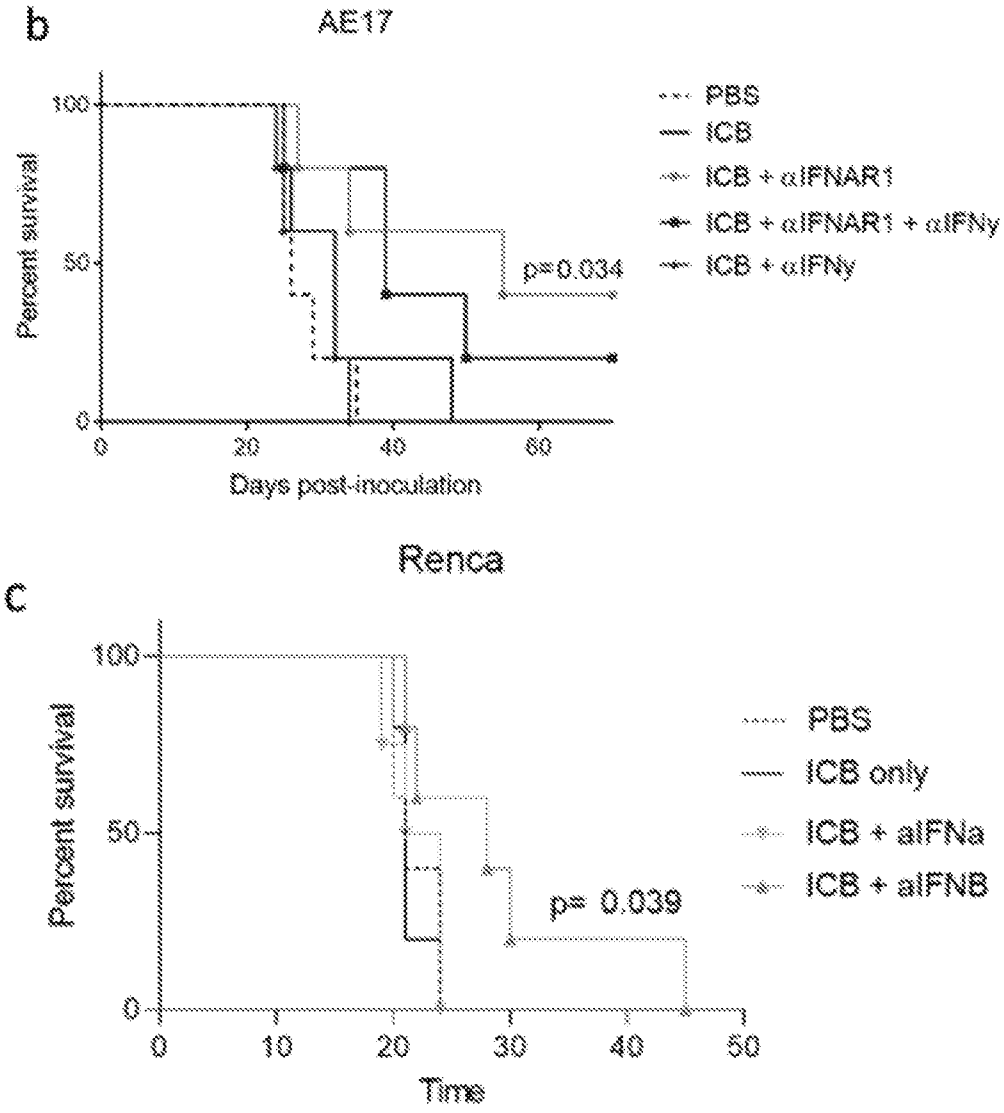

Figure 9

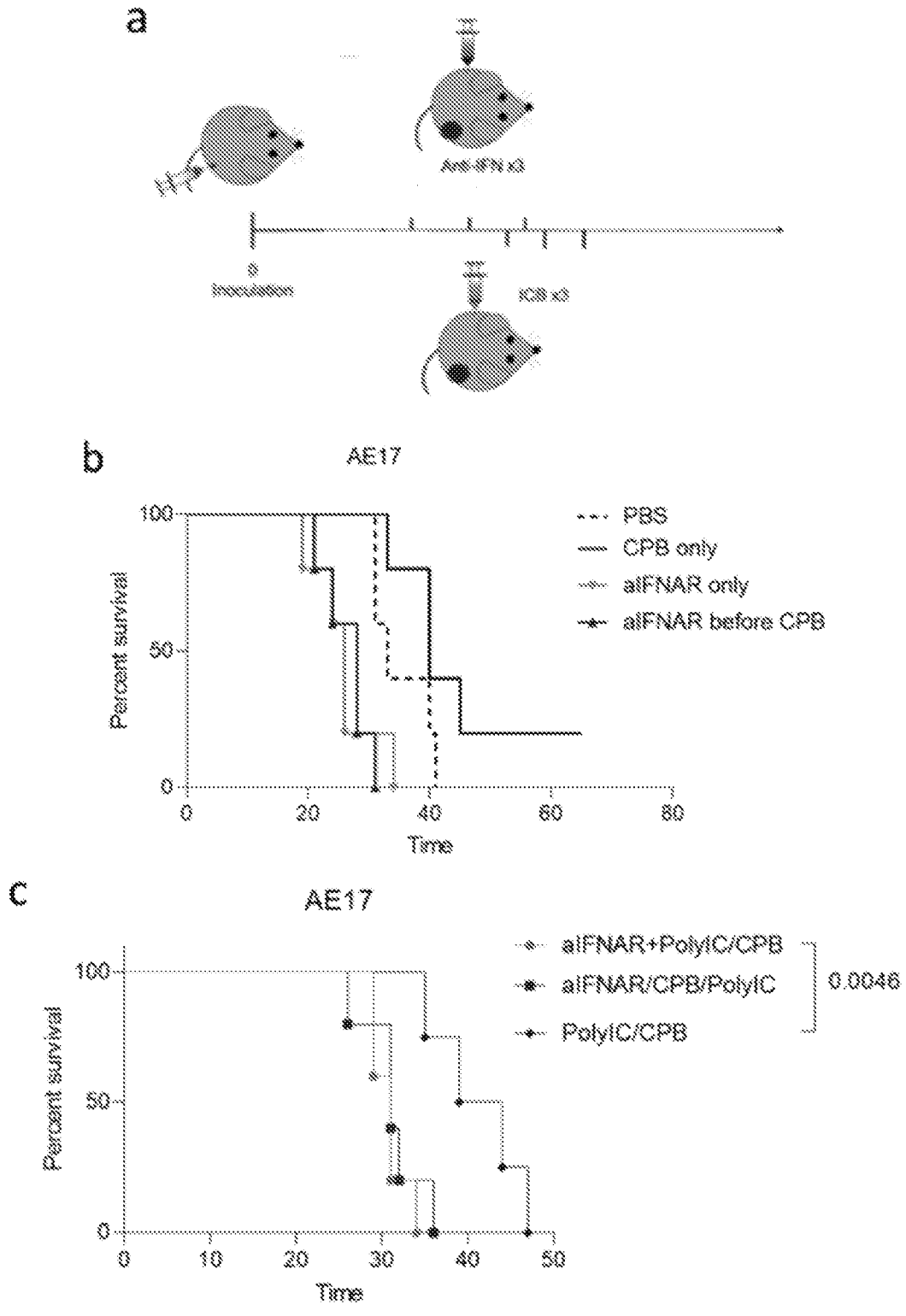
a
Anti-IFNAR
Inoculation
CPB
b
AE17
PBS
CPB only
aIFNAR only
aIFNAR before CPB
Percent survival
Time
c
AE17
aIFNAR+PolyIC/CPB
aIFNAR/CPB/PolyIC
PolyIC/CPB
0.0046
Percent survival
Time

Figure 9 continued

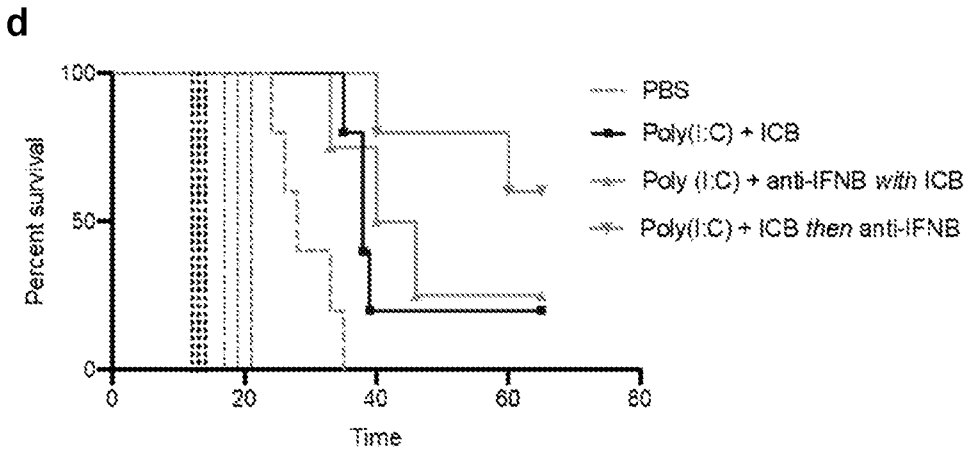

Figure 10

a

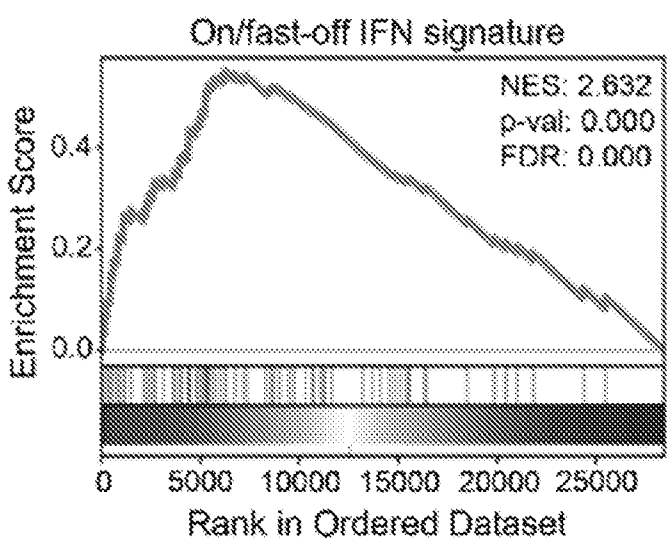

Term	ES	NES	FDR
On/fast-off IFN signature	0.549	2.632	0.0000
Interferon alpha response	0.493	2.408	0.0000
Inflammatory response	0.423	2.341	0.0000
TNFa signalling via NFKB	0.400	2.243	0.0000
Interferon gamma response	0.400	2.237	0.0000
Allograft rejection	0.393	2.162	0.0000
KRAS signalling down	0.355	1.936	0.0003
Bile acid metabolism	0.353	1.773	0.0011

Figure 10 continued

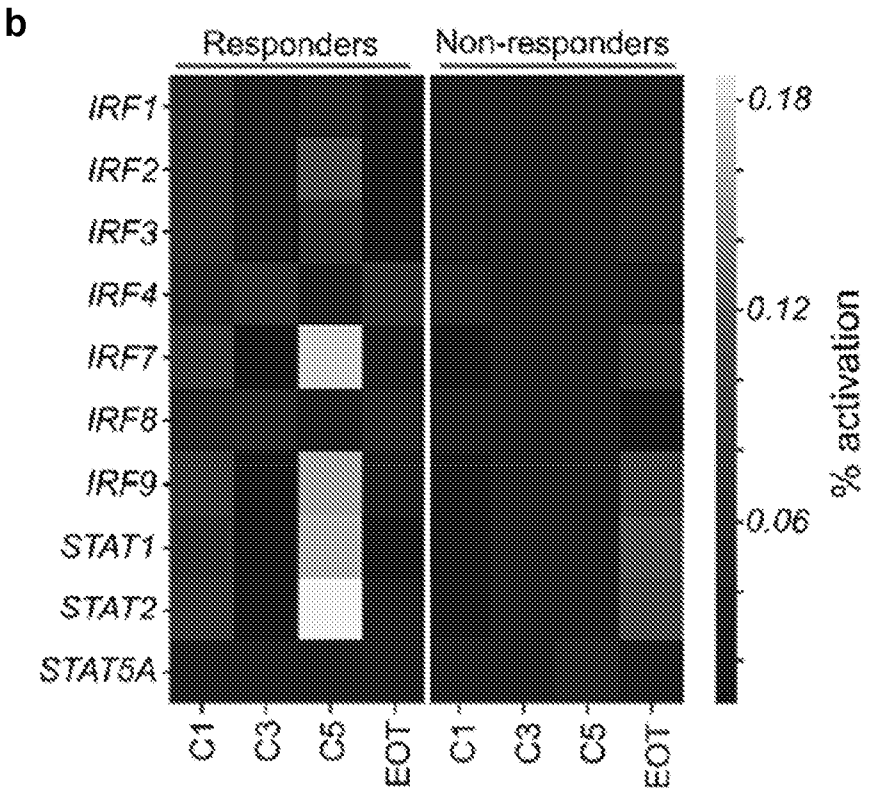

Figure 10 continued

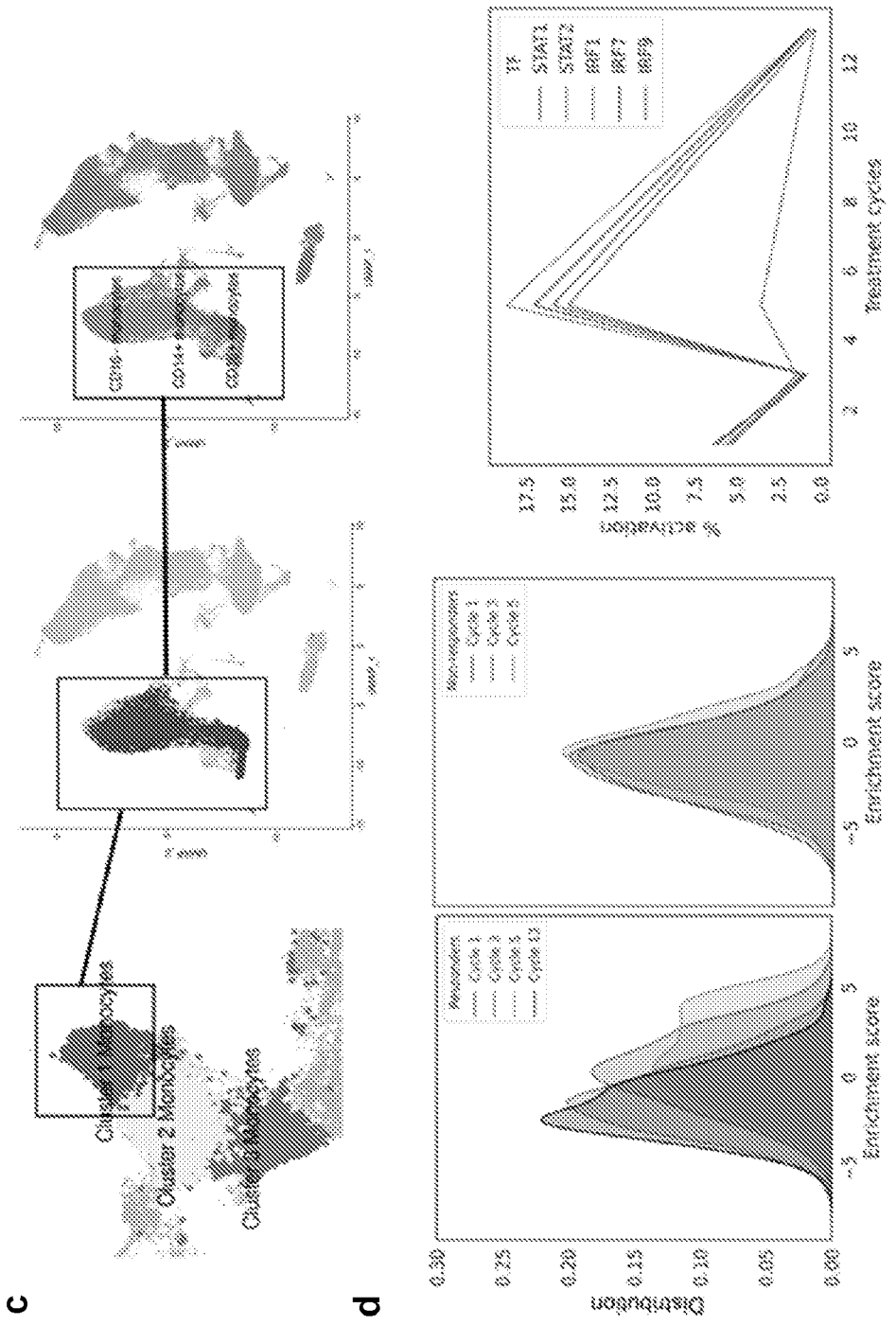

Figure 11

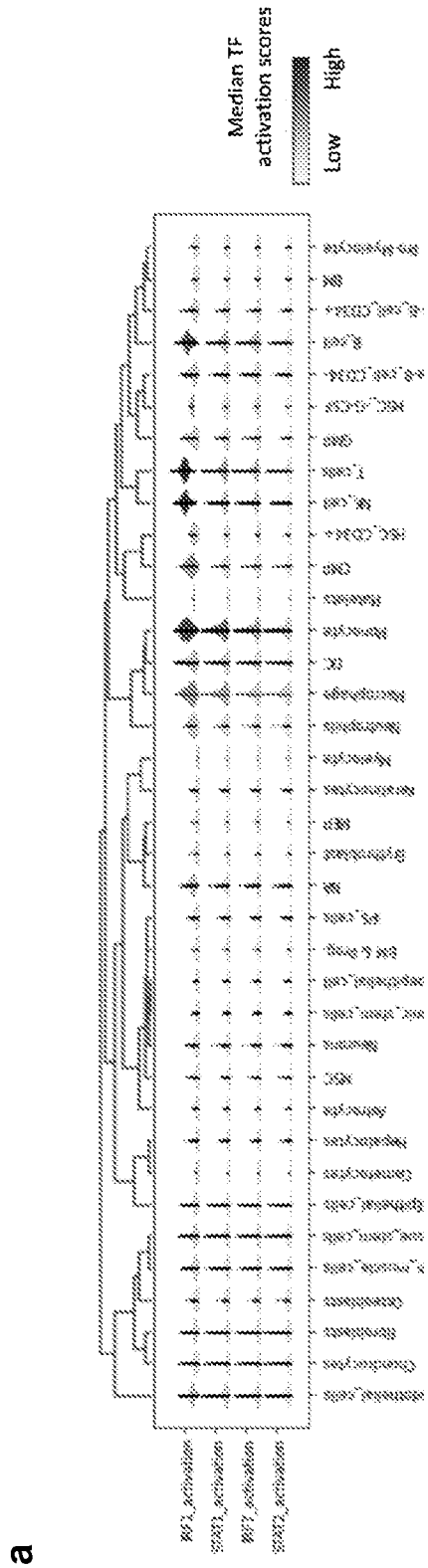

a

Figure 11 continued

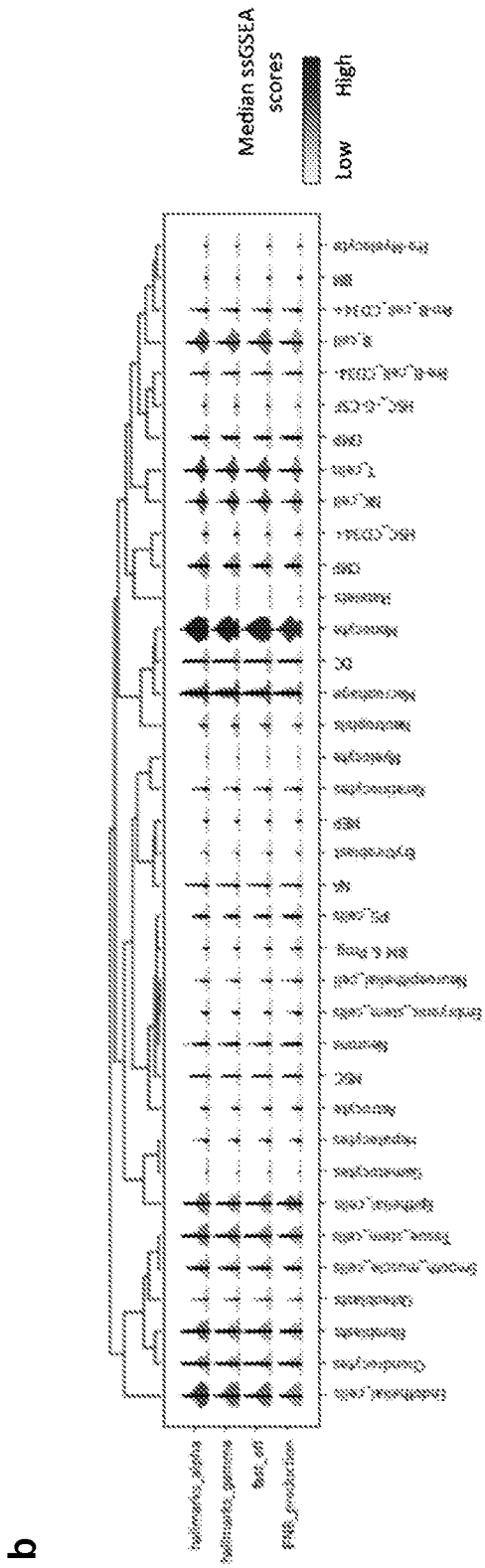

b

Figure 11 continued

C

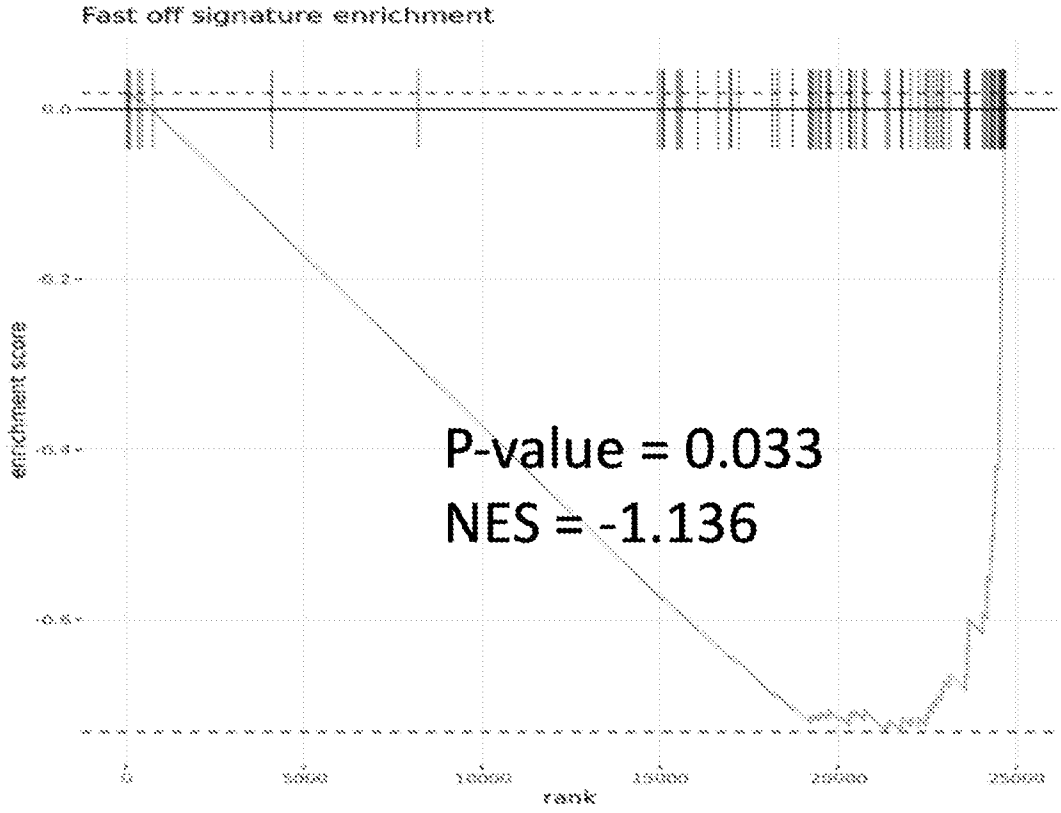

INTERNATIONAL SEARCH REPORT

International application No.
PCT/AU2021/050764

A. CLASSIFICATION OF SUBJECT MATTER

C07K 16/24 (2006.01) C07K 16/28 (2006.01) A61K 39/00 (2006.01) A61K 39/395 (2006.01) A61P 35/00 (2006.01)

According to International Patent Classification (IPC) or to both national classification and IPC

B. FIELDS SEARCHED

Minimum documentation searched (classification system followed by classification symbols)

Documentation searched other than minimum documentation to the extent that such documents are included in the fields searched

Electronic data base consulted during the international search (name of data base and, where practicable, search terms used)

Databases: PATENW (WPIAP, EPODOC and all English language full-text databases), MEDLINE, EMBASE, BIOSIS, CAPLUS, PubMed, Espacenet, Google, and internal databases provided by IP Australia.

Keywords: INTERFERON β, IFNAR and synonyms, check point inhibitors, stimulators or modulators, specific names of checkpoints, PF_06823859 OR ANIFROLUMAB, treatment of cancer and relevant terms (for more information please look at the attached SIS).

C. DOCUMENTS CONSIDERED TO BE RELEVANT

Category*	Citation of document, with indication, where appropriate, of the relevant passages	Relevant to claim No.
	Documents are listed in the continuation of Box C	

[X] Further documents are listed in the continuation of Box C

[X] See patent family annex

* Special categories of cited documents:

"A" document defining the general state of the art which is not considered to be of particular relevance

"D" document cited by the applicant in the international application

"E" earlier application or patent but published on or after the international filing date

"L" document which may throw doubts on priority claim(s) or which is cited to establish the publication date of another citation or other special reason (as specified)

"O" document referring to an oral disclosure, use, exhibition or other means

"P" document published prior to the international filing date but later than the priority date claimed

"T" later document published after the international filing date or priority date and not in conflict with the application but cited to understand the principle or theory underlying the invention

"X" document of particular relevance; the claimed invention cannot be considered novel or cannot be considered to involve an inventive step when the document is taken alone

"Y" document of particular relevance; the claimed invention cannot be considered to involve an inventive step when the document is combined with one or more other such documents, such combination being obvious to a person skilled in the art

"&" document member of the same patent family

Date of the actual completion of the international search	Date of mailing of the international search report
17 August 2021	17 August 2021

Name and mailing address of the ISA/AU

AUSTRALIAN PATENT OFFICE
PO BOX 200, WODEN ACT 2606, AUSTRALIA
Email address: pct@ipaustralia.gov.au

Authorised officer

Srgjan Chivchiristov
AUSTRALIAN PATENT OFFICE
(ISO 9001 Quality Certified Service)
Telephone No. +61262833104

Category*	Citation of document, with indication, where appropriate, of the relevant passages	Relevant to claim No.
X	WO 2020/097393 A1 (GRITSTONE ONCOLOGY, INC.) 14 May 2020 Background; Summary; Figures 12-13; Figures 26-28; sections XIX-XX.; Table 34; para 7-8, 39, 69, 78; claims 1, 24-25, 146-147, 158	1-26
X	GONG, K. et al, 'EGFR inhibition triggers an adaptive response by co-opting antiviral signaling pathways in lung cancer', Nature Cancer. Published in PMC December 2020, Vol. 1, No. 4, pages 1-51 page 11, para 3; Abstract; Introduction; Extended data Figures 3, 8; page 6; page 14, para 2; page 10, para 2	1-26
X	WO 2019/020593 A1 (INSERM (INSTITUT NATIONAL DE LA SANTE ET DE LA RECHERCHE MEDICALE) et al.) 31 January 2019 Results; Discussion; Abstract; claims 1, 5-9; pages 8-12	1-26
X	BENCI, J.L. et al., 'Tumor Interferon Signaling Regulates a Multigenic Resistance Program to Immune Checkpoint Blockade', Cell. 2016, Vol. 167, No. 6, pages 1540-1554 & Supplementary pages e1-e12 Figure 6E, D8 schedule; Figures 6F and 6G, D5 schedule; page 1551, col 1, para 1-2; page 1552, col 2, para 3	1-26
X	JACQUELOT, N. et al., 'Sustained Type I interferon signaling as a mechanism of resistance to PD-1 blockade', Cell Research. 2019, Vol. 29, pages 846-861 Abstract; page 847, col 1, para 3; page 847, col 2, para 4; Figure 2a; page 849, col 2, para 3; page 851, col 1; Figure 6; page 855, col 2, para 1-2	1-26
A	MINN, A.J. & WHERRY, E.J. et al., 'Combination Cancer Therapies with Immune Checkpoint Blockade: Convergence on Interferon Signaling', Cell. 2016, Vol. 165, No.2, pages 272-275 Figure 1; page 273, col 2, last para; page 273, col 1, first para	

INTERNATIONAL SEARCH REPORT Information on patent family members	International application No. **PCT/AU2021/050764**

This Annex lists known patent family members relating to the patent documents cited in the above-mentioned international search report. The Australian Patent Office is in no way liable for these particulars which are merely given for the purpose of information.

Patent Document/s Cited in Search Report		Patent Family Member/s	
Publication Number	**Publication Date**	**Publication Number**	**Publication Date**
WO 2020/097393 A1	14 May 2020	WO 2020097393 A1	14 May 2020
		AU 2019374874 A1	10 Jun 2021
		CA 3119752 A1	14 May 2020
		CN 112912507 A	04 Jun 2021
		KR 20210090650 A	20 Jul 2021
WO 2019/020593 A1	31 January 2019	WO 2019020593 A1	31 Jan 2019
		EP 3658173 A1	03 Jun 2020
		US 2020216530 A1	09 Jul 2020

End of Annex

Due to data integration issues this family listing may not include 10 digit Australian applications filed since May 2001.